École Doctorale en Mathématiques et Informatique de Marseille

Thèse de doctorat d'Aix-Marseille Université

Discipline : Mathématiques Appliquées

présentée par

Cécile Carrère

pour obtenir le grade de
Docteur d'Aix Marseille Université

Prise en compte de l'hétérogénéité tumorale dans l'optimisation d'une chimiothérapie : contrôle optimal, analyse théorique et numérique.

Directrices de thèse : **Assia Benabdallah** et **Guillemette Chapuisat**

Soutenue le 6 Octobre 2017 devant le jury composé de :

M^{me}	Assia Benabdallah,	*Aix-Marseille Université*	(directrice)
M^{me}	Helen Byrne,	*Oxford University*	(rapportrice)
M^{me}	Manon Carré,	*Aix-Marseille Université*	
M.	Jean-Baptiste Caillau,	*Université Côte d'Azur*	(rapporteur)
M^{me}	Guillemette Chapuisat,	*Aix-Marseille Université*	(co-directrice)
M.	Jean Clairambault,	*Inria Paris*	
M.	Thierry Colin,	*Institut Polytechnique de Bordeaux*	
M^{me}	Hasnaa Zidani,	*ENSTA*	

Résumé

Pour éviter l'apparition de cellules cancéreuses résistantes à une chimiothérapie, beaucoup de protocoles imposent de fortes doses de médicament : la dose maximale tolérée par le patient (MTD). Dans une série d'expériences in vitro menées par M.Carré au laboratoire du CRO2 à la Timone, Marseille, la présence de cellules résistantes dès le début du traitement fait échouer ce protocole, alors que l'utilisation de plus faibles doses permet de contrôler la taille de la tumeur. Afin d'expliquer et d'optimiser ce phénomène, G.Chapuisat a développé un modèle EDO reproduisant les résultats de ces expériences.

L'analyse de ce système nous permet de définir des schémas de traitements qui réduisent la taille de la tumeur, tout en limitant le nombre de cellules résistantes. Pour cela, nous étudions dans un premier temps le système sous traitement continu, ce qui nous permet d'identifier une taille minimale de tumeur sensible atteignable. Dans un second temps, nous utilisons la héorie du contrôle optimal pour déterminer des schémas de traitement minimisant en un sens la taille de la tumeur durant l'expérience. Cette étude souligne l'intérêt des chimiothérapies à faibles doses : celles-ci permettent de maintenir la tumeur à une faible taille en tuant beaucoup de cellules sensibles, tout en en épargnant suffisamment pour qu'elles continuent d'opprimer les cellules résistantes. Ainsi, des tumeurs résistantes ne peuvent pas émerger durant le traitement.

Afin de prendre en compte l'organisation spatiale des cellules, nous avons ensuite étudié un modèle EDP de compétition-diffusion de deux espèces envahissant un milieu favorable vide. Nous montrons que la différence de diffusion et de taux de doublement entre les deux types de cellules, entraîne la création de populations organisées en terrasse. En d'autres termes, sous certaines conditions sur les paramètres du système, les cellules résistantes envahissent le milieu vide favorable à une certaine vitesse, avant d'être remplacées par les cellules sensibles à une autre vitesse plus faible. Ce résultat est obtenu par des méthodes de comparaison des équations de réaction-diffusion.

Enfin, en collaboration avec H.Zidani, nous développons des méthodes d'optimisation numérique pour contrôler la taille de la tumeur au cours du temps. Nous définissons un problème de viabilité, et un problème d'atteignabilité pour le système EDO étudié dans la première partie. Dans un premier temps, nous déterminons les tumeurs initiales pour lesquelles il existe un traitement les maintenant sous un certain seuil de taille. Ensuite, pour les tumeurs initiales ne remplissant pas ce critère, nous cherchons le traitement le plus rapide atteignant ce seuil. Ces problèmes se traduisent mathématiquement par des équations de Hamilton-Jacobi-Bellman, dont nous présentons des implémentations numériques.

Abstract

To prevent the emergence of drug resistance during cancer chemotherapy, most medical protocols use the maximal tolerated dose (MTD) of drug possible. In a series of in vitro experiments, M.Carré showed that such protocols fail if resistant cells are present in the initial tumour. However, smaller doses of treatment maintain a small, stable tumour sensitive to the drug. To model and optimize such results, G.Chapuisat designed an ODE mathematical model of this experiment.

The analysis of this system leads to the design of new treatment protocols that reduce the tumour size. For this purpose, we first analyze the system under constant treatment. This allows us to identify a minimal reachable sensitive population, *i.e.* the smallest tumour composed mainly of sensitive cells that can be maintained with a constant treatment. We define an adaptive treatment that reaches this first target. Then, we use the theory of optimal control on the system to minimize a certain quantity linked to the size of the tumour during the experiment. The results from this study show the importance of low-dose treatment protocols. Indeed, they reduce the tumour volume by killing sensitive cells, but leave enough of them to continue oppressing resistant cells. This prevents the emergence of resistant populations.

Then, we study a PDE model of competition-diffusion of two species in an empty favorable environment, to understand the influence of motility on resistance emergence. We show that the differences of motility and growth factors between the two populations are responsible of the forming of a propagating terrace. In other words, for a certain range of parameters that we define, resistant cells will invade the empty favorable space at a certain speed, and then be replaced by sensitive cells at a lower speed. This result is obtained with comparison methods of reaction-diffusion equations.

Finally, we developp with H.Zidani other technics of treatment optimization, using dynamic programming. We define a problem of viability and a problem of reachability for the ODE model we studied in the first part. First, we identify for which initial tumours there exists a control maintaining it under a certain size threshold. Then, for the initial tumours that fail this criterium, we define the quickest treatment that brings them under this threshold size. These problems are modelled with Hamilton-Jacobi Bellman equations. We also present numerical implementations of these problems.

Contents

Introduction

This PhD thesis concerns chemotherapy optimization for heterogeneous tumours, regarding three different aspects : optimal control theory, competition diffusion systems and dynamic programming. The biological context is presented in Chap.1: a state of the art on chemotherapy modelling is conducted there.

0.1 Biological definitions and experiments

Cancer was the first cause of death in France in 2015. Despite serious progress in innovative treatments resulting in a lowering of its death rate, the total number of death imputed to cancer is predicted to augment, because of the aging of the population. It is thus a major public health issue. Various treatments exist and are developped against it, targeting cancerous cells or their environment. We are particularly interested in chemotherapies, and especially cytotoxic drugs, *i.e.* drugs that target cells during the division phase of their life cycle. These drugs are widely used in medical protocols, as cancer cells are dividing more often than regular cells, but might fail after a first encouraging phase because resistant cancer cells have emerged. This problem of resistance to chemotherapy has been studied by mathematical modelling in several articles, for example in [BHD08] using game theory. Also in [GSGF09], the authors mathematically design adaptive therapies to cope with the presence of resistance.

In order to have a better understanding of the phenomenon of resistance, M.Carré designed a series of experiments where two lineages of cancerous cells, sensitive or resistant to a certain drug, are cultivated in Petri wells, which are small Petri dishes. The coculture is then subject to different treatment protocols. The aim of these experiments is to investigate the role of metronomic treatments, *i.e.* low-dose chemotherapies, on resistance emergence. These treatments have proven to limit the vascularization of tumors, thus reducing their access to nutrients and oxygen, and they have less secondary effects on the immune system. However, their effect on resistance emergence is only recently studied with biological models.

The experiments are carried out on lung cancer cells lineages that are identified with fluorescent markers. Sensitive cells are marked in red, and resistant ones in green. Thanks to this, the number of cells in the two lineages can be determined through fluorescence measurements each day of the experiment. The two lineages have a similar growth rate when cultivated separately, but when they are interacting, the presence of sensitive cells oppresses resistant cells. Without treatment, sensitive cells fill the Petri well and only few resistant cells survive. Under treatment, high doses of drugs kills all sensitive cells, and lets resistant cells invade the Petri well, while smaller doses of drug maintain a low and stable population of sensitive cells, which is enough to prevent a resistant population emergence, as seen on Fig.1. The situation of having small but still controllable tumour, is interesting in a medical context. However, only constant dose treatments have been studied here, while varying dose could impact the result. We thus addressed

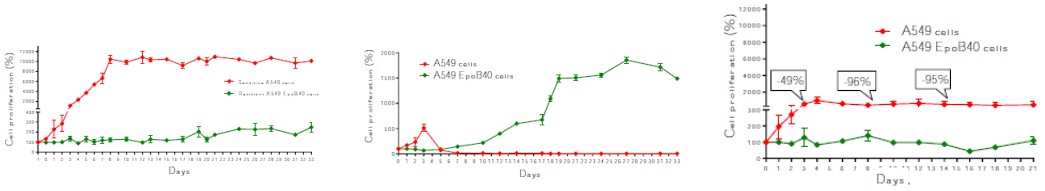

(a) Without treatment, sensitive cells fill up the Petri dish to its maximal capacity, and oppress resistant cells.

(b) Under a high dose treatment, all sensitive cells are killed, and resistant cells fill up the Petri dish.

(c) Under a low dose treatment (metronomic), the sensitive cells stabilizes at a low level, while still oppressing resistant cells.

Figure 1 – Three treatment protocols are tested on a coculture of sensitive and resistant cells. Sensitive cells are represented in red and resistant cells in green.

this problem with mathematical modelling, in order to improve treatment protocols and even optimize them.

The modelling and design of new treatments for these experiments are presented through three different mathematical aspects, in the three following chapters. In Chap.2, we present an optimization of treatments based on the theory of optimal control of ODEs, and especially the Pontryagin Maximum Principle. Then in Chap.3, cells diffusion is taken into account, to investigate the emergence of resistant cells clusters in solid tumours. Finally, in Chap.4, we use the theoretical framework of Hamilton-Jacobi-Bellman equations to address viability challenges. Each part is independant of the other, and can be read separatedly.

The main results from these chapters are presented thereafter.

0.2 Optimization of chemotherapy via optimal control theory

Chap.2 is adapted from an article in the Journal of Theoretical Biology, published in 2017 [1]. It presents a mathematical model of M.Carré's experiment as a system of coupled ordinary differential equations with control:

$$\begin{cases} \frac{ds}{dt}(t) = \rho s(t)(1 - \frac{s(t)+mr(t)}{K}) - \alpha s(t)C(t) \\ \frac{dr}{dt}(t) = \rho r(t)(1 - \frac{s(t)+mr(t)}{K}) - \beta s(t)r(t). \end{cases} \tag{1}$$

Here, s denotes the number of sensitive cells, and r the number of resistant cells. They present a logistic growth behaviour, with a similar growth rate and a total population limited by the size of the Petri well K. Parameter $m > 1$ represents the fact that resistant cells are larger than sensitive cells. In the experiments, resistant cells suffer from the interaction with sensitive cells, which is modelled by the supplementary competition term $-\beta sr$. Finally, the treatment C, on which the experimentator has a direct control, only acts on sensitive cells. It is comprised between 0 and a maximal value $C_{\max}$, which represents the maximal dose of drug one can give to a patient without triggering dangerous secondary effects. Using this model, we want to design treatment protocols that reduce the tumour volume while preventing the emergence of a large resistant population. The control we have, C, only acts on one of the equations, and several phenomena are non linear, thus technics of mathematical control of linear systems will not be

possible. We can refer to [LS06] for the control of two populations with linear evolution. Two methods to design new treatment are here considered: one relying on phase plane analysis of the system, and one using the optimal control theory.

A phase plan analysis of (1) under constant treatment gives the following result:

Theorem 1. *Given an initial condition $(s_0, r_0) \in \mathbb{T}$, the system (1) under contant treatment $C(t) \equiv C$ will evolve to different values depending on the treatment value. Denoting $C_{metro} := \frac{K\beta}{\rho+K\beta}\frac{\rho}{\alpha}$, we have:*

- *if $C = 0$ then $(s,r)(t) \underset{t\to\infty}{\longrightarrow} (K, 0)$,*
- *if $0 < C < C_{metro}$ then, depending on (s_0, r_0), either $(s,r)(t) \underset{t\to\infty}{\longrightarrow} (K\frac{\rho-\alpha C}{\rho}, 0)$ or $(s,r)(t) \underset{t\to\infty}{\longrightarrow} (0, \frac{K}{m})$,*
- *if $C \geq C_{metro}$ then $(s,r)(t) \underset{t\to\infty}{\longrightarrow} (0, \frac{K}{m})$.*

Thanks to this result, a limit population $(s_l, r_l) = (\frac{K}{\rho+K\beta}, 0)$ is identified. It is the lower limit of attractive points for (1) under constant treatments with only sensitive cells. In other words, s_l is the smallest sensitive population for which one can design a treatment protocol such that the system (1) tends to $(s_l, 0)$ as $t \to +\infty$. I define an algorithm for such an adaptive protocol:

- *Initialization* $(s,r)(0)$ cells are implanted, $\lambda_0 = 1/2$
- *Loop for $i = 1$ to end of experiment*
  1. *If $r(t_i) < \frac{K}{m}(1 - \frac{s(t_i)}{K})$*, let the system evolve with no treatment, $C_i = 0$, and $\lambda_i = \frac{1}{2}$ for reinitialization.
  2. *If $r(t_i) \geq \frac{K}{m}(1 - \frac{s(t_i)}{K})$*, set $C_i = \lambda_i C_{\text{metro}}(1 - \frac{m}{K}r(t_i))$ and $\lambda_{i+1} = \frac{1+\lambda_i}{2}$.
- *End of experiment*

This algorithm brings the system closer and closer to $(s_l, 0)$, while never entering a basin of attraction of $(0, \frac{K}{m})$, which is a population with only resistant cells.

System (1) is controlled by the drug dosage $C(t)$, we thus can use the theory of optimal control of the ODEs on it. We define the following optimization problem:

Optimal Control Problem 1. *Given an initial condition (s_0, r_0), a maximal concentration of the treatment C_{max} and a time T of experiment, find a L^∞ function $C : [0, T] \to [0, C_{max}]$ that minimizes the following cost:*

$$L_2(T) := \tilde{\psi}(s(T), r(T)) + \int_0^T L^0(s(t), r(t))dt,$$

with $\tilde{\psi}$ the Mayer part of the cost, and L^0 the Lagrange part of it:

$$\tilde{\psi}(s,r) := s^2 + r^2, \quad L^0(s,r) := As^2 + Br^2.$$

The Lagrange cost allows us to consider the size of the tumour during the whole experiment. We chose a square cost in order to penalize high level populations. Applying the Pontryagin Maximum Principle, we obtain that:

Theorem 2. *The optimal treatment for Problem 1 is a piecewise continuous function C, with three possible values at each time point. Either:*

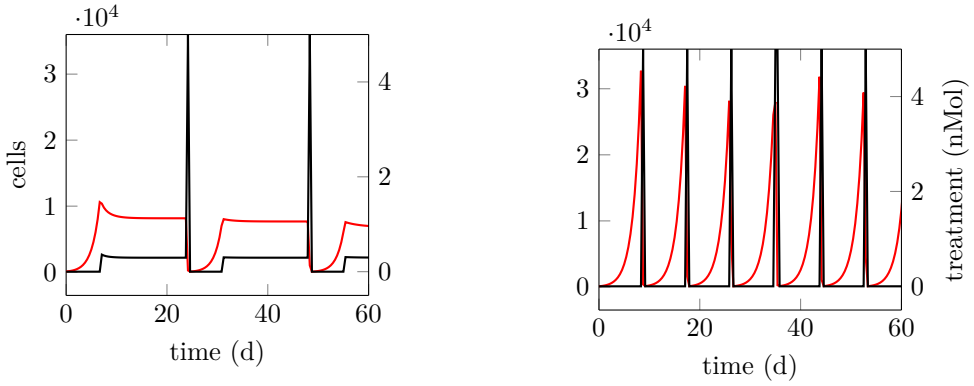

(a) A cycling treatment alterning rest, singular treatment and maximal treatment is determined to minimize the cost L_2.

(b) A cycling treatment alterning rest and maximal treatment is determined to minimize the cost L_2.

Figure 2 – Two protocols are tested for the same cost, with or without singular arc treatment. The total number of cells is represented in red, and the treatment concentration in black.

— *the control is maximal* $C = C_{max}$,
— *the control is minimal* $C = 0$,
— *the control is singular* $C = \frac{1}{\alpha s}\left(\frac{B}{A}r^2(\frac{\rho}{K}+\beta) + s\rho(1-\frac{s+2mr}{K})\right)$.
Moreover, the control is maximal at the end of the experiment: $C(T) = C_{max}$.

A singular arc of treatment corresponds in chemotherapy to a metronomic protocol, as it is a dose lower than the maximal one. This indicates that low dose chemotherapies are, for some situations, adequate to prevent resistance emergence.

However, Theorem 2 only states necessary conditions on the optimal control. We thus perform numerical simulations on periodic protocols, which suggest that for a long enough experiment, singular arcs represent a large part of optimal controls, as seen on Fig.2a. We compare it to a cycling protocol without singular arcs ($C(t) = 0$ or $C_{\max}$): the bang-bang cycle forces the tumour reach a size three times higher than with metronomic treatment, as seen on Fig.2b.

This first study gave encouraging results, as they hint on the usefulness of low-dose treatments to prevent the emergence of resistant lineages. To continue this work, the interactions between different drugs have to be taken into account. Indeed, chemotherapies usually consist of a mix of several molecules instead of only one, thus the emergence of multi-resistant lineages in this case have to be investigated.

In the following, I treat two independant extensions of this problem. In Chap.3, I examine the influence of cells diffusion on the emergence of resistant cells clusters. Indeed, the spatial repartition of cells was not taken into account in Chap.2, while this can lead to various behaviours. In another outlook, the theory of optimal control as it is presented here does not take into account uncertainties, and does not ensure that the tumour will remain small. To tackle these problems, in Chap.4, we study (1) in the theoretic framework of Hamilton-Jacobi-Bellman equations. This alllows us to define a new problem, maintaining the tumour size under a certain threshold, and to present numerical optimization methods.

0.3 Spreading of a system of competition-diffusion equations

We are now interested in a partial differential equations system. It is presented in Chap.3, which consists of an article [2]. The system is the following:

$$\begin{cases} \frac{ds}{dt}(x,t) = D\Delta s(x,t) + \rho s(x,t)(1 - \frac{s(x,t)+mr(x,t)}{K}) - \alpha s(x,t)C(t) \\ \frac{dr}{dt}(x,t) = \Delta r(x,t) + \rho r(x,t)(1 - \frac{s(x,t)+mr(x,t)}{K}) - \beta s(x,t)r(x,t). \end{cases} \tag{2}$$

We consider here constant treatments $C(t) \equiv C$, and will study this system for $(x,t) \in \mathbb{R} \times \mathbb{R}^+$. A renormalization of time, space and state variables, leads to the following system with $\gamma_0 = 1$:

$$\begin{cases} \partial_t s - \delta_0 \partial^2_{xx} s = s(\alpha_0 - s - \gamma_0 r) \\ \partial_t r - \partial^2_{xx} r = r(1 - \beta_0 s - r). \end{cases} \tag{3}$$

In the following, we study the little more general system in the following range of parameters: $1/\beta_0 < \alpha_0 < \gamma_0$. It corresponds, for the underlying ODE system, to the stability of only two points in the phase plane: $(s,r) = (\alpha_0, 0)$ and $(s,r) = (0,1)$. In the biological framework, it means that the cohabitation of the two species is unstable, but the extinction of one is a stable situation. Note that parameter α_0 represents the growth rate of s under treatment: increasing the dose of chemotherapy, all other things being equal, lowers the value of α_0.

We study there a spreading result: if initially s occupies the left half-line and is absent from $x > 0$, and r is present only on a compact set, then how will the system evolve?

This problem belongs to the field of spreading properties of reaction-diffusion and competition-diffusion equations. The fact that (3) is a coupled equations system, makes most theorems on single reaction-diffusion equations, as in [FM77] for example, unadapted. In a travelling waves framework, we would like to find a front that links the unstable point $(0,0)$ to a positive combination of s and r. However, numerical simulations suggested that for a range of parameters, the system does not evolve as a travelling wave but as a propagating terrace with two different speeds. The search for travelling waves solutions is thus not relevant in our case. In [GR16], a similar system is considered with mutations between s and r, which brings a supplementary linear term in the system of equations. This coupling is the cause of the apparition of a travelling wave. But in (3), the seggregation of the species causes this solution to vanish.

Two main results from the litterature are used in my study. The first one is the existence of travelling wave solutions of the Fisher-KPP equation, presented in [KPP37, Fis37]:

Let (D,ρ) be two positive parameters. For any $c \geq c^* = 2\sqrt{D\rho}$, there exist a unique (up to translation) solution $U \in C^2(\mathbb{R})$ of the equation:

$$\begin{cases} DU'' + cU' + U(\rho - U) = 0 \\ \lim_{\xi \to -\infty} U(\xi) = \rho \text{ and } \lim_{\xi \to +\infty} U(\xi) = 0. \end{cases} \tag{4}$$

If U is a solution of (4), then $u : (x,t) \mapsto U(x - ct)$ is a solution to $\partial_t u - D\partial^2_{xx} u = u(\rho - u)$. Moreover, a solution u of this PDE with Heavyside initial data $u(\cdot, 0) = \mathbf{1}_{x<0}$ spreads with speed c^* in the following sense: for any $c < c^*$, it satisfies $\lim_{t\to+\infty} \sup_{x<ct} |u(x,t) - 1| = 0$ and for any $c > c^*$, $\lim_{t\to+\infty} \sup_{x>ct} u(x,t) = 0$.

In the following, we will denote $c_S = 2\sqrt{\delta_0 \alpha_0}$ and $c_R = 2$; those are the minimal speeds of s and r respectively if the other species is absent.

The second result is the existence and unicity of a travelling wave solution for (3) linking the two stable states $(\alpha, 0)$ and $(0,1)$, which is proven in [KO95]:

Let $(\alpha, \beta, \gamma, \delta)$ be four positive parameters, such that $1/\beta < \alpha < \gamma$. Then there exists a unique speed $c \in (-2, 2\sqrt{\alpha\delta})$ such that the system

$$\begin{cases} \delta U'' + cU' + U(\alpha - U - \gamma V) = 0 \\ V'' + cV' + V(1 - \beta U - V) = 0 \\ \lim_{\xi \to -\infty} U(\xi) = \alpha \text{ and } \lim_{\xi \to +\infty} U(\xi) = 0 \\ \lim_{\xi \to -\infty} V(\xi) = 0 \text{ and } \lim_{\xi \to +\infty} V(\xi) = 1 \end{cases} \tag{5}$$

admits a solution $(U, V) \in C^2(\mathbb{R})$. Furthermore, this solution is unique up to translation, positive, U is decreasing and V is increasing. The speed c depends continuously on the parameters (α, β, γ), is increasing with respect to α and γ, and decreasing with respect to β.

For parameters $(\alpha, \beta, \gamma, \delta) = (\alpha_0, \beta_0, \gamma_0, \delta_0)$, we will note $c = c_{SR}$; it is the speed of the travelling wave linking the two stable states in (3).

I demonstrate in this study the following theorem:

Theorem 3. *Let (s, r) be a bounded solution of (3) with initial conditions:*

$$\begin{cases} s(x,0) = \phi(x) \text{ for } x < 0 \text{ with } 0 < \phi_m \leq \phi(x) \leq \phi_M < \alpha_0 \\ s(x,0) = 0 \text{ for } x \geq 0 \\ 1 > r(x,0) > 0 \text{ for } x < 0 \text{ and } r(x,0) = \underset{x \to -\infty}{O}(-xe^{\frac{1}{2}x}) \\ r(x,0) = 0 \text{ for } x \geq 0 \end{cases} \tag{6}$$

where the parameters $(\alpha_0, \beta_0, \gamma_0)$ satisfy the bistability criterium:

$$\frac{1}{\beta_0} < \alpha_0 < \gamma_0. \tag{7}$$

Then the following spreading results hold:

$$\forall\ c > \max(c_S, c_R), \lim_{t \to +\infty} \sup_{x > ct} |s(x,t)| + |r(x,t| = 0 \tag{8}$$

$$\forall\ c < c_{SR}, \lim_{t \to +\infty} \sup_{x < ct} |s(x,t) - \alpha_0| + |r(x,t)| = 0. \tag{9}$$

Suppose furthermore that $c_S < c_R$, then

$$\forall\ c_{SR} < c_1 < c_2 < c_R, \lim_{t \to +\infty} \sup_{c_1 t < x < c_2 t} |s(x,t)| + |r(x,t) - 1| = 0. \tag{10}$$

This result is illustrated with Fig.3.

In other words, the solution of (3) with these initial conditions forms a propagating terrace, linking the unstable state $(0, 0)$ to the stable state $(\alpha_0, 0)$ with an possible intermediary link to the other stable point $(0, 1)$. Two travelling fronts, a monostable and a bistable one, intervene in the construction of such a terrace.

The proof of this theorem relies on the following main lemma:

Lemma 1 (Comparison principle)**.** *Let (s_1, r_1) and (s_2, r_2) be such that for all $(x, t) \in D \times \mathbb{R}^+$ with $D \subseteq \mathbb{R}$, we have $0 \leq s_i(x,t) \leq \alpha_0$, $0 \leq r_i(x,t) \leq 1$ for $i = 1, 2$, such that*

$$\begin{cases} \partial_t s_1 - \delta_0 \partial^2_{xx} s_1 - s_1(\alpha_0 - s_1 - \gamma_0 r_1) \leq 0 \\ \partial_t r_1 - \partial^2_{xx} r_1 - r_1(1 - \beta_0 s_1 - r_1) \geq 0 \end{cases} \quad \text{and} \quad \begin{cases} \partial_t s_2 - \delta_0 \partial^2_{xx} s_2 - s_2(\alpha_0 - s_2 - \gamma_0 r_2) \geq 0 \\ \partial_t r_2 - \partial^2_{xx} r_2 - r_2(1 - \beta_0 s_2 - r_2) \leq 0 \end{cases}$$

and such that for all $x \in D$,

$$s_1(x,0) \leq s_2(x,0) \text{ and } r_1(x,0) \geq r_2(x,0)$$

and for all $x \in \partial D$ *and* $t \geq 0$,

$$s_1(x,t) \leq s_2(x,t) \text{ and } r_1(x,t) \geq r_2(x,t).$$

Then for all $t \geq 0$ *and for all* $x \in \mathbb{R}$,

$$s_1(x,t) \leq s_2(x,t) \text{ and } r_1(x,t) \geq r_2(x,t).$$

Note that, with this lemma, we have to construct functions (s,r) such that one is a sub-solution to its equation in (3), while the other is a super-solution.

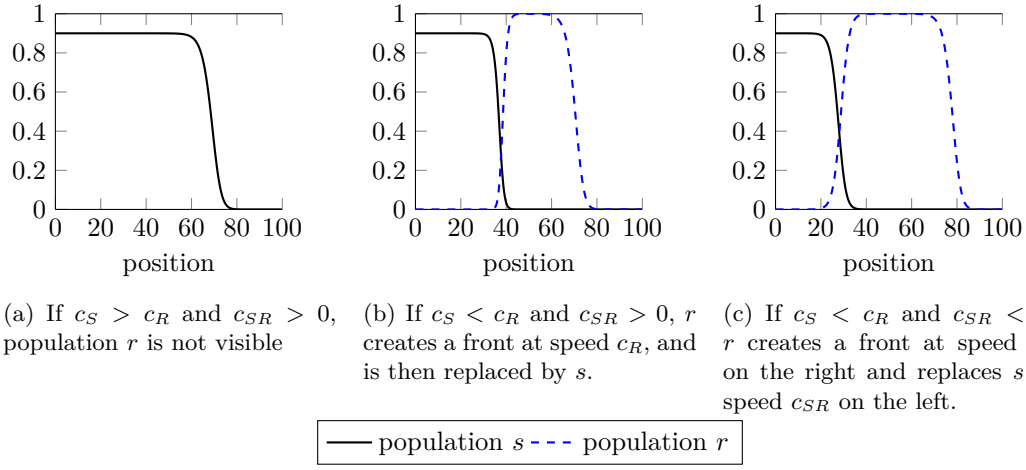

(a) If $c_S > c_R$ and $c_{SR} > 0$, population r is not visible

(b) If $c_S < c_R$ and $c_{SR} > 0$, r creates a front at speed c_R, and is then replaced by s.

(c) If $c_S < c_R$ and $c_{SR} < 0$, r creates a front at speed c_R on the right and replaces s at speed c_{SR} on the left.

Figure 3 – Numerical simulations of the system for different values of the parameters: the global behaviour depends on the comparison between c_S and c_R, and on the sign of c_{SR}. Species s is represented in black and species r is represented in dashed blue.

We demonstrate Theorem 3.1 by successive comparisons with well chosen sub-supersolutions to (3).

First, (8) is easily demonstrated by a comparison between (s,r) the solution to (3) and $(U_S, 0)$ or $(0, U_R)$, where U_S and U_R are the Fisher-KPP travelling fronts defined by (4) with adequate parameters, corresponding to the situation with only one species present.

Then, if $c_S < c_R$, one constructs successive sub-solutions to the equation in r to show that r can grow oustide of reach of s, as in [DGM]. In other words:

Lemma 2. *Let* c_1, c_2 *be two speeds such that* $c_S < c_1 < c_2 < c_R$. *Then*

$$\lim_{t \to +\infty} \sup_{c_1 t < x < c_2 t} |s(x,t)| + |r(x,t) - 1| = 0.$$

I then construct well-chosen sub-super-solutions of (3) to demonstrate (9). These functions are constructed based on the travelling front solution of:

$$\begin{cases} \partial_t s - \delta_0 \partial^2_{xx} s = s(\underline{\alpha} - s - \gamma_0 r) \\ \partial_t r - \partial^2_{xx} r = r(1 - \beta_0 s - r) \end{cases} \tag{11}$$

which is linking the stables states $(\underline{\alpha}, 0)$ and $(0, 1)$, where $\alpha_0 > \underline{\alpha}$. The method is adapted from [FM77], which was done for a single reaction-diffusion equation.

Finally, I conclude by demontrating (10) with well-chosen super-sub-solutions of (3), contructed with the travelling front solution of

$$\begin{cases} \partial_t s - \delta_0 \partial^2_{xx} s = s(\overline{\alpha} - s - \gamma_0 r) \\ \partial_t r - \partial^2_{xx} r = r(\theta - \beta_0 s - r) \end{cases} \tag{12}$$

which links the stables states $(\overline{\alpha}, 0)$ and $(0, \theta)$, where $\alpha_0 < \overline{\alpha}$ and $\theta < 1$. This result shows that s propagates at most at speed c_{SR} if there are "enough" r (more than θ for any $0 < \theta < 1$) somewhere on the right. This presence was proven in Lemma 2. Thus (10) is demonstrated.

Let us focus on the fact that if $\alpha_0 < \frac{1}{\delta_0}$, then r propagates at its Fisher-KPP speed outside of s reach. In other words, going back to a biological interpretation, if the treatment dose is weak so that $\alpha_0 > \frac{1}{\delta_0}$, then the tumour growth speed is $c_S = 2\sqrt{\alpha_0 \delta_0}$. But if the treatment dose is augmented so that $\alpha_0 < \frac{1}{\delta_0}$, then resistant cells create a growing ring encapsulating sensitive cells, and the tumour growth speed is $c_R = 2$. Thus, when designing new treatments, the motility of cells should be taken into account, to avoid the formation of resistant cells growing clusters. This results is applied in our case to tumour growth dynamics, but it falls into a more general class of applications to populations dynamics.

This result supposes chemotherapy is constant in time and uniform in space. However, treatment protocols are often periodic in time, and the presence of layers of cancerous cells could prevent the diffusion of drug, thus reducing its efficiency on cells in the tumour core. These two phenomena could be taken into account in future studies. Finally, this result was demonstrated for a class of initial conditions with s already present on the far left. An initial condition concentrated on a compact set would be more relevant biologically. Finally, the relevance of a Laplacian to model cells diffusion should be addressed, and considering crossed diffusion would enhance the accuracy of the model.

0.4 Dynamic programming

This work is a collaboration with Hasnaa Zidani.

In Chap.2, we developped treatment protocols based on optimal control theory. This presents several limitations for medical applications. First, the control and problem are defined on a finite time experiment. Thus, we are not able with this result to ensure the resistant population will not emerge after the end of the measurements. Second, biological systems are heavily subject to uncertainties, while we assumed an exact knowledge of parameters and states of the tumour. Finally, we chose to minimize a Lagrangian cost in Problem1, while a more natural idea would be to limit the maximal size of the tumour during experiment.

For all these reasons, we chose to study in Chap.4 our problem in the framework of Hamilton-Jacobi-Bellman equations and their numerical resolution, in which the different problems listed above can be adressed.

We define three models of cancer growth, based on the experiments of M.Carré presented in Chap.1. We will present here the results for the first model, and the other models have similar results. We consider the following system:

$$\begin{cases} \frac{ds}{dt}(t) = \rho s(t)(1 - \frac{s(t)+mr(t)}{K}) - \alpha s(t)C(t) \\ \frac{dr}{dt}(t) = \rho r(t)(1 - \frac{s(t)+mr(t)}{K}) - \beta s(t)r(t). \end{cases}$$

We note that it is the same model as (1). In the following, for any $x = (s, r) \in \mathbb{R}^2$ and any $C : \mathbb{R}^+ \to [0, C_{\max}]$ measurable, we will note y_x^C the solution of (1) with initial condition $y_x^C(0) = x$. We will also note $\mathcal{A}$ the set of measurable functions $C : \mathbb{R}^+ \to [0, C_{\max}]$. Finally, (1) can be re-written in a more compact way:

$$\frac{dy}{dt}(t) = f_0(y(t)) + f_1(y(t), C(t)).$$

We define two control problems on this system. The first one is a viability problem:

Problem 1 (Viability)**.** *Let $Q > 0$ be such that $Q < K$. Given $x_0 \in \mathbb{R}^2$, does there exist a control $C \in \mathcal{A}$ such that:*

$$\forall t \geq 0,\ \phi(y_x^C(t)) \leq Q$$

where $\phi(s, r) = s + mr$?

In other words, given a certain threshold Q, is it possible to maintain the tumour size $s + mr$ under this value for any time? This is an infinite time problem with constraints. The consideration of constraints is presented in [ABZ13], where the cost of a trajectory is minimized under some constraints on state variables. We adapted their proofs for our problem, where no cost is defined, but only state constraints are taken into account. In the following, we note $\mathcal{N}_{\mathbb{T}_Q}$ the viability set, *i.e.* the set of points that solve the viability problem.

The second problem is a reachability problem:

Problem 2 (Reachability)**.** *Let $Q > 0$ be such that $Q \leq K$, and let $T_0 > 0$. Does there exists a control $C \in \mathcal{A}$ such that:*

$$\forall t \geq T_0,\ \phi(y_x^C(t)) \leq Q$$

where $\phi(s, r) = s + mr$? And amongst such controls, find a control minimizing the entry time $t_{in}^C(x)$ defined by:

$$\forall x \in \mathbb{R}^2,\ \forall C \in \mathcal{A},\ t_{in}^C(x) = \inf\{t_0 \geq 0 / \forall t \geq t_0,\ \phi(y_x^C(t)) \leq Q\}.$$

For any $x \in \mathbb{R}^2$, we will note $t_{in}(x)$ this minimal value.

In other words, what are the initial tumours eligible for chemotherapy such that, after an initial treatment of duration no longer than T_0, we can ensure a tumor size less than the threshold Q? And for such eligible tumours, what is the quickest initial treatment? We note that if a point x is eligible in this problem, for any $t > t_{in}(x)$, following an optimal trajectory C^*, we have that $y_x^{C^*}(t) \in \mathcal{N}_{\mathbb{T}_Q}$. Thus the determination of $\mathcal{N}_{\mathbb{T}_Q}$ is essential to the resolution of Problem 2 ; this is a new outlook regarding dynamic programming theory.

For Problem 1, we define the following value function:

$$\forall x \in \mathbb{R}^2,\ V_Q(x) = \inf_{C \in \mathcal{A}} \max_{t \geq 0} e^{-\lambda t} g_Q(y_x^C(t))$$

where $g_Q((s,r)) = \max(-s, -r, s + mr - Q)$ for any $(s,r) \in \mathbb{R}^2$, and $\lambda > 0$ is "large enough". The determination of the value of V_Q solves the viability problem, because:

$$\forall x \in \mathbb{R}^2,\ \left(\exists C \in \mathcal{A} / \forall t \geq 0,\ \phi(y_x^C(t)) \leq 0\right) \iff V_Q(x) \leq 0.$$

The value function at point x represents the "best" outcome we can achieve for this point by control. The term $e^{-\lambda t}$ smoothes the value function, but changing $\lambda > 0$ does not change $\mathcal{N}_{\mathbb{T}_Q}$.

With small variations around a point x, we are able to show that the value function satisfies the following Hamilton-Jacobi-Bellman equation with obstacle:

$$0 = \min\left(V_Q(x) - g_Q(x), \lambda V_Q(x) + H(x, \nabla V_Q(x))\right) \tag{13}$$

where $H((s,r),p) = -f_0(s,r) \cdot p + \max(0, \alpha s C_{max} p_1)$ is the hamiltonian of this problem. The obstacle is taken into account through the term $V_Q - g_Q$. A comparison lemma allows us to demonstrate that this equation admits at most one solution.

In Problem 2, we also rely on the determination of a certain value function. Define:

$$\forall x \in \mathbb{R}^2,\ \forall t \in [0, T_0],\ W(x,t) := \min_{C \in \mathcal{A}} d_Q(y_x^C(t))$$

where d_Q is the signed distance to $\mathcal{N}_{\mathbb{T}_Q}$. Note that we thus need to determine the value function of the viability problem V_Q to define W. An illustration of $\mathcal{N}_{\mathbb{T}_Q}$ and some trajectories are shown on FIG.4.

Then, we have the following equivalence:

$$\forall x \in \mathbb{R}^2,\ \left(\exists C \in \mathcal{A} / \forall t \geq T_0,\ \phi(y_x^C(t)) \leq 0\right) \iff W(x, T_0) \leq 0.$$

Given this mapping, we can express the minimal time of entry function t_{in}:

$$\forall x \in \mathbb{R}^2,\ t_{in}(x) = \min\{t / W(t,x) \leq 0\}.$$

For any $x \in \mathbb{R}^2$, $t_{in}(x)$ is then the smallest time of treatment needed to enter $\mathcal{N}_{\mathbb{T}_Q}$. This way, after t_{in} we can ensure a tumour size smaller than the threshold Q.

We showed that the determination of W solves the reachability problem. By considering small variations around a point (x,t), we determine a Hamilton-Jacobi-Bellman that is satisfied by W:

$$0 = \partial_t W(x,t) + H(x, \nabla W(x,t)) \tag{14}$$

where H is the same hamiltonian as in the viability problem. Moreover, $W(x,0) = d_Q(x)$ for any $x \in \mathbb{R}^2$. We can demonstrate that (14) has at most one solution for initial condition $W(x,0) = d_Q(x)$, thanks to a comparison lemma.

The numerical determination of V_Q and W are thus crucial to solve Problems 1 and 2. We describe several algorithms serving this purpose. The value function V_Q is there determined by solving the Hamilton-Jacobi-Bellman equation, either by a fixed point algorithm, of by a Howard's algorithm. The value function W can be determined using the dynamic programming principle, or by solving (14) as a PDE.

Suppose functions V_Q and W are numerically constructed. Given a certain initial point x, one can determine the optimal control bringing the tumour size under the threshold value in a minimal time by following the controls minimizing W. Furthermore, for any $x \in \mathcal{N}_{\mathbb{T}_Q}$, one can determine a control maintaining the system in the viability set by following, for as long as asked, the trajectories minimizing V_Q.

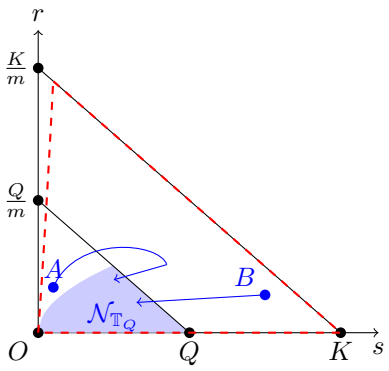

Figure 4 – The set $\mathcal{N}_{\mathbb{T}_Q}$ is determined by the calculation of V_Q. Then, the set of points from which $\mathcal{N}_{\mathbb{T}_Q}$ is reachable (inside red dashed line) is determined with W. Point A satisfies $\phi(A) \leq Q$, but all trajectories starting from it exit the triangle $\{x/\,\phi(x) \leq Q\}$. Thus A is not in $\mathcal{N}_{\mathbb{T}_Q}$. A trajectory starting from A and entering $\mathcal{N}_{\mathbb{T}_Q}$ is represented. Point B is not in the triangle $\{x/\,\phi(x) \leq Q\}$, but a trajectory starting from it can reach $\mathcal{N}_{\mathbb{T}_Q}$ quicker than T_0.

As we remarked at the beginning of this part, biological systems are subject to several uncertainties. We present here a theoretical framework in which one can express uncertainties on some parameters. We suppose here that parameter α can vary during the experiment ; the model is now:

$$\begin{cases} \frac{ds}{dt}(t) = \rho s(t)(1 - \frac{s(t)+mr(t)}{K}) - \alpha(t)s(t)C(t) \\ \frac{dr}{dt}(t) = \rho r(t)(1 - \frac{s(t)+mr(t)}{K}) - \beta s(t)r(t) \end{cases} \tag{15}$$

where for any $t \geq 0$, $\alpha(t) \in [\alpha_{min}, \alpha_{max}]$. In other words, the efficiency of the drug can vary during the experiment between two known values. We re-write (15) in a more compact way:

$$\frac{dy}{dt}(t) = f^{unc}(y, \alpha, C)$$

and we note $y_x^{\alpha,C}$ the solution of (15) under control C, efficiency α and initial condition $y_x^{\alpha,C}(0) = x$.

We define $\mathcal{B}$ the set of measurable functions $\alpha : \mathbb{R}^+ \to [\alpha_{min}, \alpha_{max}]$, and $\mathcal{AS}$ the set of non-anticipative strategies:

$$\mathcal{AS} := \Big\{ C : \mathcal{B} \to \mathcal{A} \,/\, \forall (\alpha, \alpha') \in \mathcal{B} \text{ and } \forall t \leq 0,$$
$$\big(\forall \tau \in [0,t],\, \alpha(\tau) = \alpha'(\tau)\big) \implies \big(\forall \tau \in [0,t],\, C[\alpha](\tau) = C[\alpha'](\tau)\big) \Big\}.$$

The viability problem with uncertainties is now the following:

Problem 3 (Optimal strategy)**.** *Given a threshold $Q > 0$, find the set of points $\mathcal{NS}_{\mathbb{T}_Q}$ such that for any point $x \in \mathcal{NS}_{\mathbb{T}_Q}$, there exists a strategy $C[\cdot] \in \mathcal{AS}$ such that:*

$$\forall \alpha \in \mathcal{B},\, \forall t \geq 0,\, \phi(y_x^{\alpha, C[\alpha]}(t)) \leq Q$$

where $\phi((s,r)) = s + mr$.

To solve this problem, we can define a value function adapted to the presence of uncertainties:

$$V_Q^{unc}(x) = \min_{C\in\mathcal{AS}} \max_{\alpha\in\mathcal{B}} \max_{t\geq 0} \left(e^{-\lambda t} g_Q(y_x^{\alpha,C[\alpha]}(t)) \right).$$

The value function chooses the best answer (the best treatment) to the worst case (the worst α possible). This value function satisfies a Hamilton-Jacobi-Bellman equation:

$$\min(V_Q^{unc}(x) - g_Q(x), \lambda V_Q^{unc}(x) + H^{unc}(x, \nabla V_Q^{unc}(x)) = 0 \tag{16}$$

where

$$H^{unc}(x,p) = \max_{C\in[0,C_{max}]} \min_{\alpha\in[\alpha_{min},\alpha_{max}]} (-f^{unc}(x,C,\alpha)\cdot p).$$

We are then able to derive similar numerical algorithm for the determination of V_Q^{unc}, and reconstruct trajectories from this mapping.

In conclusion, we develop in Chapter 4 a theoretical framework and numerical methods that address some biological problems that were not taken into account in Chap.2. With this, we are able to construct a tool of treatment optimization for medical use. It indicates for an initial tumour, if it is eligible for chemotherapy, *i.e.* if chemotherapy can be used to reduce it in a reasonnable time, or if the tumour should first be treated with a different drug, or by another method as surgery or radiotherapy. If the tumour is identified as eligible for our chemotherapy, it then designs a treatment protocol adapted to its size and composition. If at some point, unaccounted perturbations make the system change its trajectory, we are able to design a new protocol quickly, because the determination of V_Q and W is performed in advance for all positions.

The use of dynamic programming can offer new perspectives of optimization. For example, it is possible to take into account two or more objectives simultaneously: the different optimization problems are defined and solved independantly, and then a comparison usig Pareto fronts can be performed to choose a compromise between those objectives. For example, we considered with Problem 2 the minimization of the initial treatment time. But medical applications also take into account the immune system, which is impacted by chemotherapies. The secondary objective is then to maximize the immune system during the initial treatment. A compromize solution between these two objectives can be drawn from their study under dynamic programming and a Pareto front comparison.

Conclusion and perspectives

We study in different theoretical framework experiments on heterogeneous tuours. In Chapter 2, we design two treatment protocols that control the tumour size, while reducing the part of resistant cells. The treatment designed by optimal control theory has been tested *in vitro* by M.Bodarenko, PhD student in the team of M.Carré. These experiments showed that the model (1) did not take into account some important phenomena: especially, the drug is less efficient if too many sensitive cells are present in the Petri well. A new model for these experiments should thus be designed.

To further investigate the role of metronomic chemotherapies on resistance emergence, M.Carré designed two new sets of experiments. In a first series of experiments, a heterogeneous *in vitro* tumour shaped in a spheroid is implanted in a synthetic skin. This experiment aims at studying the interaction between healthy and cancerous cells in a Petri dish, and their response to treatment. Mathematical modelling of this setting would then take into account a third type of cells, the healthy ones, and treatments should maintain enough healthy tissues. This objective can be taken into account with optimal control theory, by setting a high cost to treatments that kill too

many healthy cells, and in dynamic programming by defining a constraint: a certain number of healthy cells should always be present. The progression of the tumour through this healthy tissue could also be investigated with partial differential equations, to determine the driving forces in its growth rate. In a second series of experiments, heterogeneous tumours are implanted in mice and resected after treatment. This way, the tumour size can be estimated during the experiment, and its composition is measured at the end of it. More complex interactions intervene in this experiment, like the presence of the immune system or the possibility for the tumour to form metastases. These mechanisms can be taken into account mathematically, for example using known models of immune therapies and metastases formation.

Chapter 1

Modélisation pour le traitement des cancers

In this chapter, we present the biological context of this thesis. We are working on chemotherapy protocols for cancer treatments. It is known that cancers often become resistant to the first drug used during the treatment. It is thus important when designing protocols to take this phenomenon into account, so that the emergence of resistance is delayed or even avoided. We describe biological experiments realized by M.Carré, that investigate the influence of low-dose treatments on heterogeneous tumours to prevent resistance emergence.

This chapter details important concepts on cancer treatments and resistance to chemotherapy, and presents a bibliography search on mathematical modelling for cancer studies. However, the concepts and definitions that are useful to this thesis are recalled in each chapter when needed.

Le cancer est actuellement la première cause de décès au niveau français [dC16]. Dû au vieillissement et à la croissance de la population, l'INCa (Institut National du Cancer) prévoit une augmentation du nombre total de cancers pour les années à venir, malgré la diminution de son taux d'incidence et de son taux de mortalité. C'est pourquoi la prévention, la détection et le traitement du cancer sont aujourd'hui des objectifs majeurs de santé publique, mobilisant la recherche à plusieurs niveaux.

Nous allons nous intéresser en particulier à certaines façons d'améliorer les traitements. La survie des patients, mais aussi leur qualité de vie durant leur maladie peuvent être grandement améliorées par l'élaboration de protocoles efficaces. Les différents moyens mis à disposition des médecins, s'il ont déjà réussi à diminuer le taux de mortalité des patients, doivent être encore perfectionnés, afin de donner une meilleure offre de soins. Les mécanismes déclenchant, maintenant et faisant croître les tumeurs sont étudiés afin de comprendre comment combattre le cancer, et comment limiter ses effets sur l'organisme.

1.1 Cellules cancéreuses : quelques caractéristiques

Nous allons dans cette partie décrire certaines caractéristiques principales des cellules cancéreuses ; la recherche de la cause de leur création est au-delà de notre sujet.

Les cellules cancéreuses partagent généralement trois caractéristiques : elles ne sont pas capables d'effectuer leur fonction primale, elles se divisent de manière incontrôlée et elles ne subissent que peu ou pas d'apoptose. D'autres effets résumés en Fig.1.2 sont importants, mais n'entrent pas dans le cadre de notre étude.

La désorganisation des tissus est l'indication la plus évidente de la présence de tumeurs [Wei13]. Des mutations, quelles que soient leur origine, permettent à la cellule de se dé-différencier partiellement ; la cellule n'est plus capable d'assurer ses fonctions normalement, et notamment ne s'organise plus comme les tissus sains environnants. On classe alors ces groupements de cellules non fonctionnelles en deux catégories générales : celles formant des tumeurs bénignes, et celles formant des tumeurs malignes. Les tumeurs bénignes restent séparées du tissu sain, et même si elles ne participent plus à l'activité normale de l'organe où elles se trouvent, elles n'empêchent pas en général le fonctionnement des autres cellules. Les tumeur malignes, en revanche, sont capables d'envahir les tissus avoisinants, créant de graves complications. Deux exemples de cellules tumorales présentes dans des tissus sains sont présentés en Fig.1.1.

Les cellules cancéreuses ont aussi la faculté de se diviser sans que les autres cellules puissent limiter leur rythme de croissance. En effet, dans les tissus sains, les cellules émettent des protéines afin de communiquer entre elles, et réguler leur nombre et leur rythme de division. Les cellules cancéreuses quant à elles, sont capables d'ignorer de tels signaux, et même d'émettre des protéines stimulant la division cellulaire des autres cellules de même type qu'elles [CD91]. La croissance tumorale n'est donc pas régulée par les phénomènes normaux dus aux autres cellules. De plus, les cellules cancéreuses dans la plupart des cas ne subissent pas la sénescence. Ce phénomène est observable dans les cellules normales du corps humain : pour une cellules donnée, seule une dizaine de divisions sont possibles au cours de sa vie ; la cellule entre ensuite dans un état dit de sénescence, où elle est active mais ne se divise plus [SPSW91]. Les cellules cancéreuses, pour leur part, ont accumulé des mutations modifiant leur expression de certaines protéines, retardant leur entrée en sénescence. Elles sont donc capables de se diviser bien plus de fois, jusqu'à 50 ou 60 fois.

Enfin, les cellules tumorales présentent des mécanismes leur permettant de ne pas mourir. Après un certain nombre de divisions, une cellule normale entre en apoptose, un processus de mort programmée. Les cellules tumorales échappent à cette mort cellulaire. Nous renvoyons à [Wei13] pour une description des mécanismes impliqués.

Dans cette thèse, nous nous intéressons aux cellules cancéreuses qui forment une tumeur solide compacte, bien différente du reste des tissus. De nombreuses études mathématiques se sont intéressées à la modélisation de la croissance tumorale. Suivant des études de dynamique des populations, [Lai64] considère des modèles de croissance de type Gompertz pour une tumeur solide. Ce modèle donne des résultats similaires à une modélisation logistique telle que présentée dans [VA82]. Les modèles logistiques sont plus appropriés à la description des petites tumeurs ; puisque nous étudions dans cette thèse des cancers en stade précoce, nous utiliserons cette modélisation. Les cellules cancéreuses peuvent entrer dans une phase de quiescence, où elles consomment moins de nutriments et ne se divisent pas, ce qui a une forte influence sur la croissance tumorale, comme présenté dans [GW89, Fri04]. Cette mise en pause est souvent due à un manque de nutriments. Nous nous intéressons à des expériences *in vitro* où les cellules sont continuellement en présence de nutriments, nous ne prendrons donc pas en compte cette hypothèse. Nous référons à [BD09] pour une revue de la modélisation de la croissance tumorale, présentant différents types de modélisations mathématiques, continue avec des EDO et EDP, ou

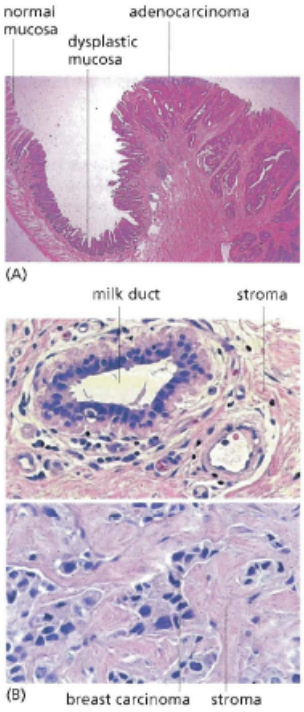

FIGURE 1.1 – Deux exemples de tissus contenant des cellules tumorales : dans (A), des cellules d'intestin sont organisées dans la gauche de la coupe, dérangées (en état dysplasique) au milieu et tout à fait tumorales (un adénocarcinome) sur la droite. Dans (B), le tissu mammaire sain en haut forme des canaux galactophores, entourés de tissu normal (*stroma*). En bas, les cellules des canaux ont perdu leurs fonctionnalité, présentent un noyau plus gros et désorganisent le tissu environnant.

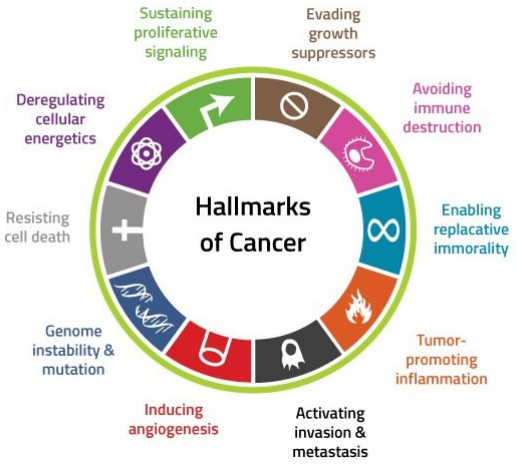

FIGURE 1.2 – Représentation synthétique des principales caractéristiques des cellules cancéreuses. Seuls certains mécanismes sont décrits dans cette thèse.

discrète avec des modèles orientés agents (*agent-based*). Dans notre travail, nous étudierons des modèles continus de croissance tumorale, utilisant des EDO ou des EDP.

Lors de sa croissance, cette tumeur initiale peut essaimer au travers des vaisseaux sanguins, et créer des tumeurs secondaires plus petites à d'autres endroits du corps humain. On parle alors de métastases. Ces tumeurs s'installant dans des organes différents de celui d'origine, elles sont rarement efficaces dans leur croissance, car peu adaptées aux nouvelles conditions. Toutefois, lorsque ces cellules réussissent à s'implanter et à proliférer, elles sont la cause d'un déréglement général de l'organe touché, et de graves complications se développent.

La modélisation de la création et croissance de métastases aide à adapter les traitements, afin d'éviter ou réduire l'essaimage de la tumeur. Ainsi, [BBHV09] développe un modèle EDP de croissance tumorale avec métastases qui pourra servir, une fois calibré, à prédire le nombre et la taille des métastases présents dans un patient. Il valide par ses résultats certaines hypothèses biologiques utilisées pour sa construction, et grâce à des résultats théoriques de convergence, peut être approché par un schéma numérique de suivi des caractéristiques. Cette idée est reprise dans [BTM$^+$16], où des données de patients sont utilisées pour prédire, chez d'autres malades, l'apparition de métastases. La théorie des jeux est utilisée dans [CBVG15] pour proposer des protocoles de traitement innovants. Ces traitements tirent parti du fait que les métastases, situées dans des organes différents de la source de la tumeur primaire (voir FIG.1.3), sont moins performantes que les tissus environnants car moins bien adaptés, ce qui les rend vulnérables à des traitements spécifiques. En un dernier exemple, [Pan96] explique l'apparition de métastases par l'utilisation de chimiothérapies pulsées, et propose des conditions sur les protocoles pour réduire ce phénomène.

Notre travail ne prend pas en compte la création de métastases. Ce phénomène étant très important dans le degré de gravité du cancer, il serait intéressant de considérer dans une nouvelle étude la capacité à essaimer d'une tumeur.

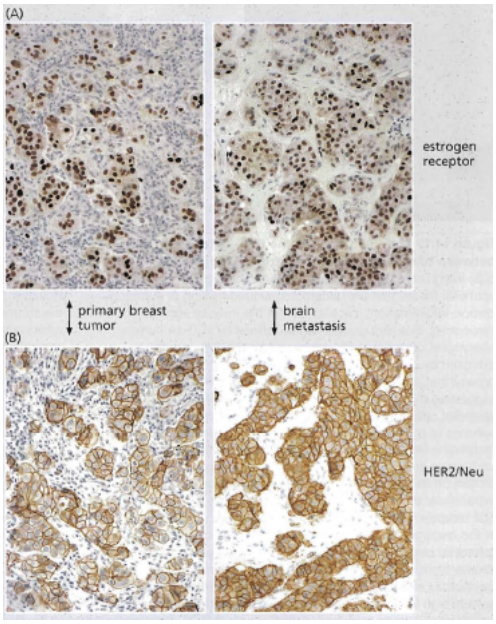

FIGURE 1.3 – Des métastases sont observées dans le cerveau d'un patient, originellement atteint d'un cancer du sein. Les cellules cancéreuses du sein sont observées à gauche, celles dans le cerveau à droite. (A) Un marquage utilisant un récepteur anti-oestrogènes et (B) un autre marqueur spécifique des cellules du sein, HER2/Neu, révèlent la nature semblable des deux amas de cellules cancéreuses.

1.2 Du laboratoire au patient

Le développement de traitements pour traiter une maladie, et le cancer en particulier, se fait en plusieurs phases.

Tout d'abord, l'étude des cellules cancéreuses doit permettre d'identifier des cibles thérapeutiques, comme une voie métabolique ou des marqueurs spécifiques, qui puissent être utilisées pour développer de nouveaux traitements. Les molécules choisies sont ensuite testées *in vitro* pour vérifier leur efficacité et leur spécificité, puis *in vivo* sur des animaux de laboratoire. Cette phase doit déterminer la toxicité annexe du médicament, c'est à dire les organes touchés, et si elle est toujours efficace dans un organisme vivant.

Ces travaux sont regroupés dans l'appellation d'essais précliniques. Ils sont suivis par les essais cliniques proprement dits, qui sont eux-même divisés en trois phases.

La phase I s'attache à déterminer la toxicité du médicament et sa pharmacocinétique pour une personne réelle. Elle est réalisée sur des volontaires sains, et parfois proposée à des patients en phase terminale de leur cancer, quand les traitements classiques ont déjà échoué. Différentes doses du médicament sont testées sur les membres de l'expérience, d'un nombre d'environ 20 à 80 participants.

Les phases II et III d'essai clinique se déroulent, quant à elles, avec des patient souffrant effectivement du cancer ciblé. La phase II détermine l'efficacité du traitement, sur une cohorte restreinte. La phase III, enfin, étudie le traitement à proprement parler sur une grande population de patients, comparant l'efficacité de la molécule aux traitements convetionnels. Ces phases de test sont indispensables à l'élaboration d'un nouveau traitement, mais coûtent généralement très cher aux laboratoires les entreprenant. En effet, la phase III d'essais cliniques doit se dérouler sur plusieurs années, et sur plusieurs centaines de patients. C'est pourquoi elle n'est envisagée que si les phases précédentes ont prouvé l'efficacité de la molécule. La modélisation mathématique pourrait permettre d'accélérer ce processus, en simulant la réponse des patients à différents rythmes et doses de traitements par exemple.

Grâce à ces études, de nombreux types de traitements ont pu être créés pour attaquer les tumeurs.

1.3 Traitements des cancers : quelle place pour la modélisation mathématique ?

Les cancers sont traités par différentes voies, dépendant de leur nature et de leur stade d'avancement. Trois grands types de traitements se différencient : la chirurgie, la radiothérapie et les traitements systémiques (utilisation de médicaments). Dans la plupart des cas, les patients passent par plusieurs phases de traitement, et reçoivent éventuellement des séances de chacun de ces types. La chirurgie et la radiothérapie sont ici brièvement présentées, mais notre travail étant plus axé sur la chimiothérapie, nous détaillerons ce sujet plus en profondeur.

1.3.1 Traitements localisés

La chirurgie était jusqu'à récemment le seul traitement des tumeurs cancéreuses. Elle a pour objectif de retirer la tumeur, certains tissus abîmés et si possible les métastases détectées. Elle est réalisée sur les tumeurs découvertes à un stade précoce, et très localisées. Parfois, elle n'est pas possible, notamment quand la tumeur se trouve trop près d'un organe essentiel, comme le cœur. Selon l'organe visé, ces opérations peuvent être très lourdes pour le patient, et très dangereuses. De plus, elles sont inefficaces contre les tumeurs déjà métastasées, car de nombreux foyers de

métastases restent invisibles à l'opérateur. Afin d'augmenter ses effets, la chirurgie est rarement pratiquée seule, mais généralement en complément d'autres traitements, comme une thérapie chimique. Dans tous les cas, le patient doit être suivi longtemps après l'opération.

Un autre traitement local de la tumeur possible est la radiothérapie. L'idée est de soumettre les cellules cancéreuses à un fort rayonnement X, ce qui les détruit. Si la tumeur se trouve proche de la surface de la peau, les rayons peuvent y être directement dirigés. Sinon, il est possible d'utiliser plusieurs sources de rayons (radiothérapie conformationnelle 3D) pour atteindre une tumeur plus profonde : chaque faisceau est insuffisamment puissant individuellement pour tuer les cellules, mais s'ils se croisent à un endroit, suffisamment d'énergie est délivrée pour impacter les tissus visés. Il est donc très important de pouvoir situer la tumeur avec précision, et évaluer l'impact des rayons sur les tissus sains. De plus, cette méthode requiert, pour la majorité du matériel actuellement en utilisation en hôpital, une parfaite immobilité du patient : une tumeur placée proche des poumons est difficile à traiter dans ces conditions.

La modélisation mathématique, en utilisant des modèles physiques, permet d'améliorer et rednre plus précises ces thérapies. Par exemple [ECH10] décrit l'action d'une radiothérapie sur des tissus sains et cancéreux, proposant un modèle réduisant la masse tumorale. Dans un cadre plus précis, [UMK$^+$14, UMK$^+$14] utilisent un modèle de croissance tumorale pour déterminer avec précision la zone à irradier et la dose à administrer lors d'une radiothérapie. En effet, seule une partie des tissus cancéreux sont détectables lors d'un scanner, les médecins choisissent donc souvent de traiter les tissus autour de la zone repérée. La modélisation mathématique et les simulations numériques permettent alors de prévoir quels sont les zones réellement à risque, celles qu'il faut donc irradier. Notre travail dans cette thèse vise les mêmes types d'objectifs, c'est à dire optimiser un traitement déjà existant, mais dans le cadre des chimiothérapies.

L'opération de radiothérapie peut être dangeureuse pour le patient, et suppose que toutes les tumeurs du corps ont été identifiées. Des traitements chimiques sont à nouveau donnés en complément, et un suivi post-opératoire du patient est indispensable à la réussite du protocole.

1.3.2 Traitements systémiques

Les traitements sytémiques sont aujourd'hui un passage quasi-obligé du traitement d'un cancer. Les molécules utilisées ont des effets, et des objectifs très diverses. Nous allons décrire ici le mode opératoire de certains traitements, mais la liste est loin d'être exhaustive. Par abus de langage, nous parlerons en général de chimiothéapies pour tout traitement utilisant l'injection de molécules dans l'organisme.

Les traitements cytotoxiques sont une première famille de médicaments, ciblant les cellules hyper-actives, notemment celles se divisant souvent. Les cellules cancéreuses entrant très régulièrement en mitose, elles sont les premières touchées par ces molécules. Des observations de l'effet de médicaments cytotoxiques sont présentés en Fig.1.4. Ce ciblage est la raison principale de la perte des cheveux lors de traitements par chimiothérapie, les cellules créant les poils se divisant elles aussi très souvent. Ce phénomène est très impressionant, mais un autre effet secondaire est plus important pour la conduite du traitement : la destruction du système immunitaire. En effet celui-ci dépend de la création permanente par division cellulaire dans la moelle épiniaire de globules blancs. Les médicaments cytotoxiques détruisent une partie des cellules à cet endroit, ce qui rend le patient vulnérable à toutes sortes d'infections. Des études comme [BFCI03] prennent en compte ce phénomène : le protocole de traitement cytotoxique est optimisé, en maintenant le système immunitaire assez haut pour que le patient ne soit pas vulnérable. L'utilisation de cytotoxiques doit se faire aussi en respectant la pharmacocinétique du médicament : son action dépend du temps passé par la molécule dans l'organe ciblé. Des modèles mathématiques permettent d'estimer ce temps [Wel97], et donc de déterminer l'efficacité du traitement.

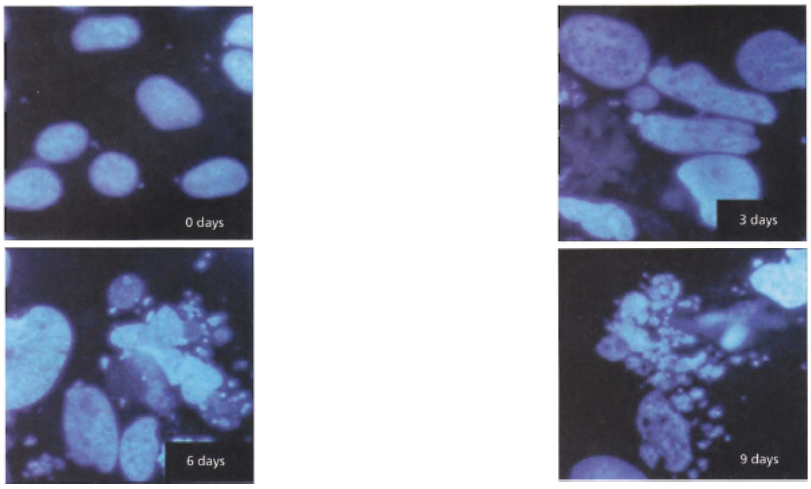

FIGURE 1.4 – Des cellules réagissent à un traitement cytotoxique : on observe ici les noyaux de cellules touchées par la molécule. À $t = 0$ jours, les noyaux sont à peu près identiques et sphériques. Ensuite ($t = 3, 6$ jours), les noyaux après quelques divisions sont déformés, plus gros ou plus petits que des noyaux de cellules cancéreuses normales. Enfin, à $t = 9$ jours, les noyaux se fragmentent en de nombreux micronoyaux, contenant chacun très peu d'information génétique, ce qui entraîne la mort de la cellule.

Cette thèse étudie un aspect de l'utilisation des traitements cytotoxiques. Les traitements cités ci-dessous ne sont donc pas considérés dans notre travail. Cependant les idées derrière ces protocoles et leur modélisation mathématique sont très intéressantes, et développent des idées novatrices qui pourraient s'insérer dans la suite de ce travail.

Les thérapies chimiques novatrices sont regroupées sous le nom de thérapies ciblées. Les chimiothérapies conventionnelles, comme les traitements cytotoxiques, ont été découverts et utilisés avant que leur mode d'action soit bien identifié. Au contraire, les thérapies ciblées sont le fruit d'une étude des comportements des cellules cancéreuses, et d'une volonté de bloquer certains mécanismes particuliers. Nous allons décrire en particulier les anti-angiogéniques, car leur découverte a été liée très rapidement à des modélisations mathématiques.

Les traitements anti-angiogéniques profitent du phénomène de vascularisation des tumeurs. Une tumeur nouvellement créée se développe habituellement jusqu'à la taille de 2-3mm de diamètre, avant de manquer de nutriments et d'oxygène. Les cellules en hypoxie peuvent produire alors des facteurs de croissance tels les VEGF (Vascular Endothelial Growth Factor), qui s'attachent à des récepteurs sur les cellules endothéliales (cellules des vaisseaux sanguins) afin de promouvoir leur croissance et leur développement dans la direction de la tumeur. Ainsi, la tumeur force le corps à développer un réseau de vaisseaux sanguins en son sein, se fournissant en nutriments et en oxygène. La tumeur entame alors une phase de croissance vasculaire, pouvant aller jusqu'à une dizaine de centimètres de diamètre. Ceci inspire un type différent de traitement, les traitements anti-angiogéniques. Ces traitements réduisent l'efficacité des VEGF créés par les tumeurs avasculaires, empêchant la production de vaisseaux irriguant la tumeur. De plus, les tumeurs vascularisées ont généralement créé de nombreux petits capillaires ; les molécules anti-angiogéniques tuent les cellules épithéliales de ces petits vaisseaux, effondrant l'apport en nutriments et en oxygène de la tumeur. Ces traitements sont généralement donnés en combinaison avec des médicaments cytotoxiques, la disparition des vaisseaux alimentant la tumeur pourraient

donc limiter l'efficacité de ceux-ci. Des études cliniques ont montré qu'au contraire, la disparition de ces capillaires améliore la distribution du médicament, car le réseau sanguin devient plus efficace. L'étude mathématique de ces traitements, et leur synergie avec les médicaments cytotoxiques, permet d'améliorer ces résultats.

La première modélisation de l'angiogénèse a été développée dans [HPFH99], puis a été suivi par de nombreux autres. Par exemple, [PHA+17] construit à l'aide de modèles mécaniques des vasculatures 3D dans le cas de tissus sains ou cancéreux, et compare les résultats obtenus : ce travail permet de mieux identifier les tumeurs au sein de tissus sains, et de mieux comprendre leur mode d'approvisionnement en nutriments et oxygène. Dans un autre cadre, [CILS14] développe des méthodes de problèmes inverse pour remonter, à partir le la répartition des cellules cancéreuses, à la position du réseau sanguin. Nous indiquons aussi [OAMB09, BRS+09], qui contruisent des modèles multi-échelle de vascularisation, et indiquent une interprétation des croissances tumorales "en escalier" (des périodes où la tumeur est stabilisée alternent avec des périodes de forte croissance). Ces modèles se penchent plus sur la compréhension des phénomènes biologiques. Dans une autre perspective, [dLMS09] utilise la théorie du contrôle optimal, et le principe du maximum de Pontryagin, pour optimiser une combinaison de traitements cytotoxique et anti-angiogénique, en prenant en compte la création de vaisseaux dans la croissance tumorale. Notre travail utilise, lui aussi, la théorie du contrôle optimal dans le but de réduire la charge tumorale, mais dans le cadre biologique de la résistance aux traitements. Utilisant une approche plus globale, [ABB+13] développe un modèle très complexe, se basant sur les interactions biologiques d'une dizaine d'agents, pour simuler cette même combinaison de traitements. Les conclusions de ces deux articles sont similaires, insistant sur l'intérêt des chimiothérapies à faible dose, et sur l'efficacité des protocoles utilisant en premier lieu les thérapies anti-angiogéniques, puis les thérapies cytotoxiques. Ces modèles ont pour but l'amélioration de traitements grâce aux simulations et à la théorie mathématique.

L'immunothérapie est un type innovant de traitement. En temps normal, le système immunitaire d'une personne saine est capable de reconnaître les cellules cancéreuses grâce à la présence de certains antigènes à leur surface et d'enclencher leur apoptose. Toutefois, on observe que les tumeurs qui ont dépassé un certain stade de croissance, contiennent des cellules cancéreuses exprimant peu d'antigènes à leur surface, et sont de fait "invisibles" au système immunitaire. D'autres mécanismes sont aussi présents et dépassent notre expertise du sujet. L'immunothérapie tente de remédier à ce problème en réactivant cette fonction du système immunitaire.

Les interactions entre système immunitaire et les tumeurs sont encore incomplètement comprises, c'est pourquoi de nombreuses études sont encore en cours sur ces traitements [JCK], pour pouvoir les donner en combinaison avec d'autres types de chimiothérapies, notemment des études utilisant la modélisation mathématique. La théorie du contrôle optimal est utilisée dans [LS14], où les interactions entre tumeur et système immunitaire sont prises en compte. Dans un autre registre, [OSM+11] utilise la modélisation à la fois par des équations de réaction-diffusion et des automates cellulaires, afin de prévoir les effets d'une combinaison de médicaments cytotoxiques et d'injection de macrophages.

1.4 Modélisation mathématique de la résistance aux anticancéreux

Malgré la large palette d'actions disponible pour les médecins, il arrive que ces traitements ne fonctionnent pas depuis le début de la chimiothérapie, ou que progressivement ils deviennent inefficaces. C'est par exemple le cas pour les médicaments cytotoxiques. Nous allons décrire certains phénomènes biologiques responsables de ce phénomène, puis détailler des études mathématiques

sur ce sujet.

1.4.1 Échec de la distribution du médicament et arrêt forcé du traitement

Une première raison de l'échec des chimiothérapies peut être leur incapacité à atteindre leur cible, étant immédiatement dégradés et évacués par le corps. Ce phénomène est appelé la résistance intrinsèque, car le corps lui-même rejette une telle molécule. L'étude de la pharmacocinétique du médicament [Wel97] est donc cruciale pour garantir son efficacité.

Une seconde raison pour arrêter un traitement cytotoxique est le fait que ses effets secondaires peuvent devenir trop dangereux pour le patient. En effet, puisqu'elles s'attaquent au cellules en cours de mitose, ces molécules détruisent en général une partie du système immunitaire. Quand celui-ci est trop bas, des maladies opportunistes telles le rhume ou la grippe peuvent être très nocives pour le patient, voire entraîner sa mort. D'autres organes vitaux, comme le foie, souffrent aussi de la présence de cytotoxiques. Afin de limiter les effets secondaires néfastes, les chercheurs définissent pour chaque molécule leur MTD, ou *Maximal Tolerated Dose*, la dose maximale de traitement qui puisse être administrée à un patient sans que les effets secondaire deviennent plus graves que le cancer traité lui-même. La plupart des traitements actuellement utilisés sont basés sur l'administration au patient de cette MTD, suivie d'une longue pause permettant au corps de reprendre des forces.

1.4.2 Les mécanismes de résistance spécifique

Un autre phénomène qui peut s'installer, et qui est d'un intérêt particulier dans notre travail, est la résistance au médicament directement de la part des cellules cancéreuses. Cette résistance peut intervenir selon différents mécanismes. Un des plus courants est l'augmentation de l'expression d'une pompe à la surface de la cellule, qui assure l'expulsion de l'intérieur de la cellule des molécules cytotoxiques. En augmentant le débit d'expulsion de ces médicaments, la cellule y est confrontée moins de temps, et donc sa probabilité d'en souffrir est réduite. Ce mécanisme est caractéristique d'une résistance simultanée à plusieurs médicaments, on parle alors de Multi-Drug Resistance 1 (MDR1). D'autres moyens peuvent être déclenchés par les cellules pour contrer les médicaments, comme l'inactivation de la cible du médicament dans le cas de thérapies ciblées, ou d'un intermédiaire lors de la transformation de la molécule. Certaines cellules peuvent, en réponse à un cytotoxique, devenir moins sujettes à l'apoptose, en augmentant l'expression de certaines protéines, ou être plus efficaces dans la réparation de leur ADN, annulant les effets de certains médicaments.

1.4.3 Hétérogénéité intratumorale

La création de résistances au sein d'une tumeur s'explique par deux principaux phénomènes.

Une tumeur solide peut, dès ses premiers stades de développement, présenter une grande hétérogénéité clonale, due à des mutations successives, même si une unique cellule est à la source de toutes les cellules cancéreuses d'une tumeur, comme illustré en Fig.1.5, et expliqué par [NCO$^+$03] (on parle d'hypothèse de monoclonalité). Ces mutations successives peuvent être modélisées par des processus stochastiques de branchement [Dur15]. La présence de plusieurs génotypes est révélée par un séquençage ADN complet dans [DLL$^+$12]. L'utilisation de traitements opère alors une sélection Darwinienne sur ces populations, car une modification des conditions de croissance élimine les traits les moins adaptés, tout en préservant les traits indifférents au traitement.

Sous cette hypothèse, de nombreux articles mathématiques considèrent que la résistance à la chimiothérapie peut être vue comme la séparation en deux populations des cellules tumorales : les cellules sensibles au traitement, et celles qui y sont résistantes. Les expériences sur lesquelles nos travaux son basées concernent deux lignées cellulaires distinctes, sensible ou résistante à un certain traitement. Nous nous plaçons donc dans ce cadre de travail. Dans [BG84], un modèle incrémentiel est proposé dans cette optique, les incréments étant le temps entre deux injections de traitement. Dans un article suivant [BRG$^+$87], ces populations sont elles-mêmes séparées entre cellules proliférantes, et cellules quiescentes (cellules au repos ne se divisant pas). Dans les deux cas, le traitement est vu comme un événement instantané, se passant à des temps prédéfinis. Notre modélisation prendra en compte des traitements continus en temps. Un cadre plus général de modélisation par des équations différentielles ordinaires (EDO) est présenté dans [MMGL87], où les interactions de compétition entre deux espèces sont considérées dans leur ensemble. Pour certaines classes de tels problèmes, deux situations sont possibles : exclusion d'une espèce, ou cohabitation entre les deux phénotypes ; une étude statistique sur de réelles tumeurs permet de voir que les deux scénarios existent. Nous nous intéressons dans cette thèse à des modèles où la cohabitation des deux espèces est instable. De tels modèles EDO sont repris par exemple dans [LS06], où la théorie du contrôle optimal est utilisée sur un système linéaire pour définir de nouveaux traitements. Notre étude dans le Chap.2 se place elle aussi dans cette perspective, mais avec un modèle EDO non linéaire, et où les interactions entre cellules sont prises en compte plus précisément. Dans [GSGF09], les auteurs définissent des traitements adaptatifs en suivant les recommandations générales suivantes : le protocole doit maintenir une population sensible au traitement, et stabiliser la taille de la tumeur à un niveau bas. Ces traitements, obtenus par des considérations purement descriptives, sont ensuite testés sur des souris [ENKD$^+$16] : les résultats sont encourageants, car la tumeur est réduite tout en restant hétérogène. Nous définirons dans cette thèse des protocoles de traitements en utilisant des méthodes mathématiques d'optimisation, ce qui permet de généraliser ces résultats.

Cependant, plusieurs études suggèrent que cette hétérogénéité clonale est accompagnée d'une multistabilité dans l'expression phénotypique du génome, c'est à dire qu'un génome peut donner lieu à différents fonctionnements cellulaires au cours de la vie d'une même cellule. L'injection de traitement pousse alors les cellules qui en sont capables à changer de phénotype, afin de survivre dans ces nouvelles conditions [PBZ$^+$13]. La résistance à un médicament est alors un phénomène réversible, car après l'arrêt du traitement, les cellules survivantes peuvent revenir à un phénotype sensible, comme illustré en Fig.1.6. Cette différence de phénotype pour un même génotype peut être observée au sein d'une seule tumeur, les cellules placées au cœur de la masse tumorale ne subissant pas les mêmes conditions de croissance que celles situées à sa surface [LCB$^+$16].

Pour prendre en compte ce phénomène, des modèles comme [LLC$^+$15] considèrent donc la résistance comme un trait continu, et modélise la croissance tumorale par des équations intégro-différentielles. Dans [ZPQH14], le modèle considéré est un système EDO étudiant les interactions entre de nombreuses espèces, avec des taux de transitions d'une espèce à l'autre élevés. Il est aussi possible d'utiliser des méthodes de modélisation stochastique [BSDB14], pour modéliser le passage d'un phénotype à un autre. Notre travail se basant sur des expériences avec seulement deux lignées cellulaires distinctes, nous ne prenons pas en compte cette hyptothèse.

Dans notre travail de thèse, nous allons baser notre modélisation sur des expériences *in vitro* où deux types distincts de cellules sont présents, et aucune mutation n'est considérée durant l'expérience. Ce modèle biologique reprend donc l'hypothèse d'une sélection Darwinienne. Cependant, l'hypothèse de multistabilité phénotypique pourra être à l'origine de modèles très intéressants.

La répartition spatiale des cellules des deux types peut avoir une importance cruciale dans le traitement, en particulier leur positionnement par rapport à la vasculature, et donc leur approvi-

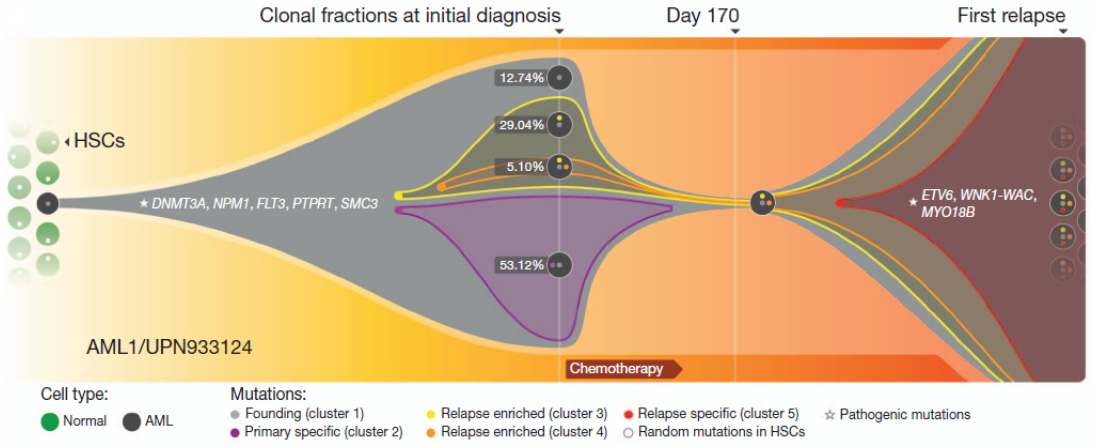

FIGURE 1.5 – Schéma tiré de [DLL+12], représentant les mécanismes de mutation/sélection à la source de la résistance à la chimiothérapie. Une seule cellule est, à gauche, source de toutes les cellules tumorales ; après des mutations successives, quatre génotypes différents existent au sein de la tumeur au moment de sa détection. Après le traitement, un génotype initialement minoritaire se retrouve majoritaire, et devient la source des cellules résistantes à la chimiothérapie.

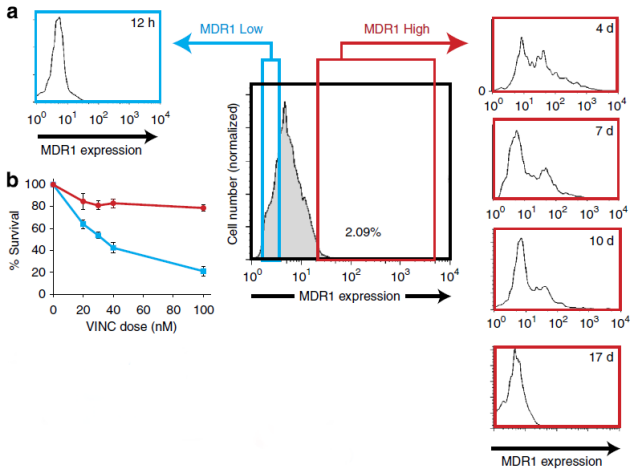

FIGURE 1.6 – Schéma tiré de [PBZ+13]. Des cellules cancéreuses présentent différent niveaux d'expression du phénotype MDR1 au sein d'une même tumeur. b) Celles exprimant peu de MDR1 (en bleu) sont globalement sensibles à la vincristine (VINC), tandis que celles expriment beaucoup de MDR1 (en rouge) y sont résistantes. a) Lorsque les cellules sensibles sont retirées de la population par utilisation du médicament (expérience de droite), après quelques jours, la tumeur retrouve sa répartition originelle d'expression de MDR1 par nombre de cellules.

sionnement en oxygène. Ce problème est étudié par [JB00], sont la forme d'équations aux dérivées partielles (EDP) modélisant la croissance d'une tumeur hétérogène. Les équations étant ensuite approchées par des EDO peuvent être résolues, ou du moins de propriétés des solutions sont exprimées, permettant de donner une idée générale des traitements intéressants. Cette étude ne prend cependant pas en compte les interactions entre les lignées cellulaires, nous étudions dans cette thèse l'influence de ces interactions sur la vitesse de croissance ; de plus les expériences que nous considérons sont *in vitro*, nous n'étudions pas l'influence du système vasculaire. Les mêmes hypothèses sont conduites par [IHRTEN+17], à l'aide d'automates cellulaires. D'autres effets spatiaux peuvent être étudiés, comme le fait que cellules sensibles et résistantes peuvent avoir des propriétés de motilité différents. Cet aspect est présenté dans [BHD08] avec des automates cellulaires et une étude de la théorie des jeux. Nous étudions ces mêmes hypothèses dans le Chap3 avec un modèle continu de compétition-diffusion.

Nour référons à [CLC16] pour une revue à grande échelle de la modélisation de la résistance à la chimiothérapie.

1.5 Amélioration des protocoles

La recherche en oncopharmacologie et thérapeutique ne s'arrête pas à la recherche de traitements innovants. Une fois un médicament créé et autorisé, son utilisation peut être améliorée en changeant son dosage, et son schéma d'administration. Ce changement est opéré soit en fonction du patient, soit de façon globale en modifiant les recommandations d'usage. Après avoir parlé des personnalisations de traitements, nous détaillerons une modification récente de posologie des médicaments anti-cancéreux : l'utilisation de schémas de traitement métronomiques.

1.5.1 Personnalisation des traitements

Les traitements définis par la communauté scientifiques ne sont pas donnés de manière identique à chaque patient, mais au contraire en s'adaptant à eux. Cette adaptation peut être très simple à réaliser, par exemple en augmetant les doses prescrites pour une personne en surpoids. Mais certains effets sont plus difficiles à prévoir, et nécessistent des informations plus précises sur le patient. La modélisation mathématique permet, à ce moment, de proposer des traitements adaptés. En effet, un modèle dont les paramètres sont ceux d'un patient permet de définir des protocoles en accord avec sa physiologie.

Dans cette optique, les modèles mathématiques développés doivent être calibrés avec les données spécifiques au patient. Dans [CCP+17], une méthode générale de confrontation aux données est présentée dans le cas particulier de tumeurs hétérogènes, mais pouvant se généraliser à d'autres systèmes biologiques. De même, [CILS12] présente une méthode utilisant des valeurs propres d'opérateurs pour retrouver les paramètres d'un modèle. Il s'agit dans ce cas de prévoir, à partir de deux clichés réalisés par IRM, l'évolution de la tumeur. En intégrant dès la création du modèle des paramètres mesurables chez le patient [RKP+12], il est aussi possible de prédire l'évolution de la maladie à partir par exemple de prises de sang et de biopsies [MBK+15].

En étudiant des cohortes de patients, il est aussi possible d'identifier par des méthodes de populations des groupes répondant de manière homogène au traitement. Ainsi, le modèle développé dans [MBC+16] propose des traitements qui sont ensuite adaptés au patient [HMB+16]. Les caractéristiques du patient permettent de déterminer l'ordre d'aministration des différentes molécules utilisées lors de cette chimiothérapie. Dans une optique similaire, les traitements proposés dans [BFCI03] sont adaptés aux patients en fonction de certains paramètres, estimés par ces méthodes de population.

La personnalisation des traitements pour chaque patient est un développement à considérer pour les travaux que nous présentons dans cette thèse. Nous étudions ici des lignées cellulaires stables et uniformes, nous n'avons donc pas l'utilité pour le moment de réaliser une personnalisation.

1.5.2 Le schéma de traitement métronomique

Dans la plupart des protocoles de chimiothérapie, le traitement est donné à sa dose maximale tolérée (MTD) sur de courtes périodes de temps, espacées par de longues pauses permettant au corps de récupérer des effets secondaires du médicament. Dans certains cas cependant, il n'est pas possible de donner une dose aussi forte : le patient est trop jeune ou trop âgé, ou atteint par plusieurs maladies à la fois, ce qui limite les choix de l'équipe médicale. Des doses moins fortes de médicament sont alors administrées, sur une période de temps plus longue. L'objectif affiché par les médecins n'est alors plus de guérir le cancer définitivement, mais de le contrôler, et d'en faire ainsi une maladie chronique [JGA15].

Lors de tels protocoles, les équipes médicales ont pu constater des résultats meilleurs que ceux attendus : des effets anti-angiogéniques [KK04], une réduction du nombre de métastases [COS+06], une amélioration de la qualité de vie [GBCC+09], une stabilisation de la progression de la tumeur [BDD+10]... Ces schémas de traitement à faible dose sont regroupés sous l'appellation de traitements métronomiques. Nous référons à [PKA10] pour une revue d'essais cliniques de ces schémas.

Ces résultats ont poussé plusieurs équipes de recherche à s'intéresser aux mécanismes créant ces améliorations. L'effet anti-angiogénique des médicaments cytotoxiques donnés à faible dose commence par exemple à être bien documenté : des doses faibles de médicaments ne sont pas capables de freiner efficacement la croissance des cellules tumorales elles-même, mais tuent les cellules épithéliales en formation, qui sont remplacées moins rapidement par la tumeur [ABB+13]. D'autres effets sont encore à expliquer, comme le retardement de l'apparition des métastases [BAB+12], ou la réduction des rechutes.

La détermination de la dose à appliquer pour des traitements métronomiques s'appuie le plus souvent simplement sur les limites imposées pas les effets secondaires (impact sur les reins, sur le système immunitaire...). Cependant, la modélisation mathématique de ces traitements peut identifier des doses optimales pour mener certains objectifs, ou des protocoles d'alternance avec d'autres chimiothérapies pour entraîner des synergies. Ces optimisations peuvent être réalisées par des expériences biologiques, mais sont bien plus rapidement effectuées avec l'aide de modélisation mathématique. Nous allons étudier dans cette thèse l'optimisation mathématique des doses de chimiothérapie pour réduire la résistance au traitement.

1.6 Données biologiques expérimentales

Dans le cadre de l'étude des schémas de traitement métronomiques, l'équipe de M. Carré au sein du CRO2 (Center for Research in Oncobiology and Oncopharmacology) de Marseille, a mis au point des modèles in vitro d'hétérogénéité intratumorale.

L'objectif de ce travail est d'étudier les interactions entre différentes populations cellulaires cancéreuses, dont les profils de réponse aux thérapeutiques varient (cellules dites sensibles ou résistantes), et de déterminer quels types de traitements sont efficaces contre ces cultures cellulaires tumorales hétérogènes. Les cellules étudiées dans la cadre de ma thèse proviennent d'une tumeur humaine du poumon (adénocarcinome pulmonaire) : la lignée A549 est sensible à des agents de chimiothérapie tels que l'épothilone B ou le paclitaxel, tandis que la lignée A549/EpoB40 qui en dérive (par sélection via une escalade de doses) est résistante à ces mêmes agents. Il faut

noter que, malgré cette différence dans la réponse aux traitements, les deux lignées cellulaires présentent une temps de doublement semblable.

Afin de pouvoir différencier et suivre sélectivement chacune de ces deux sous-populations de cellules durant les expériences, l'équipe de M. Carré s'est servie d'une méthode de transfection plasmidique pour établir des cellules stablement fluorescentes : certaines cellules peuvent ainsi exprimer la DsRed (rouge) alors que d'autres expriment la GFP (verte). Ce marquage est transmis lors des divisions cellulaires aux cellules-filles, sans perte de fluorescence. Au-delà de la visualisation (par microscopie), cette approche permet de recueillir le signal émis par chaque fluorescence et par conséquent de quantifier le nombre de cellules de chaque sous-populations (sensibles ou résistantes au traitement) au cours du temps.

Afin d'étudier la co-existence de cellules sensibles et résistantes aux traitements dans une même masse tumorales, les deux populations de cellules sont co-cultivées selon trois dispositifs (différents et apportant des informations complémentaires) :

— Le premier dispositif repose sur une co-culture des cellules adhérentes (i.e. culture « 2 dimensions ») en plaques 6 puits. Les cellules résistantes sont ensemencées dans la zone centrale du puits, séparées par un insert (en silicone) des cellules sensibles ensemencées dans la zone périphérique du même puits. Cet insert est retiré une fois l'adhérence des cellules au support effective (24h après ensemencement), permettant ainsi aux sous-populations cellulaires de proliférer, interagir et migrer librement dans l'ensemble du puits à partir de leurs zones initiales. Pendant toute la durée de l'expérience (1 mois), le milieu de culture est renouvelé 5 fois par semaine, de sorte qu'il ne constitue pas un facteur limitant à la croissance tumorale. La fluorescence de chacune des populations cellulaires est mesurée 3 à 5 fois par semaine à l'aide d'un lecteur de microplaques à fluorescence (PHERASTAR fx), via un mode dit de « well scanning ». Il est aussi possible d'observer la répartition géographique variable des cellules (GFP et DsRed) au cours de l'expérience, qui complètent les observations en microscopie à fluorescence (Nikon), comme montré en Fig.1.7.

— Dans le second dispositif, les cellules sont cultivées selon un modèle 3D que représentent les sphéroïdes. Cette structure est un meilleur modèle de l'architecture et des interactions cellule-cellule (notamment) observées dans les masses tumorales *in vivo*. Là encore, la fluorescence permet de déterminer la taille et la composition en chaque sous-population de cellules des masses 3D, comme vu en Fig.1.8a.

— Enfin, dans un troisième dispositif, les cellules sensibles et résistantes sont co-cultivées dans des systèmes Transwell®, qui reposent sur l'utilisation de deux compartiments distincts (insert et puits) séparés par une membrane perméable uniquement aux petites molécules ou vésicules. Les deux sous-populations sont donc privées d'interactions cellule-cellule, et leur communication s'effectue exclusivement à distance via leur milieu de culture, comme montré en Fig 7.1.8b.

Ces trois systèmes de co-cultures révèlent que, si aucun traitement n'est appliqué, les cellules sensibles croissent jusqu'à l'arrêt de l'expérience (qui peut être la confluence, c'est à dire le remplissage, du puits), alors que la population résistante se voit restreinte à une minorité de cellules, comme montré en Fig.1.9a. Par ailleurs, le dispositif Transwell permet de caractériser l'effet répresseur des cellules sensibles sur les cellules résistantes, puisque celui ci se produit indépendamment de tout contact cellule-cellule par une voie de communication à distance. Une étude complémentaire réalisée par M. Bondarenko, doctorante dans l'équipe de M. Carré, a finalement permis de déterminer que les cellules sensibles produisent un excédent de lactate, affectant la prolifération et la survie des cellules résistantes.

Afin de reproduire les protocoles basés sur l'utilisation de la dose maximale tolérée (MTD), les cellules sont ensuite exposées à un traitement hebdomadaire à forte dose (5 nM d'EpoB, 1 fois par semaine, avec changement du milieu de culture maintenu les autres jours). Comme attendu,

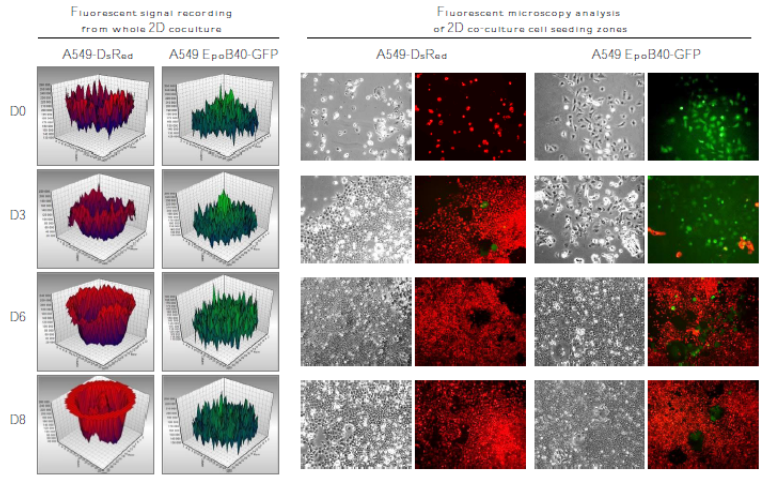

FIGURE 1.7 – Les cellules sensibles et résistantes sont cocultivées dans des plaques 6 puits, selon un modèle de culture 2D. Leur répartition dans l'ensemble du puits est présentée sur le panel de gauche (graphique issu des quantifications au PHERAStar), et des exemples de plans de co-cultures sont présentés sur le panel de droite (photos acquises en microscopie à fluorescence). Dans cette expérience, les cellules sensibles A549 sont indiquées en rouge (DsRed) et les résistantes A549/Epo40 en vert (GFP)

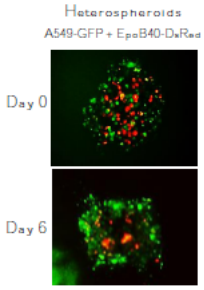

(a) Les cellules sont cultivées sous la forme de sphéroïdes, et sont imagées (microscope à fluorescence) et quantifiées (PHERAStar) au cours du temps. Dans cette série d'expérimentations, les cellules sensibles A549 sont en vert (GFP) et les cellules résistantes A549/Epo40 en rouge (DsRed).

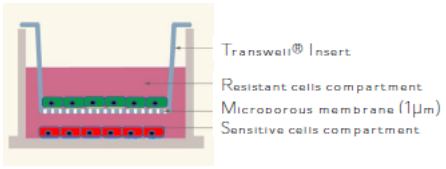

(b) Les deux sous-populations cellulaires sont cultivées dans deux compartiments distincts, séparés par une paroi perméable uniquement aux petites molécules et vésicules, mais ne laissant pas passer les cellules d'un compartiment à l'autre.

FIGURE 1.8 – Deux dispositifs supplémentaires sont mis en place : une coculture des cellules en sphéroïdes, et une culture des cellules dans deux compartiments séparés.

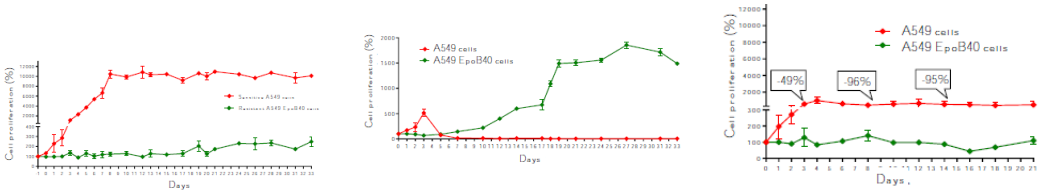

(a) Sans traitement, les cellules sensibles remplissent le puits et oppriment les cellules résistantes.

(b) Sous un traitement fort (5nM) et espacé, les cellules sensibles sont presque toutes tuées, ce qui laisse les cellules résistantes proliférer et remplir le puits de Pétri.

(c) Sous un traitement faible (0,5nM) et régulier, la prolifération des cellules sensibles et freinée, mais il en reste suffisamment pour opprimer les cellules résistantes.

FIGURE 1.9 – Résultats des trois protocoles sur l'expérience de coculture en 2 dimensions en puits de Pétri. Les deux autres dispositifs donnent des résultats similaires.

ce traitement est dans un premier temps très efficace, car il tue toutes les cellules répondeuses (sensibles) des co-cultures. Cependant, l'éradication complète de cette population de cellules sensibles lève l'inhibition qu'elle exerçaient sur les cellules résistantes, permettant alors à ces dernières de reprendre leur croissance et former des masses tumorales entièrement insensibles à la première ligne de traitement FIG.1.9b.

Enfin, la chimiothérapie métronomique est ici reproduite par exposition chronique des cellules à une faible dose (10 fois inférieure à celle du protocome MTD, soit 0,5 nM cinq fois par semaine). Grâce à ce protocole, la population de cellules sensibles se stabilise à un niveau très bas par rapport à la situation de contrôle (sans traitement), mais reste suffisante pour continuer à empêcher l'émergence des cellules résistantes au traitement FIG.1.9c.

Le traitement de type métronomique donne donc une situation très intéressante, avec une population *in vitro* de cellules cancéreuses réduite, mais toujours majoritairement sensible au traitement. Ces expériences suggèrent donc que les traitements métronomiques peuvent réduire les risques de rechute après chimiothérapie.

Dans le cadre d'une collaboration, G.Chapuisat a construit un modèle mathématique reproduisant ces expériences. Son étude, et l'utilisation de méthodes mathématiques d'optimisation, aboutissent dans cette thèse à l'élaboration de protocoles de traitements qui réduisent la taille de la tumeur en conservant son hétérogénéité.

Chapter 2

Optimization of an *in vitro* chemotherapy to avoid resistant tumours

Chemotherapy use against solid tumours often results in the resistance of the cancer cells to the molecule used. In this paper, we will set up and analyse an ODE model for heterogeneous *in vitro* tumours, consisting of cells that are sensitive or resistant to a certain drug. We will then use this model to develop different protocols, that aim at reducing the tumour volume while preserving its heterogeneity. These drug administration schedules are determined through analysis of the system dynamics, and optimal control theory.

This chapter consists of an article published in the *Journal of Mathematical Biology* in 2017 [1], except section 2.3.2, which was added for coherence in this thesis.

Keywords: Chemotherapy; Mathematical model; Optimal control; Metronomics

2.1 Introduction

Resistance to chemotherapy is a major problem when treating cancer. Diverse factors can be the cause of such a phenomenon. The resistance might be caused by an overall bad adsorption of the drug by the organism: it is possible that the chemical agent is directly evacuated, without even reaching the target cells. This problem is mainly referred as an intrinsic resistance. Another reason is due to the nature of the cancerous cells themselves. Mutations can create new lineages of cells less sensitive to the drug, or an epigenetic behaviour might be selected to tackle the chemical aggression. The way those cells consume nutrients, or divide up, might evolve under the selection pressure imposed by the drug injection. In that case, either the mutation (or the epigenetic behaviour) is present in some cells before the beginning of the treatment, and then selected, or a secondary metabolism way might be chosen to bypass the first one, blocked by the drug action. Either way, when resistance to the chemotherapy appears, the medical team often has no choice but to switch to a different therapy, sometimes more harmful than the first one for the rest of the patient's organism. To prevent such a scenario, different strategies are studied. Anti-angiogenic drugs for example, target endothelial cells, which are less likely to mutate and develop resistance, in order to prevent vascularization of the tumour and maintaining it at a small size [ABB$^+$13]. Another approach is to change the rhythm of drug injections, as low dose treatments or resting times can have a resensitizing action [HFH03].

In many chemotherapy protocols, the usual procedure is to try to kill as many cancerous cells as possible and very quickly, so that the patient gets rid of his tumour with a maximum probability. Thus a large dose of drug is delivered during very short periods: such a protocol uses the Maximal Tolerated Dose (MTD), which is considered the highest dose of this drug you can give to a patient before side effects are too harmful for him. Such a strategy is justified if the resistance is considered as an acquired trait, and the aim is to destroy the tumour before any mutation occurs. But if resistant cells exist in the tumour even before the chemotherapy begins, then killing all sensitive cells would suppress the only natural control we had on them.

In this outlook, lower and more frequent drug doses that maintain a small sensitive population should be preferred. If a certain amount of them is still present, they might impose a competition pressure on resistant cells, and prevent them from proliferating. Such low dose protocols are called metronomic treatments. By using them, cancer would then be viewed as a long term disease that needs maintenance treatments, because no complete eradication of the disease is considered. They are developed today because they are less harmful for the patient's immune system, and can have an anti-angiogenic effect. Concerning the resistance phenomenon, the doses must be finely tuned to be sure sensitive cells never disappear, while reducing the tumour size to a minimum. This could be done by constant observation of the tumour state, or predicted for example by multiple *in vitro* experiments, or more efficiently by theoretical and numerical modelling. Moreover, because their advantages over MTD protocols are only effective over a long time, models can help predict the efficiency of such therapies. For both these reasons, mathematical modelling of this competitive environment and analysis of treatment solutions is now crucial. This hindsight can then lead *in vitro* or *in vivo* experiments, as it was done in [ENKD$^+$16].

Treatment optimization has been studied in applied mathematics under different perspectives. Two main trends appear regarding applied analysis and differential equations: numerical optimization for complex systems, or theoretical optimal control of simple systems. In the first category, several drug effects are often taken into account [ABB$^+$13]: cytotoxicity, anti-angiogenesis, toxicity for the rest of the organism, action on the immunosystem... Those models might use ODEs to describe a complex system with a lot of interactions [ABB$^+$13]. An other form of models is to use replicator dynamics, using individual rules that later infer on the whole system behaviour, as in [SG10, BHD08]. In that case, numerical methods are used to compute an optimal treatment to reduce, for example, the volume of the tumour under some conditions. But the complexity of such models can hide the driving phenomena of the real system, and they are not practical to predict the general behaviour of the tumour. In the second approach, the model is chosen extremely simple, with few differential equations, so that it can be analytically studied and theoretical optimal control theory can be used. The optimal treatment is determined, or at least characterized by the method given by the Pontryagin Maximum Principle [Tré05]. One can cite [LS14] for an optimal control of a vascularized tumour through two different drugs given in combination, but also [dLMS09, BH13] for recent applications of optimal control to chemotherapy. This approach gives an insightful comprehension of the model dynamics, and a mathematical justification for the chosen treatment schedule. In order to apply this method to the reduction of a tumour without selecting the resistant cancerous cells, we will work with a simple compartmented ODE cancer model.

In order to gain a better understanding of cancer dynamics, it is now important to see tumours not as homogeneous populations of cells, but as a complex ecosystem with a large variety of phenotypes. When a patient enters a chemotherapy, the medical team chooses to use drugs that target the most common cells in the tumour: this choice divides the cells into two different populations, one that is sensitive to the drug, and one resistant to it. In many cases, this phenotypic difference does not affect the global behaviour of the cells before the chemotherapy.

Biological observations are difficult to produce, since it may be hard to differentiate the two lineages. In a series of ongoing experiments, M. Carré at the CRO2 uses fluorescent marking to follow lung cancer cells implantation in Petri wells. A different transmissible marker is implanted to two lineages of cells, one sensitive to Epothilene, coloured in red, and one resistant to it, coloured in green. A first observation is that, when little or no treatment is applied, sensitive cells fill up the well, while resistant cells only survive in a small number, for a large diversity of initial composition.

Modelling this heterogeneity now depends on the assumptions that are made on the nature of resistant cells. The resistant trait can be considered as continuous, leading to partial differential equations of time and trait [LLC+15]. In our case, only two kind of cells are taken into account, so ordinary differential equations describing each population dynamics will be used. Random processes occurring in living organisms can be taken into account, like in [MBOVD04, CG86, GV03]. But since we want to model *in vitro* experiments, and use the model to develop optimal treatments, we chose a deterministic model. In this line of work, [BRG+87, BG84] developed simple, linear compartmented models of competing cancer cells, and [LS06] use optimal control theory on them to determine new treatment schedules that will delay the emergence of a resistance. In these models, the two lineages have the same growth rates, and do not compete for nutrients nor space. This does not explain the dominance of sensitive cells over resistant cells in normal conditions, so further complexifications should be taken into account. A trade-off in growth rate for resistant cells is introduced in [GSGF09], so that sensitive cells are selected over them during the experiment, and [MMGL87, Pan96] insist on the role of space and nutrients competition. But in M.Carré's experiments, the dominance of sensitive cells is seen very quickly, even if a first treatment injection has reduced greatly their population at the beginning. Models that do not consider an actual repressive effect of sensitive cells on resistant cells cannot reproduce this phenomenon.

This paper is divided into three main parts. The first part will present a mathematical model for heterogeneous *in vitro* tumours. Then, after an analysis of the system behaviour under a constant injection of a drug, we investigate a first way to mathematically enhance the treatment protocol, by minimizing the tumour size at the experiment end. This first example being unsatisfactory, the second part studies two other choices of protocols. First, an adaptive stabilization protocol is designed to control indefinitely the system at a low, stable state. Second, we choose to minimize analytically a new cost taking into account the tumour size during the whole experiment. Finally, in the third part, we focus on numerical results, to compare our two protocols with a constant treatment and a cycling MTD protocol.

2.2 General study of a heterogeneous *in vitro* tumour model

2.2.1 Mathematical modelling

We use phenotypical observations of lung cancer cells A549, sensitive to Epothilene, and their resistant version, A549 Epo40. These lineages are used by M. Carré, researcher at the CRO2 [1] in experiments on cancerous cells interactions. We also only consider two months *in vitro* experiments, where only the two types of cells are present, and nutrients are distributed in abundance.

The cell population is divided into two compartments: the sensitive cells, denoted s, and the resistant cells, denoted r. We neglect any mutation or metabolism change that would make sensitive cells become resistant during the experiment: such events are rare, and would not

1. Center for Research in Oncobiology and Oncopharmacology

contribute a lot to the global resistance over two months of treatment. Moreover, the resistant ligneage of cells is resistant to very high concentrations of Epothilene (40 nMol), while dosages in this kind of experiment is limited to tolerable levels for an animal organism (5 nMol). Hence the selective pressure is not sufficient to make A549 cells mutate into A549 Epo40 cells. We thus decided to focus on other dynamics that explain the emergence of a globally resistant tumour. When cultivated alone, the cells behave as in a logistic model, which we will use for the rest of the study. This model is expressed for a generic population x as:

$$\frac{dx}{dt}(t) = \rho x(t)(1 - \frac{x(t)}{K})$$

where ρ is the initial growth rate of the population, and K the carrying capacity of the environment. The term $\frac{x}{K}$ represents the total space already occupied in the environment. In our case, the two kinds of cells consume space, so this term should be $\frac{s+r}{K}$. But we should take into account the difference of size between the two lineages: resistant cells are bigger than sensitive cells in M. Carré's experimental setting. For that purpose, the term representing the used space is $\frac{s(t)+mr(t)}{K}$, with $m > 1$. The growth rates of s and r are denoted, respectively, ρ_s and ρ_r.

$$\begin{cases} \frac{ds}{dt}(t) & = \rho_s s(1 - \frac{s+mr}{K}), \\ \frac{dr}{dt}(t) & = \rho_r r(1 - \frac{s+mr}{K}). \end{cases} \tag{2.1}$$

When cultivated together without any treatment, A549 cells will outgrow the A549Epo40 population quickly. But in the framework of a logistic model, (2.1) is not sufficient to describe this phenomenon, as the quantity $\rho_r \ln(s(t)) - \rho_s \ln(r(t))$ here remains constant. Moreover, when cultivated separately, the two lineages seem to have very similar growth coefficients ρ_s and ρ_r (see Tab.2.1). Thus, we add a supplementary competition term $-\beta sr$ for the resistant cells. This ensures that the tumour will be, after some time, composed of almost only sensitive cells. It is coherent with our idea of a resistance that cannot be detected before treatment, as very few cells present this trait.

Finally, the concentration $C(t)$ of the drug only acts on the sensitive cells, and its action is proportional to the number of those cells. We restrict our model to the case $0 \leq C(t) \leq C_{\max}$, where $C_{\max}$ is the maximal tolerated dose for a patient (MTD). Resistant cells A549Epo40, for this range of concentration, are completely unaffected by the drug. The system is now:

$$\begin{cases} \frac{ds}{dt}(t) = \rho_s s(1 - \frac{s+mr}{K}) - \alpha s C(t), \\ \frac{dr}{dt}(t) = \rho_r r(1 - \frac{s+mr}{K}) - \beta sr. \end{cases} \tag{2.2}$$

The different parameters in Tab.2.1 are estimated values for A549 (sensitive) and A549 Epo40 (resistant) cells.

Theorem 4. *For any bounded Lebesgue measurable function $C : [0, T] \to [0, C_{max}]$ with $T \leq \infty$, the triangle $\mathbb{T} := \{s > 0\} \cap \{r > 0\} \cap \{s + mr < K\}$ is positively invariant under the dynamical system of equations (2.2).*

Proof. A direct application of theorem 2.1.1. in [BP07, p. 14] ensures that for any $(s_0, r_0) \in \mathbb{T}$ and measurable control $C : [0, T] \to [0, C_{\max}]$, the initial value problem (2.2) with $(s, r)(0) = (s_0, r_0)$ has a global unique solution $(s, r) : [0, T] \to \mathbb{R}^2$, which is absolutely continuous on $[0, T]$ and depends continuously on the initial condition.

Let $\{(s, r)(t), t \in [0, T]\}$ be a trajectory of the system (2.2) for a certain Lebesgue measurable function $C : [0, T] \to [0, C_{\max}]$ and such that $(s, r)(0) = (s_0, r_0)$.

Symbol	Meaning	Value	Unit
s_0	sensitive cells number	initial : 5000	cells
r_0	resistant cells number	initial : 5000	cells
K	Petry dish carrying capacity	4800000	cells
m	size ratio between s and r	30	adimensional
ρ_s	sensitive cells growth rate	0.031	cells/hour
ρ_r	resistant cells growth rate	0.026	cells/hour
C	drug concentration	maximum : 5	nM/hour
α	drug effect	0.06	nM^{-1}
β	action of sensitive on resistant	$6.25 \cdot 10^{-7}$	cells^{-1}
T	experiments duration	720	h

Table 2.1 – Parameters for the equations and their value used in the simulations

On the set $\{s = 0\}$ (resp. $\{r = 0\}$), the system (2.2) yields $\frac{ds}{dt} = 0$ (resp. $\frac{dr}{dt} = 0$). So according to the uniqueness of the solution (s, r), if there exists a certain t_0 such that $s(t_0) = 0$ (resp. $r(t_0) = 0$), then for all $t \in [0, T]$, $s(t) = 0$ (resp $r(t) = 0$). Moreover, the points $O = (0, 0)$ and $E_r = (0, \frac{K}{m})$ are fixed points, and at the point $K = (K, 0)$ the derivative on s satisfies $\frac{ds}{dt} \leq 0$. Hence the sets $\{s = 0, 0 \leq r \leq \frac{K}{m}\}$ and $\{0 \leq s \leq K, r = 0\}$ are both stable under the system (2.2).

Now suppose a trajectory $\{(s, r)(t), t \in [0, T]\}$ satisfies $(s, r)(0) \in \mathbb{T}$, and there exists $t > 0$ such that $(s, r)(t) \notin \mathbb{T}$. Then by continuity there exists a smallest time $t_0 > 0$ such that $(s, r)(t_0) \in \partial\mathbb{T}$. The cases were $s(t_0) = 0$ or $r(t_0) = 0$ are ruled out by the stability of the sets $\{s = 0\}$ and $\{r = 0\}$. Hence the only possibility is $s(t_0) + mr(t_0) = K$ with $s(t_0) > 0$ and $r(t_0) > 0$. But then $\frac{ds}{dt}(t_0) + m\frac{dr}{dt}(t_0) = -\alpha s(t_0)C(t_0) - \beta s(t_0)r(t_0) < 0$, so there exists $\epsilon > 0$ such that $s(t_0 - \epsilon) + mr(t_0 - \epsilon) > K$. This is absurd since t_0 was the first exiting time by definition.

Hence $\mathbb{T}$ is positively stable under system (2.2). □

In equations (2.2), the two growth rates are taken different. For the lineages we consider, they are quite similar (see Tab.2.1). Thus in the rest of this article we consider $\rho_s = \rho_r = \rho = 0.03$cells/hour. This will simplify the computations, but the results remain similar if the difference is kept. The treatment effect could also be considered as a saturated function, with αC replaced by $\frac{\alpha C(t)}{E + C(t)}$, but this does not change much the different results we obtained, so we decided to keep a simple model.

In the end, the system we will study is:

$$\begin{cases} \frac{ds}{dt}(t) = \rho s(1 - \frac{s+mr}{K}) - \alpha s C(t), \\ \frac{dr}{dt}(t) = \rho r(1 - \frac{s+mr}{K}) - \beta s r \\ s(0) = s_0 \quad , \quad r(0) = r_0 \end{cases} \tag{2.3}$$

2.2.2 Phase plan analysis for a constant treatment

In order to understand the system (2.3) dynamic, we first study its behaviour under a constant treatment over time $C(t) = C$

$$\begin{cases} \frac{ds}{dt}(t) = \rho s(1 - \frac{s+mr}{K}) - \alpha s C, \\ \frac{dr}{dt}(t) = \rho r(1 - \frac{s+mr}{K}) - \beta s r. \end{cases} \tag{2.4}$$

This study will highlight the global behaviour of the system, and show important points in the phase plan. Under this assumption, for a constant treatment, we have the following theorem:

Theorem 5. *Given an initial condition $(s_0, r_0) \in \mathbb{T}$, the system (2.4) will evolve to different values depending on the treatment value. Denoting $C_{metro} := \frac{K\beta}{\rho+K\beta}\frac{\rho}{\alpha}$, we have:*

- *if $C = 0$ then $(s,r)(t) \underset{t\to\infty}{\longrightarrow} (K, 0)$,*
- *if $0 < C < C_{metro}$ then, depending on (s_0, r_0), either $(s,r)(t) \underset{t\to\infty}{\longrightarrow} (K\frac{\rho-\alpha C}{\rho}, 0)$ or $(s,r)(t) \underset{t\to\infty}{\longrightarrow} (0, \frac{K}{m})$,*
- *if $C \geq C_{metro}$ then $(s,r)(t) \underset{t\to\infty}{\longrightarrow} (0, \frac{K}{m})$.*

Proof. A study of the system (2.4) fixed points and their stability, depending on the value of C, shows that three different cases emerge. They are summed up on Fig.2.1.

- **Case 1: No treatment**
  If no treatment is applied, then the only attractive fixed point of the system is $E_s(0) := (K, 0)$, where the well is completely filled and with only sensitive cells. All trajectories starting in $\mathbb{T}$ are attracted to it, as illustrated on Fig.2.1a.
- **Case 2: Strong treatment**
  If a strong treatment is injected, namely $C \geq C_{\text{metro}} := \frac{K\beta}{\rho+K\beta}\frac{\rho}{\alpha}$, then the only attractive fixed point is $E_r := (0, \frac{K}{m})$, where the well is filled with only resistant cells at their maximal stacking capacity. All trajectories starting inside $\mathbb{T}$ are attracted to this point, as illustrated in Fig.2.1c.
- **Case 3: Weak treatment**
  In the case where $0 < C < C_{\text{metro}}$, two fixed points are now stable: $E_r = (0, \frac{K}{m})$ with only resistant cells, and $E_s(C) := (K\frac{\rho-\alpha C}{\rho}, 0)$, with only sensitive cells, but at a lower level than if no treatment is used. Depending on the initial number of both sensitive and resistant cells, trajectories will evolve towards one or the other of the fixed points. The triangle $\mathbb{T}$ is thus divided into two attraction basins, corresponding to $E_s(C)$ and E_r.

In each case, Poincaré-Bendixson theorem allows us to conclude.

A third fixed point exists, which is always unstable: $E_u(C) := (s_u(C), r_u(C))$ with $s_u(C) := \frac{\alpha C}{\beta}$ and $r_u(C) = \frac{\rho+K\beta}{m\beta\rho}(\frac{\rho K\beta}{\rho+K\beta} - \alpha C)$, a mixed population state. Numerically, we can estimate that the attraction basins delimitation is a convex curve going through $O := (0,0)$ and $E_u(C)$. In any case, one sees that if at a certain time t we have $s(t) > s_u(C)$ and $r(t) = r_u(C)$, then $\frac{dr}{dt}(t) < 0$, and if $s(t) = s_u(C)$ and $r(t) < r_u(C)$ then $\frac{ds}{dt}(t) > 0$. Hence the plane portion $\{s > s_u(C)\} \cap \{r < r_u(C)\}$ is positively stable, so it is contained into $E_s(C)$ attraction basin.

When C approaches the limit value C_{metro}, the point $E_s(C)$ approaches its limit value $E_{s,l} := (\frac{K\rho}{\rho+K\beta}, 0)$. It is an interesting value, as no smaller population with only sensitive cells is stable.

Fig.2.1b represents the situation of a weak treatment.

□

With values from Tab.2.1, we find that $C_{\text{metro}} = 0.495nM/h$. This corresponds to a coherent value for metronomic treatments, that use a dose ten times weaker than the MTD in classical protocols.

2.2.3 Optimal control of the tumour size at the end of the experiment

Our model is able to reproduce the phenomena we desired. It now should be used to determine treatments that achieve medical purposes. The choice of an objective, mathematically, will greatly influence the form of the corresponding optimal treatment. Thus, we investigate different kinds

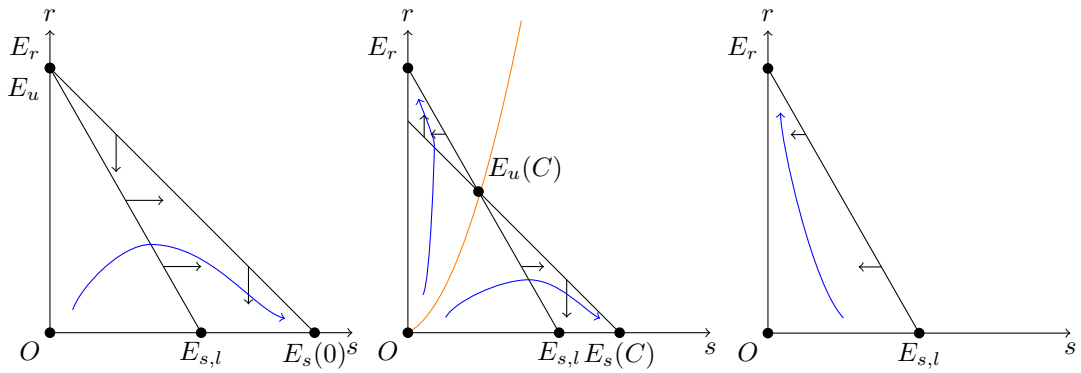

(a) No treatment (b) Weak treatment (c) Strong treatment

Figure 2.1 – Phase planes for the three different situations, the model is able to reproduce the results from experiments

of objectives to present their advantages and drawbacks. We present here a first example, to reduce the tumour size at the end of the experiment.

Optimal Control Problem 2. *Given an initial condition $(s_0, r_0) \in \mathbb{T}$, a maximal concentration of the treatment C_{max} and a duration T of experiment, find a Lebesgue measurable function $C : [0, T] \to [0, C_{max}]$ that minimizes the global quantity of effective cancerous cells:*

$$\psi(s, r) := s(T) + mr(T)$$

at the final time T.

This is a Mayer problem [Tré05]. The answer of this problem highlights how it is not relevant for medical purposes:

Theorem 6. *The optimal treatment for Problem 2 is "bang-bang", and up to a certain time $t_{start} \in [0, T]$ depending on the parameters, we have $C(t) = 0$, and from t_{start} to T the treatment is maximal $C(t) = C_{max}$.*

A first step towards Theorem 6 proof is the existence of optimal solutions to Problem 2.

Lemma 3. *For any $(s_0, r_0) \in \mathbb{T}$, there exists a Lebesgue measurable control $C^* : [0, T] \to [0, C_{max}$ which is optimal for Problem 2.*

Proof. We denote $f : ((s, r), t, C) \mapsto (\rho s(1 - \frac{s+mr}{K}) - \alpha s C, \rho r(1 - \frac{s+mr}{K}) - \beta s r)$. For any $t \in [0, T]$ and any $(s, r) \in \mathbb{T}$, the set of velocities $F((s, r), t) = \{f((s, r), t, C), C \in [0, C_{\max}]\}$ is convex and compact. Moreover, f is Lipschitz-continuous with respect to each variable on $\bar{\mathbb{T}} \times [0, T] \times [0, C_{\max}]$. Then, according to Filippov's theorem from [BP07, p. 88], for any $(s_0, r_0) \in \mathbb{T}$, the reachable set defined by:

$$\begin{aligned}\mathcal{R}^T_{s_0,r_0} := \{(s_T, r_T) \in \bar{\mathbb{T}} / \exists C : [0, T] \to [0, C_{\max}] \text{ Lebesgue measurable,} \\ \text{solution of (2.3) with } (s, r)(0) = (s_0, r_0) \text{ satisfies } (s, r)(T) = (s_T, r_T)\}\end{aligned}$$

is compact. Thus, if (s_T, r_T) minimizes ψ over $\mathcal{R}^T_{s_0,r_0}$, then $(s_T, r_T) \in \mathcal{R}^T_{s_0,r_0}$ and there exists a control C^* associated to it. This control solves Problem 2. Note that if $(s_0, r_0) \in \mathbb{T}$, then $\mathcal{R}^T_{s_0,r_0} \subset \mathbb{T}$, thus any $(s_T, r_T) \in \mathcal{R}^T_{s_0,r_0}$ satisfies $s_T > 0$ and $r_T > 0$. □

We can now perform the proof of Theorem 6.

Proof. We want to characterize optimal solutions of Problem 2. The necessary conditions for the optimality of the control $C : [0,T] \to [0, C_{\max}]$ of the Pontryagin Minumum principle state that there exist a constant $p_0 \geq 0$ and an absolutely continuous adjoint vector $p : [0,T] \to \mathbb{R}^2$ satisfying the following conditions. First, for all $t \in [0,T]$ we have $(p_0, p(t)) \neq 0$, that is the condition of non-triviality. Second, the optimality condition: the optimal control $C^*(t)$ minimizes along the optimal trajectory $(p_0, p(t), s^*(t), r^*(t))$ the Hamiltonian:

$$H(s,r,p_1,p_2,C) := p_1 \cdot \left(\rho s(1 - \frac{s+mr}{K}) - \alpha s C\right) + p_2 \cdot \left(\rho r(1 - \frac{s+mr}{K}) - \beta s r\right),$$

over the set $[0, C_{\max}]$. Third, p satisfies the adjoint equations and transversality condition:

$$\begin{cases} \dot{p}(t) = -\begin{pmatrix} \frac{\partial H}{\partial s} \\ \frac{\partial H}{\partial r} \end{pmatrix}(t) = -\begin{pmatrix} \rho(1 - \frac{2s+mr}{K}) - \alpha C & -(\frac{\rho}{K} + \beta) r \\ -\rho s \frac{m}{K} & \rho(1 - \frac{s+2mr}{K}) - \beta s \end{pmatrix} p(t), & (2.5) \\ p(T) = \nabla \psi(s(T), r(T)) = p_0 \begin{pmatrix} 1 \\ m \end{pmatrix}. & (2.6) \end{cases}$$

If $p_0 = 0$, then (2.6) implies that $p_1(T) = p_2(T) = 0$: this contradicts the non-triviality condition, so $p_0 \neq 0$. Hence we can normalize $p_0 = 1$ without loss of generality.

The hamiltonian H is linear in the control C: the function $-\alpha p_1 s$ is called the switching function of the problem. In order to minimize H along the optimal trajectory, we see that:

— if $\alpha p_1^*(t) s^*(t) < 0$ then $C^*(t) = 0$,

— if $\alpha p_1^*(t) s^*(t) > 0$ then $C^*(t) = C_{\max}$,

— if $\alpha p_1^*(t) s^*(t) = 0$ we need more information.

Since $\frac{dp_1^*}{dt}(t) = -(\rho(1 - \frac{2s^*+mr^*}{K}) - \alpha C^*(t)) p_1^*(t) + (\frac{\rho}{K} + \beta) p_2^*(t)$, we have $p_1^*(t) \equiv 0$ on a non empty interval I if and only if $p_2^*(t) \equiv 0$ on that same interval. But then according to the Cauchy-Lipschitz theorem $I = (0,T)$, so $p(T) = 0$. This is absurd, so p_1^* does not vanish on an interval. Hence the optimal treatment is for every $t \in [0,T]$ either 0 or $C_{\max}$.

A study of p phase plan FIG.2.2 shows that any trajectory ending on $\begin{pmatrix} 1 \\ m \end{pmatrix}$ either satisfies $p_1(t) > 0$ for every $t > 0$, or there exists $t_0 > 0$ such that $p_1(t) < 0$ for every $0 < t < t_0$ and $p_1(t) > 0$ for every $t > t_0$.

If $p_1^*(0) > 0$ then $p_1^* > 0$ during the whole experiment, so $\forall t \in [0,T],\ C(t) = C_{\max}$, so $t_{\text{start}} = 0$. If $p_1^*(0) < 0$ then $\forall t \in [0, t_0),\ p_1^*(t) < 0$ and $\forall t \in (t_0, T],\ p_1^*(t) > 0$, so with $t_{\text{start}} = t_0$ we have $\forall t \in [0, t_{\text{start}}),\ C(t) = 0$, and $\forall t \in (t_{\text{start}}, T],\ C(t) = C_{\max}$.

□

Remark 1. This proof can also be performed using the framework of geometric optimal control, as in [dLMS09].

In other words, we wait for the sensitive cells to invade the dish and kill almost all resistant cells, then just before the measurement time we release a huge dose of drugs to clear off the sensitive cells. The treatment starting time t_{start} can be determined numerically.

This is not an acceptable strategy for clinical research: indeed, it supposes that we only want a pointwise result, without looking at the intermediate states of the system, nor the long term consequences of such a protocol. Indeed, it is possible that we let the tumour reach its maximal capacity K during the experiment, as seen in FIG.2.3a, which would be really bad in a medical context. Moreover, according to our model, if after the end of the experiment T one maintains

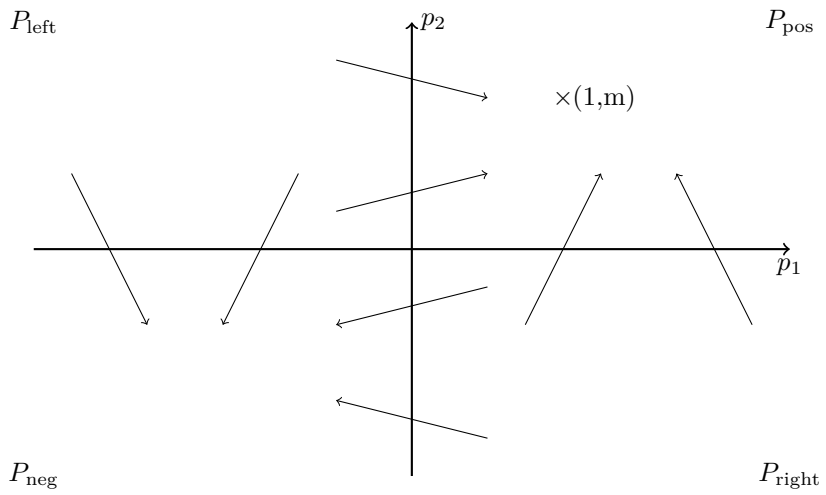

Figure 2.2 – The phase plane of the adjoint vector p reveals two positively stable zones

the treatment $C = C_{\max}$, then the resistant cells will invade the now free space left over by the sensitive cells as seen on FIG.2.3b. Otherwise, if one stops the treatment after T, so $C = 0$, then the sensitive cells will progressively resettle in the well as seen on FIG.2.3c. Even worse, such a large drug dose might have killed, in reality, all the sensitive cells: even if we stop the treatment after T, we are no longer able to control the tumour. To tackle this problem, new treatment protocols should take into account the quantity of cells in the well during the whole experiment, from 0 to T, and have an outlook on future behaviour on the solution.

This example highlighted that the choice of a cost ψ is very important to define an optimal therapy. It depends on medical objectives, and should be chosen after discussions with biologists.

2.3 Treatment protocols with different aims

Since the optimal treatment defined in 2.2.3 is not very well suited for medical protocols, we define two new problems. The first one based solely on the study of trajectories in 2.2.2 gives a way to stabilize the tumour at low, constant state. The second one is a new optimal control problem, which takes into account the size of the tumour during the whole experiment.

2.3.1 Adaptive stabilization protocol

A consequence of Theorem 5 is that the total tumour $s + r$ never goes extinct. For medical reasons, it is interesting to reach a constant state, with mostly sensitive cells, and at the lowest possible level. If we define a treatment so that the tumour reaches such a state, the cancer will no longer be considered a single-event disease, but a chronic one, that requires constant care but is under medical control.

In this outlook, we want to stabilize the system at the fixed point with only sensitive cells $E_s(C)$, with this point as close as possible to $O = (0, 0)$, with the constraint of $E_s(C)$ being stable. The fixed point $E_s(C)$ is stable for $0 < C < C_{\text{metro}}$, so our objective is the point $E_{s,l} := (\frac{K\rho}{\rho + K\beta}, 0)$, that is the position of $E_s(C)$ for $C = C_{\text{metro}}$.

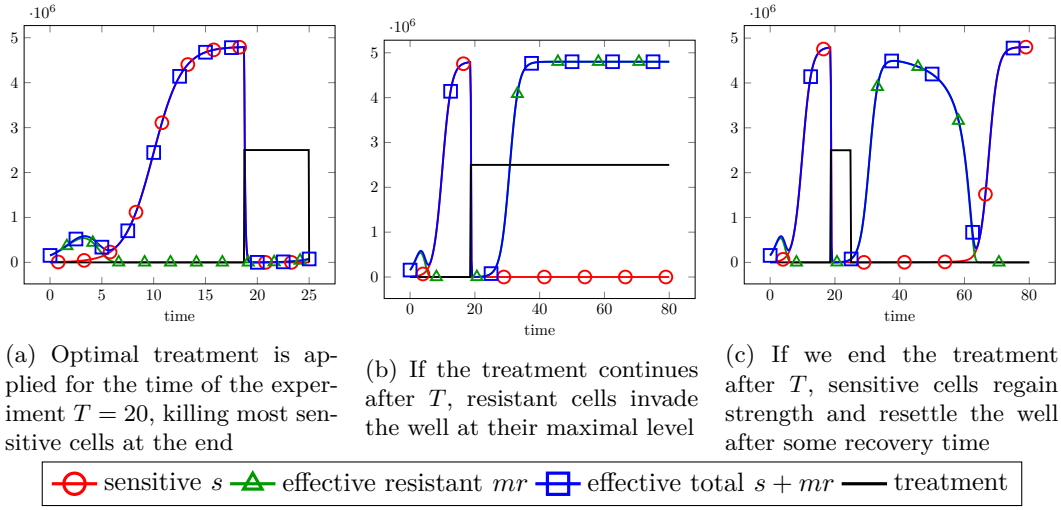

(a) Optimal treatment is applied for the time of the experiment $T = 20$, killing most sensitive cells at the end

(b) If the treatment continues after T, resistant cells invade the well at their maximal level

(c) If we end the treatment after T, sensitive cells regain strength and resettle the well after some recovery time

Figure 2.3 – Cells populations evolutions during an optimal treatment when only the final population is take into account

We now propose a strategy to approach this point. We want to define a treatment for our system such that, at any moment t, the trajectory of the system (s, r) is in the basin of attraction of $E_s(C)$, which position depends on the value of $C(t)$. Thus, one can assure the patient that his tumour is controlled. We also impose $C(t)$ to be piecewise constant, and its value can only be changed each day (which corresponds to an experimental situation). The initial population is supposed to be a mix of sensitive and resistant cells ($s(0) > 0$, $r(0) > 0$). This strategy is an adaptive, iterative medical protocol.

The beginning of the ith day is denoted t_i, and the value of C during the ith day is denoted C_i. We use a coefficient $\lambda_i \in (0, 1)$ that is also modified each day. Measures of $(s, r)(t_i)$ define the treatment value each day:

— *Initialization* $(s, r)(0)$ cells are implanted, $\lambda_0 = 1/2$
— *Loop for* $i = 1$ *to end of experiment*

1. *If* $r(t_i) < \frac{K}{m}(1 - \frac{s(t_i)}{K})$, let the system evolve with no treatment, $C_i = 0$, and $\lambda_i = \frac{1}{2}$ for reinitialization.
2. *If* $r(t_i) \geq \frac{K}{m}(1 - \frac{s(t_i)}{K})$, set $C_i = \lambda_i C_{\text{metro}}(1 - \frac{m}{K}r(t_i))$ and $\lambda_{i+1} = \frac{1+\lambda_i}{2}$.

— *End of experiment*

This protocol is illustrated by Fig.2.4, during four days: Fig.2.4a shows the action of a first step of the protocol, without treatment, while Fig.2.4b and 2.4c represent two days with treatment. During the loop, theoretically, phase 1 can only be encountered for a few days at the experiment beginning, and when phase 2 begins it lasts until the end of our protocol. However, biological variations could occur and bring us back to phase 1.

We have presented the general idea of an algorithm reaching the plateau $(s, r) = E_{s,l} = (\frac{K\rho}{\rho + K\beta}, 0)$. As shown on Fig.2.5, the sensitive population reaches a maximal level shortly after the treatment started, then slowly decreases to reach asymptotically the point $E_{s,l}$. The different parameters (time delay before starting the treatment, pace of changes in C, λ parameter...) could

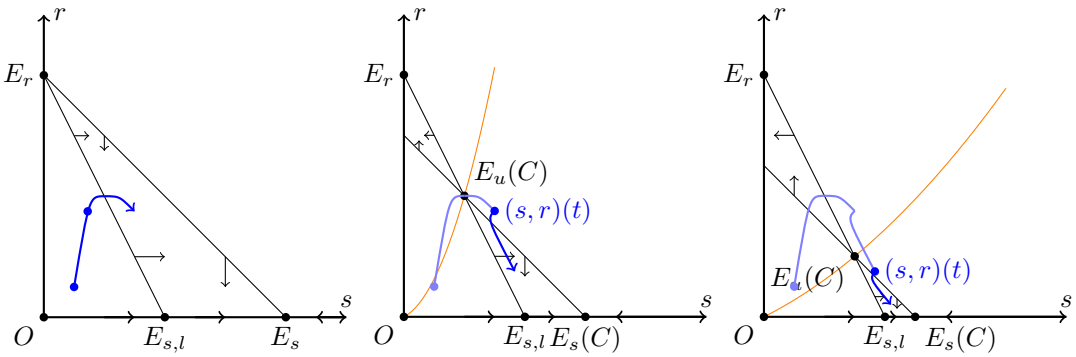

(a) Day 1 and 2: the quantity of resistant cells is still growing, so no treatment is applied

(b) Day 3: the system has crossed the designated threshold to start the treatment

(c) Day 4: the treatment value is actualized to bring $E_s(C)$ closer to $E_{s,l}$

Figure 2.4 – Several steps of the adaptive protocol are represented on the phase plane

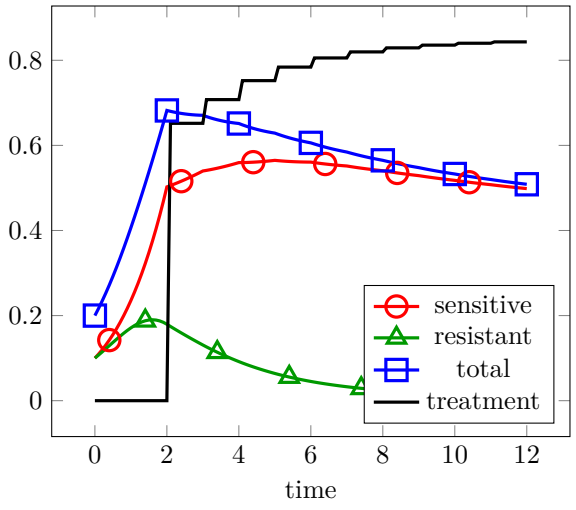

Figure 2.5 – Adaptive stabilization protocol in the time scale: the treatment is increased each day, and the cells population approaches the desired level

be optimized by the choice of λ_i, depending on the medical constraints (rhythm of the patient presence at the hospital, toxicity of the treatment) and objectives: reaching the plateau as soon as possible, using the less treatment point-wise or cumulated...

In the following, this protocol will be referred to as the adaptive protocol. It treats the tumour as a chronic disease: we do not try to suppress the cancerous cells, but to control them for an indefinite time.

2.3.2 Optimal control of the tumour size during the whole experiment

The adaptive protocol is designed through qualitative considerations on the system behaviour. We now want to determine another type of protocol, that will have a quantitative objective.

Expression of the singular control for an integral cost

A natural way to take into account the treatment effects for an entire period is to use an integral cost: $L_{\text{int}}(T) = \int_0^T (As(t)+Br(t))dt$. For medical reasons, it is also important that during the experiment, the tumour remains small. To ensure that, we will use a cost that penalizes high values of $s(t)$ and $r(t)$, *i.e* a L^2-norm: $\int_0^T (As^2(t) + Br^2(t))dt$. Our new problem is the following:

Optimal Control Problem 3. *Given an initial condition $(s_0, r_0) \in \mathbb{T}$, a maximal concentration of the treatment C_{max} and a time T of experiment, find a piecewise continuous function $C : [0, T] \to [0, C_{max}]$ that minimizes the following cost:*

$$L_2(T) := \tilde{\psi}(s(T), r(T)) + \int_0^T L^0(s(t), r(t))dt,$$

with $\tilde{\psi}$ the Mayer part of the cost, and L^0 the Lagrange part of it:

$$\tilde{\psi}(s, r) := s^2 + r^2, \quad L^0(s, r) := As^2 + Br^2.$$

We find that the optimal treatment for this problem is of a particular form:

Theorem 7. *The optimal treatment for Problem 3 is a piecewise continuous function C, with three possible values at each time point. Either:*
- *the control is maximal $C = C_{max}$,*
- *the control is minimal $C = 0$,*
- *the control is singular $C = \frac{1}{\alpha s}\left(\frac{B}{A}r^2(\frac{\rho}{K} + \beta) + s\rho(1 - \frac{s+2mr}{K})\right)$.*

Moreover, the control is maximal at the end of the experiment: $C(T) = C_{max}$.

Proof. First, the existence of optimal solutions to Problem 3 is ensured by Theorem 5.2.1 from [BP07], on p.94. The assumptions of this theorem are satisfied by our system inside $\mathbb{T}$, so a cut-off far from it is enough to apply the theorem.

We will once again use the framework of Optimal control theory, and in particular the Pontryagin Minimum Principle. Because the cost functional now has an Lagrangian part, the system hamiltonian is modified:

$$H(s, r, p_1, p_2, C) = As^2 + Br^2 + p_1 \cdot \left(\rho s(1 - \frac{s + mr}{K}) - \alpha sC\right) + p_2 \cdot \left(\rho r(1 - \frac{s + mr}{K}) - \beta sr\right). \tag{2.7}$$

From this we deduce the differential equations on the adjoint vector $p = \begin{pmatrix} p_1 \\ p_2 \end{pmatrix}$

$$\begin{cases} \frac{dp_1}{dt} = -\frac{\partial H}{\partial s} = -2As - p_1(\rho(1 - \frac{2s+mr}{K}) - \alpha C) + p_2(\frac{\rho}{K} + \beta)r, & (2.8) \\ \frac{dp_2}{dt} = -\frac{\partial H}{\partial r} = -2Br + p_1\rho\frac{m}{K}s - p_2(\rho(1 - \frac{s+2mr}{K}) - \beta s). & (2.9) \end{cases}$$

In (2.7), the treatment C only appears as $-\alpha s p_1 C$: the switch function is once again $-\alpha s p_1$. From the Pontryagin Minimum Principle we know that:

— if $\alpha s p_1 > 0$ then $C = C_{\max}$,

— if $\alpha s p_1 < 0$ then $C = 0$,

— if $\alpha s p_1 = 0$ then C is to be determined.

Let us now investigate the case $p_1(t) \equiv 0$ on I, where I is an interval of non-empty interior. In optimal control theory, such an interval is called a singular arc. We want to deduce an expression for C on that interval. First consider (2.8) on that particular interval:

$$0 = -2As + p_2(\frac{\rho}{K} + \beta)r. \tag{2.10}$$

Differentiating this expression gives us:

$$\begin{aligned} \dot{p}_2(\frac{\rho}{K} + \beta)r &= 2A(\rho s(1 - \frac{s+mr}{K}) - \alpha s C) - p_2(\frac{\rho}{K} + \beta)(\rho r(1 - \frac{s+mr}{K}) - \beta s r) \\ &= 2A(\rho s(1 - \frac{s+mr}{K}) - \alpha s C) - 2As(\rho(1 - \frac{s+mr}{K}) - \beta s) \\ &= 2A(\beta s - \alpha C)s. \end{aligned}$$

Moreover, injecting (2.10) in (2.9):

$$\dot{p}_2(\frac{\rho}{K} + \beta)r = -2Br^2(\frac{\rho}{K} + \beta) - 2As(\rho(1 - \frac{s+2mr}{K}) - \beta s).$$

So that in the end:

$$(\beta s - \alpha C)s = -\frac{B}{A}r^2(\frac{\rho}{K} + \beta) - s(\rho(1 - \frac{s+2mr}{K}) - \beta s).$$

We now have an expression for C on a singular arc :

$$\begin{aligned} C(t) &= \frac{1}{\alpha s}\left(\frac{B}{A}r^2(\frac{\rho}{K} + \beta) + s\rho(1 - \frac{s+2mr}{K})\right)(t) & (2.11) \\ &= \frac{1}{\alpha s}\left(r(\frac{B}{A}(\frac{\rho}{K} + \beta)r - s\rho\frac{m}{K}) + s\rho(1 - \frac{s+mr}{K})\right)(t). & (2.12) \end{aligned}$$

One should note that this can only hold if $0 \leq C \leq C_{\max}$.

Moreover, if we denote $\tilde{\psi}(t) = s^2(t) + r^2(t)$, such that $\psi(T) = \tilde{\psi}(T) + \int_0^T (As^2(t) + Br^2(t))dt$, the Pontryagin Minimum Principle states that the adjoint p corresponding to the optimal control satisfies $p(T) = p_0\nabla\tilde{\psi}(T)$. An argument similar to the proof of Theorem 6 allows us to take $p_0 = 1$, so $p_1(T) = 2s(T) > 0$. Hence we have $C(T) = C_{\max}$.

□

In the following, treatments that contain such a singular arc will be called biologically optimal treatments (BOD).

Legendre-Clebsch condition

Theorem 7 only states the possible forms of an optimal treatment. Depending on the parameters in the equations, the time T and the initial condition, it might happen that the optimal treatment does not provide any singular arc (or minimal). The second order condition of Legendre-Clebsch [BC03] states that, on a singular arc,

$$\frac{\partial}{\partial C}\frac{d^2}{dt^2}\frac{\partial H}{\partial C} < 0.$$

We will show the following property:

Theorem 8. *On any singular arc defined by 7, the Legendre-Clebsch second order condition is satisfied.*

Proof. We want to compute the succesive derivatives of the Hamiltonian H to investigate the Legendre-Clebsch second order condition.

$$\frac{\partial H}{\partial C} = -p_1 \alpha s$$

We define

$$f(s,r) = \begin{pmatrix} \rho s(1 - \frac{s+mr}{K}) \\ \rho r(1 - \frac{s+mr}{K}) - \beta sr \end{pmatrix}$$
$$g(s,r) = \begin{pmatrix} -\alpha s \\ 0 \end{pmatrix}$$
$$x = \begin{pmatrix} s \\ r \end{pmatrix}$$

so that $-p_1 \alpha s = \langle p, g \rangle$.

We then note the following result: for $x : [0,T] \to \mathbb{R}^2$ a solution of (2.3), p the associated adjoint, and h any differentiable vector field, we have

$$\frac{d}{dt}\langle p, h(x)\rangle(t) = -2A\langle x(t), h(x(t))\rangle + \langle p(t), [f + Cg, h](x(t))\rangle$$

where $[a,b](x) = Db(x)a(x) - Da(x)b(x)$ is the Lie bracket, and Da and Db are the matrices of partial derivatives. This result comes from (2.8) and (2.9).

Thus we get:

$$\begin{aligned}\frac{d}{dt}\frac{\partial H}{\partial C}(t) &= -2A\langle x(t), g(x(t))\rangle + \langle p(t), [f + Cg, g](x(t))\rangle \\ &= 2A\alpha s^2 + \langle p(t), [f,g](x(t))\rangle\end{aligned}$$

so that

$$\frac{d^2}{dt^2}\frac{\partial H}{\partial C}(t) = 4A\alpha s(\rho s(1 - \frac{s+mr}{K}) - \alpha s C) - 2A\langle x, [f,g]\rangle + \langle p, [f + Cg, [f,g]]\rangle$$
$$\frac{\partial}{\partial C}\frac{d^2}{dt^2}\frac{\partial H}{\partial C} = -4A\alpha^2 s^2 + \langle p, [g, [f,g]]\rangle$$

Let us perform some intermediary calculations:

$$Df = \begin{pmatrix} \rho(1 - \frac{2s+mr}{K}) & -\frac{\rho m}{K}s \\ -(\frac{\rho}{K} + \beta)r & \rho(1 - \frac{s+2mr}{K}) - \beta s \end{pmatrix} \quad , \quad Dg = \begin{pmatrix} -\alpha & 0 \\ 0 & 0 \end{pmatrix}$$

$$[f,g] = (Dg)f - (Df)g = -\alpha s \begin{pmatrix} \frac{\rho}{K}s \\ (\frac{\rho}{K}+\beta)r \end{pmatrix} \quad , \quad D[f,g] = -\alpha \begin{pmatrix} \frac{2\rho}{K}s & 0 \\ (\frac{\rho}{K}+\beta)r & (\frac{\rho}{K}+\beta)s \end{pmatrix}$$

$$[g,[f,g]] = (D[f,g])g - (Dg)[f,g] = \alpha^2 s \begin{pmatrix} \frac{\rho}{K}s \\ (\frac{\rho}{K}+\beta)r \end{pmatrix}$$

thus:

$$\frac{\partial}{\partial C}\frac{d^2}{dt^2}\frac{\partial H}{\partial C} = -4A\alpha^2 s^2 + p_1\alpha^2 s^2 \frac{\rho}{K} + p_2\alpha^2(\frac{\rho}{K}+\beta)rs$$

On a singular arc, we then get:

$$\begin{aligned} \frac{\partial}{\partial C}\frac{d^2}{dt^2}\frac{\partial H}{\partial C} &= -4A\alpha^2 s^2 + p_1\alpha^2 s^2 \frac{\rho}{K} + p_2\alpha^2(\frac{\rho}{K}+\beta)rs \\ &= s\alpha^2(p_2(\frac{\rho}{K}+\beta)r - 4As) \\ &= -2A\alpha^2 s^2 < 0 \end{aligned}$$

Thus the Legendre-Clebsch second order condition is satisfied for any (s,r).

□

Because of this result, we cannot draw supplementary descriptions of the singular arc from this theorem.

2.4 Comparison of numerical results

Theorem 7 states the values that an optimal treatment C for cost L_2 can take at each time t. Using this information, we want to numerically answer Problem 3.

To simplify the numerical optimization and get it closer to a medical treatment, some conditions are added. To help the patient recover after a large dose of drug, any period of MTD treatment ($C(t) = C_{\max}$) must be followed by a period without treatment ($C(t) = 0$), so that the patient's organism can have a rest. Also, the treatment is given by cycles, during a period of one month (30 days), as it is performed in clinical tests. The numerical optimization is performed on the length of each time arc, using built-in optimization tools from Scilab. We chose $B/A = m^2$ for size coherence.

We have thus transformed the optimization probem 3 into the following problem: minimize the cost L_2 on periodic functions $\tilde{C} : [0,T] \to [0, C_{\max}]$ of period $t_1 + t_2 + t_3$, where

$$\tilde{C}(t) = \begin{cases} 0 \text{ on } [0,t_1) \\ C_{\text{sing}}(s(t),r(t)) \text{ on } [t_1, t_1+t_2) \\ C_{\max} \text{ on } [t_1+t_2, t_1+t_2+t_3) \end{cases}$$

where C_{sing} is the singular arc defined by (2.12).

During some numerically tested treatments, long periods without or with little treatment make the resistant population decrease a lot. Numerical errors might then let $r < 0$ on such periods. To prevent this effect, we include a reserve of quiescent resistant cells: a constant amount of resistant cells $q := 10^{-3}$ that can produce resistant cells r. The equation on r now becomes:

$$\frac{dr}{dt} = \rho r(1 - \frac{s+mr}{K}) - \beta sr + q.$$

	FTO	Adaptive	BOD	MTD	Unit
Initial number of sensitive/resistant cells	5000/500	5000/500	5000/500	5000/500	cells
Total L_2 cost	1.2	2.9	1.5	3.0	cells^2
Maximal cells number	90700	86900	97400	228700	cells
Total used drug	380	310	320	300	nM
Cycles number	×	×	3	5	
Total time under $C = C_{\max}$	48	0	72	144	h
Total time with less than 5000 cells	24	0	96	144	h
Mean percentage of resistant cells the ten last days	3.98	0.0001	1.25	1.45	%

Table 2.2 – Comparison between FTO, adaptive, BOD and MTD protocols

The results presented on Fig.2.6c show how the number of cells is kept at a low level for the whole experiment. Periods without treatment allow the sensitive population to gain strength, until they are enough to kill the resistant cells. Then the therapy begins at a low level, maintaining the cells at a certain population number. When resistant cells are almost killed off, massive therapy begins to swipe the remaining sensitive cells. Then the resting time allows the sensitive cells population to recover again.

In order to compare this schedule to others, we determined three different protocols for the same problem. First, we used a numerical optimization software, AMPL, to solve Problem3. Time is discretized with steps of $1h$. Its results are presented on Fig.2.6a: we will later refer to this protocol as the Fixed Time Optimal (FTO). Second, we implemented the stabilization strategy we defined in 2.3.1: the results are presented on Fig.2.6b. Finally, to illustrate the advantage of metronomic treatments over the ones currently in use in medical protocols, we optimized the cost L_2 for cycling treatments that only allow $C(t) = 0$ or $C(t) = C_{\max}$. It is represented on Fig.2.6d. Several interesting informations on those different protocols are summed up in Tab.2.2.

The cost L we chose is minimized by the FTO treatment. The BOD protocol, which includes forced cycles, fares also well under this criterion, while MTD and adaptive protocols present a high cost. The four of them use roughly the same amount of drug during the experiment, but the adaptive protocol is the only one to never use the maximal dosage of $5nM/h$. For a clinical use, the time with small tumoral charge will be important too: the adaptive protocol does not provide any, while during the two cycling schedules, the Petri dish is regularly ridden of almost all cancerous cells. In the FTO protocol, at the end of the experiment the resistant population is no longer under control: thus, contrary to the other strategies, the mean resistant cells proportion in the tumour at the end is really higher for this situation than the other. Especially, because the aim of the adaptive strategy is to reach a limit population with no resistant cells, it fares way better than the other three protocols on this criterion.

The uses and drawbacks of those different protocols will be discussed in 2.5.

2.5 Discussion

We developed a mathematical model to predict the behaviour of competing cancerous cells under various treatment schedules. A study of the dynamical system gives then an idea of an interesting schedule of the drug, to stabilize the tumour at a low level, and a further optimization gives an other interesting schedule.

The Tab.2.2 compares the numerical results of the FTO, adaptive, BOD and an optimal MTD protocols. The FTO protocol answers numerically Problem 3, but would not be considered

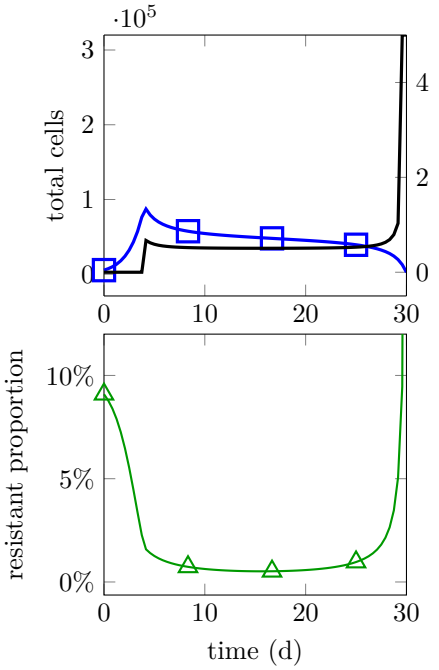

(a) Numerical optimal treatment: Fixed time optimum

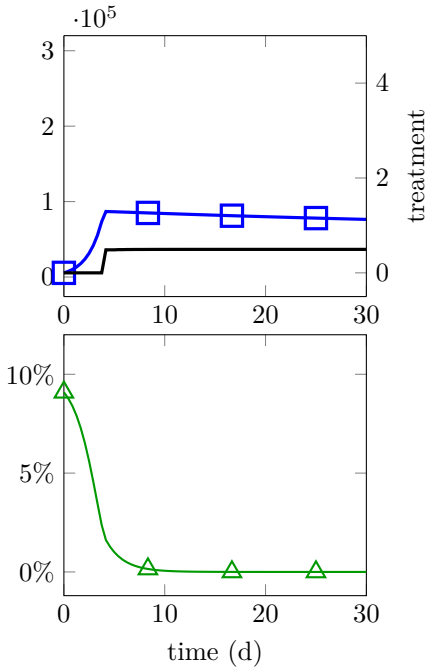

(b) Adaptive protocol

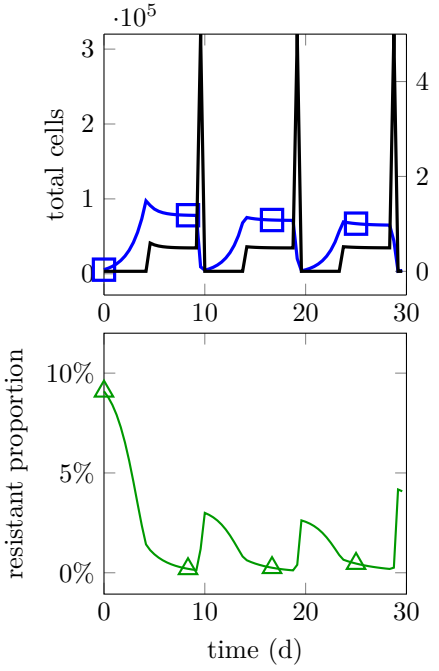

(c) Biologically optimal dose protocol

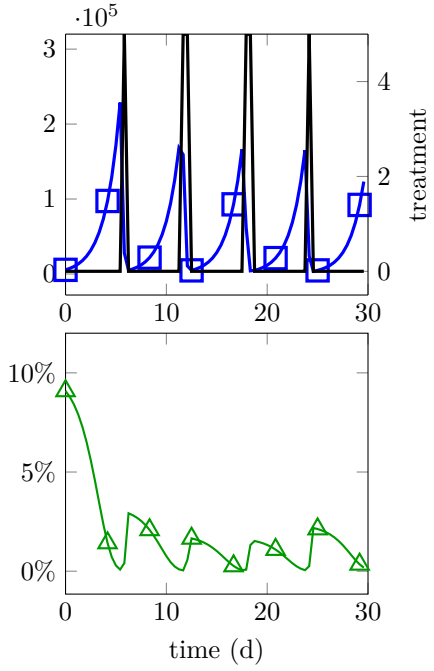

(d) Maximal tolerated dose protocol

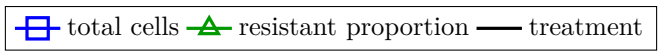

Figure 2.6 – Four different protocols are presented, with the total number of cells in the well coloured in red, the treatment evolution in black, and the resistant cells proportion in green

for a medical trial. Indeed, even if the mathematical cost L is minimal for this protocol among the four schedules we study, it does not ensure a control on the tumour over a long time. As we see in FIG.2.6a, at the end of the experiment, a large dose of drug is released in order to kill a maximum of sensitive cells. Thus, the resistant cells proportion becomes very important: keeping a control over this tumour after the 30 days treatment might prove more difficult.

The MTD protocol is widely used in medical applications: because it regularly kills a large amount of cancer cells, it is expected that in some cases the tumour will be completely eradicated after the treatment. According to our model, although it does provide the patient a long cumulated time with a reduced tumour charge, it still fares bad on other arguments. First, in order to maintain the resistant cells at a low level, the protocol forces us to allow the tumour to reach a large size at each cycle, which can trigger new effects as the vascularization or metastasis creation, or even kill the patient. Second, as we see on FIG.2.6d, the resistant cells proportion in the tumour is almost always high, meaning we might be losing control on the disease. Moreover, large doses of drug not only harm the cancerous cells but also the immune system, so long periods under $C_{\max}$ and short recovery times should be avoided as they are very toxic.

The adaptive protocol we described in 2.3.1 does not use maximal drug dose delivery: the maximal dose in this treatment is $C_{\text{metro}} = 0.296nM/h$, which is far from the maximal $5nM/h$. This really lessens the treatment toxicity. Its design ensures that the proportion of resistant cells is really low, and decreasing, so that the tumour evolution is really controlled. Moreover, our adaptive protocol can be easily processed *in vitro*, as it even takes into account some of the variability inherent to real experiments. Further studies of its robustness to the parameters and its speed to reach the interesting equilibrium $E_{s,l}$ should be performed.

The BOD protocol we defined in 2.3.2 gives an interesting intermediate to the last two protocols. Although we chose the cost L quite arbitrarily, the resulting optimal schedule stabilizes the tumour at a small level, and regularly reduces it to a group of less than 5000 cells. The presence of resting periods in the schedule is also a good point for medical purposes.

Thus, our study highlighted four treatment protocols, that have diverse advantages and drawbacks. It would be a task for medical teams to chose between them, or to define new objectives for us to study if possible.

These results, although encouraging, should be taken into perspective with the model we used.

By construction, our model does not cover the cancer cells total extinction. A simple approach to address this problem is to consider that when s or r is less than one cell, then the corresponding population went extinct. But that is not a satisfactory behaviour for the resistant population, as we supposed that even when no treatment is applied, resistant cells exist: r should never be extinct in such model. Even worse, a strong drug dose can in practice kill absolutely all sensitive cells, without any chance of rebound. Knowing that, a MTD protocol as in FIG.2.6d would probably kill all sensitive cells at one of the drug injections, so that we would loose all control over the resistant population. BOD protocol fares a little better, as periods with maximal dose are shorter, but it still creates a risk of total extinction. In that outlook, our adaptive protocol ensures that the tumour is always controlled, for an indefinite time.

This model highly relies on two hypotheses about the phenomenon of resistance. First, that there exists two genuine populations of cells, one strictly sensitive to the drug and one resistant to it, rather than a continuous trait of resistance. Second, that a lineage never evolves from one category to the other. This might not be the case for a different lineage of cancer cells, and especially not for *in vivo* experiments. However, this biological model already shows that an intermediate dose of treatment might be better to prevent the resistance of a tumour to a certain drug, rather than MTD treatment schedule.

Another limitation of our model is the fact that no spatial terms are taken into account. It

might be interesting to do so, as further experiments by M. Carré performed on tumour spheroids showed that the initial repartition of the cells can have an impact on the outcome. Indeed, at the end of experiments where sensitive cells are predominant, remaining resistant cells tend to be found in clusters. In that case, the Optimal Control Theory will be more complex to use, so numerical optimization solvers could become a more interesting strategy. Finally, for the moment, the toxicity of the drug is not taken into account in the cost L: that may be a further work to consider.

Nonetheless, since this model was developed from considerations of simple, *in vitro* experiment, it has several advantages. First, very few parameters are needed to simulate effectively the behaviour of the system. They have a good biological interpretation, and can easily be measured. Second, *in vitro* experiment can be conducted easily compared with experiments involving living animals. Our hypothesis will thus be easy to check, and new experiments do not cost much.

Now that our model produced some optimal schedules, it will be interesting to test them *in vitro*. This will be performed at the CRO2, and the results will be analysed and commented by both the medical and the mathematical team. Especially, the adaptive strategy is quite easy to test, and is more likely to be chosen by medical teams.

Although this study presents qualitative and quantitative results on optimal treatments for *in vitro* experiments, no *in vivo* direct application is considered: cancerous cells tend to act very differently inside real organs than in a Petri dish, as too many biological phenomenons are set aside in the latter. Our results can be used as guidelines, or hindsight for further experiments, but not as an actual treatment schedule.

Acknowledgements

I thank Hasnaa Zidani for the numerous discussions we had on optimal control theory and for her help in understanding and manipulating AMPL. I thank Manon Carré for her explanations on cancerous cells interactions, and for having the courage to test our theoretical protocols on *in vitro* tumours. This work has been carried out in the framework of the project NONLOCAL (ANR-14-CE25-0013), funded by the French National Research Agency (ANR).

Chapter 3

Spreading speeds for a two-species competition-diffusion system

In this paper, spreading properties of a competition-diffusion system of two equations are studied. This system models the invasion of an empty favorable habitat, by two competing species, each obeying a logistic growth equation, such that any coexistence state is unstable. If the two species are initially absent from the right half-line $x > 0$, and the slowest one dominates the fastest one on $x < 0$, then the latter will invade the right space at its Fisher-KPP speed, and will be replaced by or will invade the former, depending on the parameters, at a slower speed. Thus, the system forms a propagating terrace, linking an unstable state to two consecutive stable states.

3.1 Introduction

This paper is devoted to the study of the spreading of the following competition-diffusion system between two species s and r:

$$\begin{cases} \partial_t s - \delta_0 \partial^2_{xx} s = s(\alpha_0 - s - \gamma_0 r), \\ \partial_t r - \partial^2_{xx} r = r(1 - \beta_0 s - r) \end{cases} \tag{3.1}$$

with positive parameters α_0, β_0, γ_0, δ_0 satisfying $1/\beta_0 < \alpha_0 < \gamma_0$, which ensures that equilibria $(\alpha_0, 0)$ and $(0, 1)$ are both stable for the corresponding ODE system. More precisely, for initial conditions where both species are absent from the right half-line $x > 0$, and s dominates r around $x = -\infty$ initially, if s spreads in absence of r slower than r in absence of r, then solutions of (3.1) will approach a propagating terrace, which connects the unstable equilibrium $(0, 0)$ to the stable equilibrium $(0, 1)$, and then the stable equilibrium $(0, 1)$ to the other stable equilibrium $(\alpha_0, 0)$.

Propagating terraces arise when two phenomena spread successively with two different speeds. Two types of speeds are used in the system (3.1): one is linked to a monostable scalar equation, the Fisher-KPP equation, and the second derives from a bistable system of differential equation, which was studied by Y.Kan-On [KO95]. Spreading results for reaction-diffusion equations often use a comparison principle, which derives from a maximum principle on ellipic equations. In

the case of systems of competition-diffusion equations, maximum principles are rarely applicable directly. Moreover, the appearance of two different propagating speeds forming a propagating terrace prevents the direct application of most classical methods of scalar reaction-diffusion equations.

System (3.1) arises from a biological problematic: it describes the propagation of two competing species in a favorable environment. More specifically, it derives from a study on heterogeneous tumours, composed of cancerous cells that are sensitive or resistant to a certain drug. But this result can be applied to several other biological systems, for example invading species in ecology, or also to chemical reactions.

Definition and properties of Fisher-KPP and bistable competition-diffusion travelling waves, alongside with developments linked to these equations, are recalled in the following. This will allow us to define some notations that will be used in the rest of the article.

Fisher-KPP equation In the model (3.1), if $r(x,t) \equiv 0$ or $s(x,t) \equiv 0$, the other function obeys a Fisher-KPP equation, which is a classical model for species growth and propagation [KPP37, Fis37]. It models the evolution of a population $n = n(x,t)$ depending on both position $x \in \mathbb{R}$ and time $t \geq 0$. Individuals move randomly in space, divide at a certain maximal rate ρ and compete over nutrients:

$$\partial_t u(x,t) - D\Delta_x u(x,t) = u(x,t)(\rho - u(x,t)). \tag{3.2}$$

When system (3.2) is considered on $x \in \mathbb{R}$, it admits travelling fronts solutions, *i.e.* solutions of the form $u(x,t) = U(x-ct)$ where c is a constant. For sake of notations, the following well-known result from [KPP37] is recalled:

Let (D,ρ) be two positive parameters. For any $c \geq c^* = 2\sqrt{D\rho}$, there exist a unique (up to translation) solution $U \in C^2(\mathbb{R})$ of the equation:

$$\begin{cases} DU'' + cU' + U(\rho - U) = 0, \\ \lim_{\xi\to-\infty} U(\xi) = \rho \text{ and } \lim_{\xi\to+\infty} U(\xi) = 0. \end{cases} \tag{3.3}$$

If U is a solution of (3.3), then $u : (x,t) \mapsto U(x-ct)$ is a solution to (3.2). Moreover, a solution u of (3.2) with Heavyside initial data $u(\cdot,0) = \mathbf{1}_{x<0}$ spreads with speed c^* in the following sense: for any $c < c^*$, it satisfies $\lim_{t\to+\infty} \sup_{x<ct} |u(x,t) - 1| = 0$ and for any $c > c^*$, $\lim_{t\to+\infty} \sup_{x>ct} u(x,t) = 0$.

In the rest of this article, c_S (resp. c_R) will denote the minimal speed associated with parameters $(D,\rho) = (\delta_0, \alpha_0)$ (resp. $(D,\rho) = (1,1)$) for system (3.3). Since all solutions are invariant up to translation, U_S (resp. U_R) will denote one fixed solution of (3.3) for parameters $(D,\rho) = (\delta_0,\alpha_0)$ (resp. $(D,\rho) = (1,1)$) and speed c_S (resp. c_R).

The articles of Fisher [Fis37] and Kolmogorov-Petrovskii-Piscounoff [KPP37] have been a milestone for the field of reaction diffusion equations. In general, we refer to [VVV94] for results on travelling waves in physics and biology, and to [Xin00] for a review of this field of research. In [Bra83], the speed of convergence of solutions u of (3.2) with Heavyside initial data is investigated with more details: the authors show that level sets of u travel at a speed slower than c^*. On an other hand, [HR10] exhibited a family of initial conditions for (3.2) such that the solution spreads with accelerated speed.

System of competition-diffusion equations System (3.1) is a model of two different species competing and dispersing in the same habitat. They both follow a Fisher-KPP model for growth and interaction, but the parameters might differ from one species to another. After a change of

variables and states, the system can be reduced to (3.1), where α_0, β_0, γ_0 and δ_0 are positive constants. Results on the behaviour of (3.1) depend on the values of the parameters, and on the behaviour of the corresponding ODE system:

$$\begin{cases} \partial_t s = s(\alpha_0 - s - \gamma_0 r), \\ \partial_t r = r(1 - \beta_0 s - r). \end{cases} \tag{3.4}$$

The asymptotic behaviour of this system depends on parameters $(\alpha_0, \beta_0, \gamma_0)$. If $\alpha_0 \leq \min(\gamma_0, 1/\beta_0)$, then $\lim_{t\to+\infty}(s,r)(t) = (0,1)$: the r population is the only one stable. If $\gamma_0 < \alpha_0 < 1/\beta_0$, then

$$\lim_{t\to+\infty}(s,r)(t) = \left(\frac{1-\alpha_0\beta_0}{1-\beta_0\gamma_0}, \frac{\alpha_0-\gamma_0}{1-\beta_0\gamma_0}\right)$$

which means that a mixed population is stable. If $1/\beta_0 < \alpha_0 < \gamma_0$, then both $(\alpha_0, 0)$ and $(0,1)$ are stable: almost every solution converges to one of them as $t \to +\infty$. Finally, if $\alpha_0 \geq \max(1/\beta_0, \gamma_0)$, then $\lim_{t\to+\infty}(s,r)(t) = (\alpha_0, 0)$: the s population is the only one stable. In this paper, the bistable case is considered: $1/\beta_0 < \alpha_0 < \gamma_0$.

This range of parameters defines a set of competition-diffusion bistable PDE systems. There exists diverse results on such systems, especially in ecology modelling. In [KO95], Y. Kan-On demonstrates the following result:

Let $(\alpha, \beta, \gamma, \delta)$ be four positive parameters, such that $1/\beta < \alpha < \gamma$. Then there exists a unique speed $c \in (-2, 2\sqrt{\alpha\delta})$ such that the system

$$\begin{cases} \delta U'' + cU' + U(\alpha - U - \gamma V) = 0, \\ V'' + cV' + V(1 - \beta U - V) = 0, \\ \lim_{\xi\to-\infty} U(\xi) = \alpha \text{ and } \lim_{\xi\to+\infty} U(\xi) = 0, \\ \lim_{\xi\to-\infty} V(\xi) = 0 \text{ and } \lim_{\xi\to+\infty} V(\xi) = 1 \end{cases} \tag{3.5}$$

admits a solution $(U, V) \in C^2(\mathbb{R})$. This solution is furthermore unique up to translation, positive, U is decreasing and V is increasing. The speed c depends continuously on the parameters (α, β, γ), is increasing with respect to α and β and decreasing with respect to γ.

Since solutions of (3.5) are unique up to translation, in the rest of this article, (S, R) will denote a fixed pair of solutions and c_{SR} the speed solution of (3.5) for parameters $(\alpha, \beta, \gamma, \delta) = (\alpha_0, \beta_0, \gamma_0, \delta_0)$.

In relation to this result, [Gar82] showed with a degree theoretic approach that such travelling waves are $\mathcal{C}^0$ stable. Recently [GN15] shows that travelling waves still exist if the competition becomes strong, which is to be expected for very aggressive species. In the setting of this article, it corresponds to fixing $\gamma = \beta k$, and letting $k \to +\infty$. Finally, [BW13] demonstrated the existence and stability of pulsating waves if the parameters α_0, β_0, γ_0 and δ_0 are all periodic in time with the same period: this would, for example, model a periodic external action on the environment.

Propagating terraces Bearing in mind that travelling waves exist between the two stable states, a spreading result will here be demonstrated, *i.e.* the long-time behaviour of the system for a class of initial conditions. Suppose species s and r are present on the left side of the plane, with r smaller than a certain exponential function at $t = 0$:

$$\begin{cases} s(x,0) = \phi(x) \text{ for } x < 0 \text{ with } 0 < \phi_m \leq \phi(x) \leq \phi_M < \alpha_0, \\ s(x,0) = 0 \text{ for } x \geq 0, \\ 1 > r(x,0) > 0 \text{ for } x < 0 \text{ and } r(x,0) = \underset{x\to-\infty}{O}(-xe^{\frac{1}{2}x}), \\ r(x,0) = 0 \text{ for } x \geq 0. \end{cases} \tag{3.6}$$

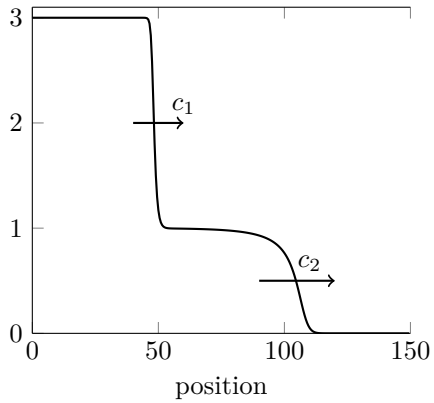

Figure 3.1 – Numerical simulation of a propagating terrace for $f(u) = u(u-1)(u-1.2)(u-3)$

Numerical experiments suggest that the long-time behaviour of this system is organized in a propagating terrace, which means that several speeds of invasion can be observed, depending on the parameters. Propagating terraces have been first exhibited by [FM77] for a scalar equation $\partial_t u - \Delta u = f(u)$, with f bistable on range $[0, a]$ with speed c_1, and bistable on range $[a, 1]$ with speed $c_2 > c_1$.

Figure 3.1 shows a numerical example of propagating terrace, performed on Scilab.

In recent developments, [DGM14] proved that such propagating terraces exist and are stable in a sense for periodic in space medium. The proof of theorem 9 will develop technics to show the existence of a propagating terrace for a system of coupled differential equations. In [DGM], the authors show that a prey-predator system will develop such propagating terraces. If the prey is faster than its predator, it will develop out of the predator's reach, at its natural speed (*i.e.* the speed at which it would propagate if there was no predators), then it is preyed on at a lower speed. The proof of invasion of the empty space relies on properties of the growth function of preys similar to Fisher-KPP. As growth functions in (3.1) are of Fisher-KPP type, the invasion of empty space will rely on a similar proof. On another hand, competition will intervene in the proof of replacement of one species by the other in (3.1): this competition is not symmetrical in [DGM], thus their results do not apply in the present paper case.

Statement of the theorem and outline of the paper The aim of this paper is to demonstrate the following theorem:

Theorem 9. *Let* (s, r) *be a bounded solution of* (3.1) *with initial conditions* (3.6) *where the parameters* $(\alpha_0, \beta_0, \gamma_0)$ *satisfy the bistability criterium:*

$$\frac{1}{\beta_0} < \alpha_0 < \gamma_0 \tag{3.7}$$

Then the following spreading results hold:

$$\forall\ c > \max(c_S, c_R), \lim_{t\to+\infty} \sup_{x>ct} |s(x,t)| + |r(x,t| = 0, \tag{3.8}$$

$$\forall\ c < c_{SR}, \lim_{t\to+\infty} \sup_{x<ct} |s(x,t) - \alpha_0| + |r(x,t)| = 0. \tag{3.9}$$

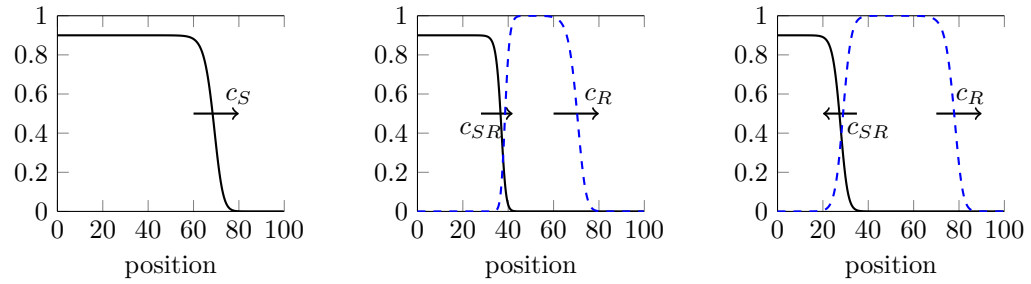

(a) If $c_S > c_R$ and $c_{SR} > 0$, population r is not visible.

(b) If $c_S < c_R$ and $c_{SR} > 0$, r creates a front at speed c_R, and is then replaced by s.

(c) If $c_S < c_R$ and $c_{SR} < 0$, r creates a front at speed c_R on the right and replaces s at speed c_{SR} on the left.

Figure 3.2 – Numerical simulations of the system for different values of the parameters: the global behaviour depends on the comparison between c_S and c_R, and on the sign of c_{SR}.

Suppose furthermore that $c_S < c_R$, then

$$\forall\ c_{SR} < c_1 < c_2 < c_R, \lim_{t\to+\infty} \sup_{c_1 t<x<c_2 t} |s(x,t)| + |r(x,t) - 1| = 0. \tag{3.10}$$

In the case $c_S > c_R$, the behaviour of the system depends on the sign of c_{SR} and on the initial conditions. Indeed, if $c_{SR} > 0$, one can adapt the proof to show that

$$\forall\ c > c_S, \lim_{t\to+\infty} \sup_{x>ct} |s(x,t)| + |r(x,t| = 0, \tag{3.11}$$

$$\forall\ c < c_S, \lim_{t\to+\infty} \sup_{x<ct} |s(x,t) - \alpha_0| + |r(x,t)| = 0. \tag{3.12}$$

The system thus almost eliminates species r: it does not appear in the long time behaviour. If $c_{SR} < 0$, the global behaviour depends on the initial repartition of s and r, this case is not treated in this paper.

Figure 3.2 shows numerical simulations of the evolution of (3.1), preformed on Scilab for different values of the parameters.

A partial result for (3.10) can be extended to a more general type of growth functions. More specifically, the limit result:

$$\forall\ c_S < c_1 < c_2 < c_R, \lim_{t\to+\infty} \sup_{c_1 t<x<c_2 t} |s(x,t)| + |r(x,t) - 1| = 0$$

still holds if instead of system (3.1) we consider:

$$\begin{cases} \partial_t s - \partial^2_{xx} s = sF(s,r), \\ \partial_t r - \delta \partial^2_{xx} r = rG(s,r) \end{cases}$$

where F, G are $\mathcal{C}^1$ functions satisfying:

— $\forall s > 0$ (resp. $r > 0$), $r \mapsto F(s,r)$ (resp. $s \mapsto G(s,r)$) is stricly decreasing,
— there exists $a, b > 0$ such that $F(a,0) = 0$ and $G(0,b) = 0$,
— $\forall s \in [0,a)$ (resp. $r \in [0,b)$, $F(s,0) > 0$ (resp. $G(0,v) > 0$),
— $\forall s, r \geq 0$, $F(s,r) \leq F(0,r)$ and $G(s,r) \leq G(s,0)$.

The first hypothesis ensures that there is competition between the two species. The second and third ones give us a hair-trigger effect: when only one of the species is present, it will grow until it reaches its maximum capacity, a or b. The last hypothesis, finally, states that the species attain their maximal growth rates for small densities ; this suggests that their propagation speeds can be determined by the leading edge, as in the Fisher-KPP framework. For more details on this proof, see [DGM].

However, the proofs of (3.9) and (3.10) heavily rely on the existence of a travelling wave connecting the two stable states $(\alpha_0, 0)$ and $(0,1)$, and on the dependance of the speed c_{SR} on α_0 and other parameters. These results all are present in [KO95], but as far as the author knows, they have not been generalized to other types of growth functions. Theorem 9 is thus stated only under the Fisher-KPP hypothesis.

This paper is organized as follows. The first part will present the biological problem which called for the study of system (3.1), and an interpretation of Theorem 9. In the second part, a lemma that will be useful for the whole study is stated ; the system behaviour far from competition is then studied, showing that the fastest species can grow out of reach of the slowest one. The third part is concerned with what happens in the competition zone, and will show that the replacement of one species by the other will in fact occur at the speed defined by Kan-On [KO95].

3.2 Biological interpretation: a model of cancer growth

Model (3.1) has been used to study heterogeneous tumour growth. Solid tumours are subject to non uniform phenomena, and as such, can develop heterogeneous behaviours. Especially, the use of chemotherapy to cure cancers often triggers the emergence of resistant lineages, that will not be affected by the drug, by selecting them against more sensitive cells. When the tumour does not reply to the treatment any more, medical doctors then have to find a different drug, if it exists, to tackle this new kind of cancerous cells, which can be more harmful for the patient. In any case, appearance of a resistance to the chemotherapy is a cause of treatment failure, and should be avoided. Moreover, cytotoxic drugs, which are widely used in classical protocols, cause unwanted toxic side effects, thus their dosage should be carefully designed.

These problems can be addressed by *in vivo* or *in vitro* experimentation, and also by mathematical modelling of the different phenomena inside tumours. Therapy optimization in the case of heterogeneous tumours, for example, has been studied among others with the use of cellular automata [RTGGA15, GSGF09], with the construction of complex systems and their numerical studies [ABB+13], and also with the construction of simple models and their analytical studies, using, for example, Pontryagin Maximum Principle [dLMS09, LS14]. We refer to [CLC16] for a review of mathematical modelling of resistance apparition in solid tumours.

In a previous article [1], the author studied the effect of chemotherapy on heterogeneous tumours. A series of biological experimentations on *in vitro* tumours, composed of sensitive and resistant cells, showed that large doses of chemotherapy would kill all sensitive cells and let resistant cells grow to a maximum population. A mathematical ODE model adapted to these experimentations was designed, and different adaptive treatment protocols to reduce risks of resistance to chemotherapy were constructed, notably with optimal control theory. The main idea is to choose the maximal drug dosage such that, in the model (3.4), a population with only

sensitive cells is stable and locally attractive, and to bring the system in this bassin of attraction. In order to better understand the experiments, it appeared crucial that spatial diffusion should be taken into account, which is why system (3.1) was constructed.

Spatial heterogeneity has a great influence on cancer virulence and evolution, as illustrated in [GG96]. In [LLC+15], the authors construct a model of solid tumours taking into account spatial diffusion of nutrients, treatment and cells, as well as the resistance of cells as a continuous trait. Diverse treatment protocols can be tested and compared in this framework, like combination of constant infusion and alternative maximum-minimum delivery of cytotoxic drugs. Game theory is used in [BHD08] to explain how a more invasive lineage can be selected against a proliferative one. It uses cellular automata, and support the use of therapies that would increase the cost of motility, in order to maintain the tumour at a benign state. We are developing in our article a PDE model that enhances this idea, that cytotoxic drugs will be efficient as long as it does not favour a more motile lineage.

In model (3.1), s represents the population of cells that are sensitive to a certain drug, and r a lineage of resistant cells. They divide, spread and compete at different rates. We do not investigate how the resistant trait emerge, but only how they spread with the tumour once they have appeared. Thus, we do not take into account mutations of sensitive cells into resistant cells, or resistant cells into sensitive cells. Using the hypothesis of mutations, [GR16] showed the existence of a travelling wave connecting $(0,0)$ to a coexistence state. Finally, the action of chemotherapy is taken into account through parameter α_0, the growth rate of s. If no treatment is applied, α_0 is at a maximal value, and as treatment dosage increases, α_0 decreases. The bistability criterium (3.7) states that if $\alpha_0 < 1/\beta_0$, then the sensitive population $(s,r) = (\alpha_0, 0)$ is no longer stable: this property gives us a limit value for treatment dosage. Since we are interested in biological coherent solutions, we only consider bounded solutions of (3.1).

Theorem 9 states that the fastest species will escape the region where the slowest one is present, and act as if there was no competition. Let us rephrase these results in the framework of cancer modelling. If $\alpha_0 > 1/\delta_0$, then the overall growth speed of the tumour is $2\sqrt{\delta_0\alpha_0}$, this speed decreases as we augment the drug dosage. But as soon as $\alpha_0 < 1/\delta_0$, resistant cells are selected by the treatment, and form a growing ring around the sensitive core ; the global growth speed becomes 2 and does not depend on the treatment any more. Even worse, as α_0 decreases, c_{SR} may become negative: resistant cells will replace sensitive cells in already invaded environments. In a previous paper [1] where no spatial effects were taken into account, we stated that treatment protocols could be designed for the ODE system (3.4), such that the steady state with only sensitive cells is always stable, and that reduce the number of cancerous cells to a minimum. We thus proposed $\alpha_0 > 1/\beta_0$ as a limiting value for the treatment. With spatial effects, we see that the motility of cells – that is, their ability to move – should also be taken into account when designing a treatment protocol, as explained also in [BHD08].

With results from [BW13], we could extent our theorem to time periodic coefficients. This would model, for example, periodic chemotherapy dosages, or periodic growth cycles for cells. As the overall behaviour of solutions from [BW13] only depends on the means and extrema of the parameters, our results would not be drastically modified ; we thus decided not to take this phenomenon into account.

3.3 Outside of competition

3.3.1 Comparison lemma

The following comparison lemma for competitive systems will be crucial in the demonstration of Theorem 9.

Lemma 4 (Comparison principle)**.** *Let (s_1, r_1) and (s_2, r_2) be such that for all $(x,t) \in D \times \mathbb{R}^+$ with $D \subseteq \mathbb{R}$, we have $0 \leq s_i(x,t) \leq \alpha_0$, $0 \leq r_i(x,t) \leq 1$ for $i = 1, 2$, and such that*

$$\begin{cases} \partial_t s_1 - \delta_0 \partial^2_{xx} s_1 - s_1(\alpha_0 - s_1 - \gamma_0 r_1) \leq 0, \\ \partial_t r_1 - \partial^2_{xx} r_1 - r_1(1 - \beta_0 s_1 - r_1) \geq 0 \end{cases} \quad \text{and} \quad \begin{cases} \partial_t s_2 - \delta_0 \partial^2_{xx} s_2 - s_2(\alpha_0 - s_2 - \gamma_0 r_2) \geq 0, \\ \partial_t r_2 - \partial^2_{xx} r_2 - r_2(1 - \beta_0 s_2 - r_2) \leq 0 \end{cases}$$

and such that for all $x \in D$,

$$s_1(x,0) \leq s_2(x,0) \text{ and } r_1(x,0) \geq r_2(x,0),$$

and for all $x \in \partial D$ and $t \geq 0$,

$$s_1(x,t) \leq s_2(x,t) \text{ and } r_1(x,t) \geq r_2(x,t).$$

Then for all $t \geq 0$ and for all $x \in D$,

$$s_1(x,t) \leq s_2(x,t) \text{ and } r_1(x,t) \geq r_2(x,t).$$

This lemma is a consequence of both a comparison theorem for cooperative systems (applied here to $(s, -r)$), which can be found in [PW12], and the Phragmèn-Lindelöf principle, also demonstrated in [PW12].

In order to simplify notations, in the rest of the article the functionals N_1 and N_2 are defined on functions $(u, v) : \mathbb{R} \times \mathbb{R}^+ \to \mathbb{R}$ by:

$$N_1[u,v](x,t) = \partial_t u(x,t) - \delta_0 \partial^2_{xx} u(x,t) - u(\alpha_0 - u - \gamma_0 v), \tag{3.13}$$

$$N_2[u,v](x,t) = \partial_t v(x,t) - \partial^2_{xx} v(x,t) - v(1 - \beta_0 u - v). \tag{3.14}$$

We will also note $(s_1, r_1) \preceq (s_2, r_2)$ if $s_1 \leq s_2$ and $r_1 \geq r_2$.

3.3.2 Limitation of speeds in both directions

This first part will show that the species s and r do not develop faster than if they were without competition.

Recall U_S is a solution of

$$\begin{cases} \delta_0 U_S'' + c U_S' + U_S(\alpha_0 - U_S) = 0, \\ U_S(-\infty) = \alpha_0 \text{ and } U_S(+\infty) = 0 \end{cases} \tag{3.15}$$

with $c = c_S$: it is the KPP front defined in (3.3). There exists $x_0 \in \mathbb{R}$ such that for all $x \in \mathbb{R}$, $\phi(x) \leq U_S(x - x_0)$. Then $(\bar{s}, \underline{r}) : (x,t) \mapsto (U_S(x - x_0 - c_S t), 0)$ satisfies:

$$\begin{aligned} N_1[\bar{s}, \underline{r}](x,t) &= \partial_t \bar{s}(x,t) - \delta_0 \partial^2_{xx} \bar{s}(x,t) - \bar{s}(x,t)(\alpha_0 - \bar{s}(x,t)) \\ &= -c_S U_S'(x - x_0 - c_S t) - \delta_0 U_S''(x - x_0 - c_S t) - U_S(x - x_0 - c_S t)(\alpha_0 - U_S(x - x_0 - c_S t)) \\ &= 0 \end{aligned}$$

and $N_2[\bar{s}, \underline{r}](x,t) = 0$. Thus, according to the comparison lemma 4, $(s, r) \preceq (\bar{s}, \underline{r})$.

Then, let $c > c_S$: the first population s satisfies for every $t \geq 0$ and every $x > ct$:

$$s(x,t) \leq U_S(x - x_0 - c_S t) \leq U_S((c - c_S)t - x_0)$$

because U_S is decreasing. Using that $\lim_{\xi\to+\infty} U_S(\xi) = 0$, we conclude that:

$$\lim_{t\to+\infty} \sup_{x>ct} s(x,t) = 0. \tag{3.16}$$

Reasonning similarly on r we show that, for every $c > c_R$,

$$\lim_{t\to+\infty} \sup_{x>ct} r(x,t) = 0.$$

Moreover, [KPP37] gives an asymptotic estimation on U_R around $+\infty$: there exists $C > 0$ such that

$$U_R(\xi) = C\xi e^{-\frac{c_R}{2}\xi}(1 + \underset{\xi\to+\infty}{o}(1)). \tag{3.17}$$

Thus, we can deduce a similar result around $-\infty$: for any $c > c_R$,

$$\lim_{t\to+\infty} \sup_{x<-ct} r(x,t) = 0$$

in the other direction.

These results conclude the demonstration of (3.8).

3.3.3 Invasion of the empty space by the fastest species

In this section, we will show that the fastest species invades the right empty space at its Fisher-KPP speed. Let us suppose that, for example, $c_R > c_S$.

Lemma 5. *Let c_1, c_2 be two speeds such that $c_S < c_1 < c_2 < c_R$. Then*

$$\lim_{t\to+\infty} \sup_{c_1 t<x<c_2 t} |s(x,t)| + |r(x,t) - 1| = 0.$$

It is a partial proof of (3.10). We already know because of 3.3.2 that

$$\lim_{t\to+\infty} \sup_{c_1 t<x<c_2 t} |s(x,t)| = 0$$

for any $c_S < c_1 < c_2 < c_R$. The idea of this lemma is that because r moves faster than s, it does not see any competition ahead of $c_S t$, and thus acts as a Fisher-KPP front.

To prove this, we will need an intermediate lemma:

Lemma 6. *For any c such that $c_S < c < c_R$, for any $x \in \mathbb{R}$, we have*

$$\lim_{t\to+\infty} r(x + ct, t) = 1$$

where the convergence is uniform on every compact for x.

Proof. This proof will be divided into three steps. Let c be such that $c_S < c < c_R$.

Step 1: Let c' be such that $c < c' < c_R$. We claim that there exists $a > 0$, $x_2 \in \mathbb{R}$ and $\eta_1 > 0$ such that:

$$\liminf_{t\to+\infty} \inf_{x\in(-a,a)} r(x + ct + x_2, \frac{ct}{c'}) \geq \eta_1. \tag{3.18}$$

In other words, the solution r is greater than a small bump travelling at the speed c'.

To prove this, let $\epsilon > 0$ be such that:

$$c' < 2\sqrt{1 - \epsilon\beta_0} < c_R. \tag{3.19}$$

For any $a > 0$, we define $\psi_a : \mathbb{R} \to \mathbb{R}$ the principal eigenfunction of the Laplace operator on a ball $[-a, a]$ with Dirichlet boundary conditions, normalized with $||\psi_a||_\infty = 1$, *i.e*:

$$\begin{cases} \partial^2_{xx}\psi_a = \lambda_a\psi_a \text{ on } (-a, a), \\ \psi_a(-a) = \psi_a(a) = 0, \\ \psi_a > 0 \text{ on } (-a, a), \\ ||\psi_a||_\infty = 1. \end{cases} \tag{3.20}$$

Here, λ_a is the principle eigenvalue and satisfies $\lambda_a < 0$ for any $a > 0$, and tends to 0 as a tends to $+\infty$. In the following, we extend the definition of ψ_a on the whole space by setting $\psi_a(x) = 0$ if $|x| \geq a$.

We now define:

$$\underline{r}(x, t) := \eta e^{-\frac{c'}{2}(x-c't)}\psi_{2a}(x - c't - x_2)$$

where a, x_2 and η will be characterized later. Let $\bar{s}(x, t) := U_S(x - x_0 - c_S t)$, where x_0 is such that $(s, r) \preceq (\bar{s}, 0)$. There exists $x_1 \in \mathbb{R}$ such that for any $x > x_1 + x_0 + c_S t$, we have $\bar{s}(x, t) < \epsilon$. We will choose a, x_2 and η such that $(s, r) \preceq (\bar{s}, \underline{r})$. First,

$$\begin{aligned} N_1[\bar{s}, \underline{r}](x, t) &= \partial_t\bar{s}(x, t) - \delta_0\partial^2_{xx}\bar{s}(x, t) - \bar{s}(x, t)(\alpha_0 - \bar{s}(x, t) - \gamma_0\underline{r}(x, t)) \\ &= \gamma_0 U_S(x - c_S t - x_0)\underline{r}(x, t) \\ &\geq 0. \end{aligned}$$

Moreover, by taking $x_2 \geq x_1 + 2a$, we ensure that for $-2a < x - c't - x_2 < 2a$, we have $\underline{r}(x, t) > 0$ and $\bar{s}(x, t) = U_S(x - c_S t - x_0) \leq U_S(x - c't - x_0) \leq U_S(-2a + x_2 - x_0) \leq \epsilon$. Thus:

$$\begin{aligned} N_2[\bar{s}, \underline{r}](x, t) &= \partial_t\underline{r}(x, t) - \partial^2_{xx}\underline{r}(x, t) - \underline{r}(x, t)(1 - \beta_0\bar{s}(x, t) - \underline{r}(x, t)) \\ &\leq \left(\frac{c'^2}{4} - \lambda_{2a}\right)\underline{r}(x, t) - \underline{r}(x, t)(1 - \beta_0\epsilon - \underline{r}(x, t)) \\ &\leq \underline{r}(x, t)\left(\frac{c'^2}{4} - \lambda_{2a} - (1 - \beta_0\epsilon - \underline{r}(x, t))\right). \end{aligned}$$

We can then choose a large enough such that $\frac{c'^2}{4} - \lambda_{2a} - (1 - \beta_0\epsilon) < 0$ because of (3.19), and η small enough such that $\frac{c'^2}{4} - \lambda_{2a} - (1 - \beta_0\epsilon - \eta e^{-\frac{c'}{2}(x_2-2a)}) < 0$. Then $N_2[\bar{s}, \underline{r}](x, t) \leq 0$ for all $(x, t) \in \mathbb{R} \times \mathbb{R}^+$.

Finally, for any fixed $t_0 > 0$, we can further reduce η such that $r(x, t_0) \geq \underline{r}(x, t_0)$. Then, by the comparison lemma 4, $(s, r) \preceq (\bar{s}, \underline{r})$. By setting

$$\eta_1 := \eta e^{-\frac{c'}{2}(x_2+a)} \min_{x\in(-a,a)} \psi_{2a}(x),$$

we get that, since $r(x, \frac{ct}{c'}) \geq \underline{r}(x, \frac{ct}{c'}) = \underline{r}(x - ct, 0)$, the limit (3.18) is satisfied.

Step 2: We now claim that there exists $b > 0$, $\eta_2 > 0$ and $x_3 \in \mathbb{R}$ such that

$$\liminf_{t\to+\infty} \inf_{\substack{x\in(-b,b)\\ t'\in(\frac{ct}{c'},t)}} r(x+ct+x_3,t') > \eta_2. \tag{3.21}$$

In other words, the bump does in fact persist under r for time t' between $\frac{ct}{c'}$ and t.

For that, let us fix $t > 0$, and define:

$$\underline{\underline{r}}(x,t') := \eta'\psi_a(x-ct-x_2)$$

where η' will be characterized later. For any $t' < t$, the pair $(\bar{s}, \underline{\underline{r}})$ satisfies $N_1[\bar{s}, \underline{\underline{r}}](x,t') \geq 0$, and:

$$\begin{aligned} N_2[\bar{s}, \underline{\underline{r}}](x,t') &= \partial_t \underline{\underline{r}}(x,t') - \partial^2_{xx}\underline{\underline{r}}(x,t') - \underline{\underline{r}}(x,t')(1-\beta_0\bar{s}(x,t') - \underline{\underline{r}}(x,t')) \\ &\leq -\underline{\underline{r}}(x,t')(1+\lambda_a - \underline{\underline{r}}(x,t') - \beta_0\epsilon). \end{aligned}$$

By increasing a if necessary, we can suppose $1+\lambda_a-\beta_0\epsilon > 0$. Then, by taking $\eta' < 1+\lambda_a-\beta_0\epsilon$, we get that $N_2[\bar{s}, \underline{\underline{r}}](x,t') \leq 0$ for any $t' < t$. We can further reduce η' such that $r(x+ct+x_2, \frac{ct}{c'}) \geq \underline{\underline{r}}(x, \frac{ct}{c'})$. Because of (3.18), for t large enough, η' does not depend on t. Then, by the comparison lemma 4, we have $(s,r) \preceq (\bar{s}, \underline{\underline{r}})$ for any $x \in \mathbb{R}$ and any t' such that $\frac{ct}{c'} < t' < t$. By setting $b = \frac{a}{2}$ and $\eta_2 = \eta' \min_{x\in(-b,b)} \psi_a(x)$, we get (3.21).

Step 3: Now we demonstrate the convergence towards 1 of $r(x+ct,t)$ when $t \to +\infty$, uniformly on compact subsets. Let $(t_n)_n$ be such that $t_n \to +\infty$. We define the following sequence of functions:

$$r_n(x,t) = r(x+ct_n, t+t_n) \quad \forall (x,t) \in \mathbb{R}\times[-t_n, +\infty).$$

Standard parabolic estimates allow us to use Arzela theorem: we can extract a subsequence still denoted t_n such that r_n converges locally uniformly to r_∞, which satisfies:

$$\partial_t r_\infty - \partial^2_{xx} r_\infty - r_\infty(1-\beta_0\epsilon - r_\infty) \geq 0 \quad \forall (x,t) \in \mathbb{R}^2$$

Moreover, because of (3.21), we know that for any $t \leq 0$, $\inf_{x\in(-b,b)} r_\infty(x+x_3,t) \geq \eta_2$. Let r_ϵ be the solution of

$$\begin{cases} \partial_t r_\epsilon - \partial^2_{xx} r_\epsilon - r_\epsilon(1-\beta_0\epsilon - r_\epsilon) = 0, \\ r_\epsilon(x,0) = \eta_2 \mathbf{1}_{(-b,b)}(x-x_3). \end{cases}$$

Then for any $x \in \mathbb{R}$ and any $t \geq 0$, by the classical comparison principle, $r_\infty(x,0) \geq r_\epsilon(x,t)$. But r_ϵ converges locally uniformly to $1-\beta_0\epsilon$ [KPP37], thus for any $x \in \mathbb{R}$ we have $r_\infty(x,0) \geq 1-\beta_0\epsilon$.

Looking back at the definition of r_∞, we deduce that for all $(x,t) \in \mathbb{R}\times\mathbb{R}^+$ we have

$$\liminf_{t\to+\infty} r(x+ct,t) \geq 1-\beta_0\epsilon$$

locally uniformly with respect to x. This is true for any $\epsilon > 0$ small enough, so we have

$$\lim_{t\to+\infty} r(x+ct,t) = 1$$

which concludes the proof of lemma 6. □

We are now equipped to prove lemma 5.

Proof. Let c_1 and c_2 be two speeds such that $c_S < c_1 < c_2 < c_R$. Let $\epsilon > 0$ be such that $c^* = 2\sqrt{1-\beta_0\epsilon}$ satisfies $c_2 < c^* < c_R$. For any $\theta < 1-\beta_0\epsilon$ close enough to $1-\beta_0\epsilon$, the following system:

$$\begin{cases} \hat{R}'' + c^*\hat{R}' + \hat{R}(1-\beta_0\epsilon-\hat{R}) = 0, \\ \hat{R}(0) = \theta \text{ and } \hat{R}'(0) = 0 \end{cases}$$

admits a solution $\hat{R}$ that satisfies $\hat{R}(b) = 0$ for a certain $b > 0$, and $\hat{R}'(\xi) < 0$ for any $\xi \in (0, b]$. We refer for example to [AW78] for a proof of existence of such a solution ; it relies mostly on phase plane analysis. We then define $\underline{r} : \mathbb{R} \times \mathbb{R}^+ \to \mathbb{R}$ by:

$$\underline{r}(x,t) = \begin{cases} \theta \text{ if } x - c^*t < \rho, \\ \hat{R}(x - c^*t - \rho) \text{ if } \rho \leq x - c^*t < \rho + b, \\ 0 \text{ if } x - c^*t \geq \rho + b \end{cases}$$

where ρ is to be chosen later.

Consider now $(\bar{s}, \underline{r})$ where $\bar{s}(x,t) = U_S(x - c_S t - x_0)$ is a Fisher-KPP front satisfying $\bar{s}(x,0) \geq s(x,0)$ for any $x \in \mathbb{R}$. There exists $x_1 \in \mathbb{R}$ such that for any $x > x_1$, we have $U_S(x) \leq \epsilon$ .Then, for any $(x,t) \in \mathbb{R} \times \mathbb{R}^+$:

$$N_1[\bar{s}, \underline{r}](x,t) = \gamma_0 U_S(x - c_S t - x_0)\underline{r}(x,t) \geq 0$$

and for any (x,t) such that $x \geq x_1 + c_S t$:

$$\begin{aligned} N_2[\bar{s}, \underline{r}](x,t) &= \begin{cases} \theta(\beta_0 U_S(x - c_S t - x_0) - 1 + \theta) \text{ if } x - c^*t < \rho \\ \beta_0 \hat{R}(x - c^*t - \rho)(U_S(x - c_S t - x_0) - \epsilon) \text{ if } \rho \leq x - c^*t < \rho + b \\ 0 \text{ if } x - c^*t \geq \rho + b \end{cases} \\ &\leq 0. \end{aligned}$$

Moreover, we know that $\lim_{t\to+\infty} r(c_1 t, t) = 1$ because of lemma 6, thus there exists $T > 0$ such that for any $t > T$, $r(c_1 t, t) \geq \theta$.

Finally, consider the situation at time $t = T$. By setting $\rho \leq -b + (c_1 - c^*)T$, we have $\underline{r}(x,T) = 0$ for any $x \geq c_1 T$. Thus, by using the comparison lemma 4, for any $t \geq T$ and $x \geq c_1 t$,

$$r(x,t) \geq \underline{r}(x,t). \tag{3.22}$$

For t large enough, $\rho + c^*t > c_2 t$, thus

$$\liminf_{\substack{t\to+\infty \\ c_1 t < x < c_2 t}} r(x,t) \geq \theta.$$

This is true for any $\theta < 1 - \beta_0\epsilon$ close enough to $1 - \beta_0\epsilon$ and for any $\epsilon > 0$ small enough, so we can pass to the limit as $\epsilon \to 0$ and $\theta \to 1$, and deduce that

$$\liminf_{\substack{t\to+\infty \\ c_1 t < x < c_2 t}} r(x,t) \geq 1 \tag{3.23}$$

which concludes the proof of lemma 5.

□

This proof uses loosely the Fisher-KPP hypothesis: we could have taken more general growth functions for sensitive and resistant cells, and still have this result of invasion, as stated in 3.1.

With a similar reasoning, we can prove the following lemma:

Lemma 7. *For all $c < -c_R$,*

$$\lim_{t\to+\infty} \sup_{x<ct} |s(x,t) - \alpha_0| + |r(x,t)| = 0.$$

This lemma is an intermediate proof of (3.9).

3.4 Competition between species

We are now interested in an intermediate zone, where competition between species can have an influence on their behaviour. We will first prove (3.9). In a second part, we will complete the proof of (3.10) by studying the zone of interaction of s and r.

3.4.1 Left side of the interaction zone

We know that $\lim_{t\to+\infty} \sup_{x<ct} |s(x,t)-\alpha_0|+|r(x,t)| = 0$ for any $c < -c_R$ because of Lemma 7. Let us now prove that it is the case for any $c < c_{SR}$. The method we use here is developed for a scalar equation in [FM77].

Let c be such that $c < c_{SR}$. We recall that as stated in the introduction 3.5 and in [KO95], c_{SR} depends continuously on the parameters and is increasing with respect to α_0. Thus, there exists $\underline{\alpha} < \alpha_0$ such that $1/\beta_0 < \underline{\alpha} < \gamma_0$ and the Kan-On speed $\underline{c}_{SR}$ corresponding to parameters $(\underline{\alpha}, \beta_0, \gamma_0, \delta_0)$ satisfies $c < \underline{c}_{SR} < c_{SR}$. We define $(\underline{S}, \overline{R})$ the corresponding Kan-On front; it satisfies:

$$\begin{cases} \delta_0 \underline{S}'' + \underline{c}_{SR}\underline{S}' + \underline{S}(\underline{\alpha} - \underline{S} - \gamma_0\overline{R}) = 0, \\ \overline{R}'' + \underline{c}_{SR}\overline{R}' + \overline{R}(1 - \beta_0\underline{S} - \overline{R}) = 0, \\ \lim_{\xi\to-\infty} \underline{S}(\xi) = \underline{\alpha} \text{ and } \lim_{\xi\to+\infty} \underline{S}(\xi) = 0, \\ \lim_{\xi\to-\infty} \overline{R}(\xi) = 0 \text{ and } \lim_{\xi\to+\infty} \overline{R}(\xi) = 1. \end{cases}$$

We now define $(\underline{s}, \bar{r})$ on $\mathbb{R}\times\mathbb{R}^+$ by:

$$\begin{cases} \underline{s}(x,t) = \max(0, \underline{S}(x - \underline{c}_{SR}t - \xi(t)) - q(t)), \\ \bar{r}(x,t) = \min(1, \overline{R}(x - \underline{c}_{SR}t - \xi(t)) + p(t)) \end{cases}$$

where ξ, p and q will be characterized later.

Let $\epsilon > 0$ be such that $\epsilon < \min(\underline{\alpha}, \underline{\alpha} - \frac{1}{\beta_0}, \frac{\gamma_0-\alpha_0}{\gamma_0}, \frac{1}{3})$ (this is possible because of (3.7) and the definition of $\underline{\alpha}$). Because $\underline{S}$ is strictly decreasing and $\overline{R}$ is strictly increasing, there exists $\eta > 0$ such that, for any ζ satisfying either $\epsilon < \underline{S}(\zeta) < \underline{\alpha} - \epsilon$ or $\epsilon < \overline{R}(\zeta) < 1 - \epsilon$, we have $\underline{S}'(\zeta) < -\eta$ and $\overline{R}'(\zeta) > \eta$. We then state the following lemma, that will impose conditions on p, q and ξ.

Lemma 8. *We choose ξ, p and q of the form*

$$\begin{cases} \xi(t) = \xi_1 + \xi_0 e^{-\mu t}, \\ p(t) = p_0 e^{-\mu t}, \\ q(t) = q_0 e^{-\mu t} \end{cases}$$

where p_0, q_0 and $\mu > 0$, p_0 satisfies

$$p_0 < \frac{\alpha_0 - \underline{\alpha}}{2\gamma_0}, \tag{3.24}$$

q_0 and μ satisfy

$$q_0 < \frac{\epsilon p_0}{2\beta_0}, \tag{3.25}$$

$$q_0 + \mu < \gamma_0(1-\epsilon) - \alpha_0, \tag{3.26}$$

$$\beta_0 q_0 + \mu < \beta_0(\underline{\alpha} - \epsilon) - 1, \tag{3.27}$$

$$q_0(\alpha_0 + \mu + q_0) < (\underline{\alpha} - \epsilon)\frac{\alpha_0 - \underline{\alpha}}{2}, \tag{3.28}$$

$$\mu < \frac{1-3\epsilon}{2}, \tag{3.29}$$

$$\mu < \gamma_0 - \alpha_0, \tag{3.30}$$

and ξ_0 satisfies

$$\xi_0 > \frac{q_0\gamma_0(1-\epsilon)}{\mu\eta}, \tag{3.31}$$

$$\xi_0 > \frac{p_0\beta_0(\underline{\alpha} - \epsilon)}{\mu\eta}. \tag{3.32}$$

Then we have for any $(x,t) \in \mathbb{R} \times \mathbb{R}^+$ that:

$$N_1[\underline{s}, \bar{r}](x,t) \leq 0,$$
$$N_2[\underline{s}, \bar{r}](x,t) \geq 0.$$

Proof. For any $(x,t) \in \mathbb{R}\times\mathbb{R}^+$, we have with $\zeta = x - \underline{c}_{SR}t - \xi(t)$ and if $\underline{s}(x,t) > 0$ and $\bar{r}(x,t) < 1$:

$$\begin{aligned} N_1[\underline{s}, \bar{r}](x,t) &= \partial_t \underline{s}(x,t) - \delta_0 \partial^2_{xx}\underline{s}(x,t) - \underline{s}(x,t)(\alpha_0 - \underline{s}(x,t) - \gamma_0 \bar{r}(x,t)) \\ &= -\xi'(t)\underline{S}'(\zeta) - q'(t) + \underline{S}(\zeta)(\underline{\alpha} - \alpha_0 + \gamma_0 p(t) - q(t)) \\ &\quad + q(t)(\alpha_0 - \underline{S}(\zeta) - \gamma_0 \overline{R}(\zeta) + q(t) - \gamma_0 p(t)) \end{aligned}$$

and

$$\begin{aligned} N_2[\underline{s}, \bar{r}](x,t) &= \partial_t \bar{r}(x,t) - \partial^2_{xx}\bar{r}(x,t) - \bar{r}(x,t)(1 - \beta_0 \underline{s}(x,t) - \bar{r}(x,t)) \\ &= -\xi'(t)\overline{R}'(\zeta) + p'(t) + \overline{R}(\zeta)(p(t) - \beta_0 q(t)) - p(t)(1 - \overline{R}(\zeta) - \beta_0 \underline{S}(\zeta) - p(t) + \beta_0 q(t)) \end{aligned}$$

Around $\pm\infty$ Let (x,t) be such that $\underline{S}(x - \underline{c}_{SR}t - \xi(t)) > \underline{\alpha} - \epsilon$ and $\overline{R}(x - \underline{c}_{SR}t - \xi(t)) < \epsilon$. Then:

$$\begin{aligned} N_1[\underline{s}, \bar{r}](x,t) &= -\xi'(t)\underline{S}' - q'(t) + \underline{S}(\underline{\alpha} - \alpha_0 + \gamma_0 p(t) - q(t)) + q(t)(\alpha_0 - \underline{S} - \gamma_0 \overline{R} + q(t) - \gamma_0 p(t)) \\ &\leq -q'(t) + \underline{S}(\underline{\alpha} - \alpha_0 + \gamma_0 p_0) + q(t)(\alpha_0 + q_0) \\ &\quad \text{if we take } \xi_0 > 0 \\ &\leq q_0 e^{-\mu t}(\mu + \alpha_0 + q_0) + (\underline{\alpha} - \epsilon)\frac{\underline{\alpha} - \alpha_0}{2} \text{ because of (3.24)} \\ &\leq 0 \end{aligned}$$

because of (3.28). Furthermore,

$$\begin{aligned} N_2[\underline{s}, \bar{r}](x,t) &= -\xi'(t)\overline{R}' + p'(t) + \overline{R}(p(t) - \beta_0 q(t)) - p(t)(1 - \overline{R} - \beta_0 \underline{S} - p(t) + \beta_0 q(t)) && (3.33) \\ &\geq p'(t) + p(t)(\beta_0(\underline{\alpha} - \epsilon) - 1 - \beta_0 q(t)) \text{ because of (3.25)} && (3.34) \\ &\geq p(t)(\beta_0(\underline{\alpha} - \epsilon) - 1 - \beta_0 q_0 - \mu) && (3.35) \\ &\geq 0 && (3.36) \end{aligned}$$

because of (3.27).

Now, let (x,t) be such that $\underline{S}(x-\underline{c}_{SR}t-\xi(t))<\epsilon$ and $\overline{R}(x-\underline{c}_{SR}t-\xi(t))>1-\epsilon$. Then:

$$\begin{aligned}
N_1[\underline{s},\bar{r}](x,t) &= -\xi'(t)\underline{S}' - q'(t) + \underline{S}(\underline{\alpha}-\alpha_0+\gamma_0 p(t)-q(t)) + q(t)(\alpha_0-\underline{S}-\gamma_0\overline{R}+q(t)-\gamma_0 p(t)) \\
&\leq -q'(t) + q(t)(\alpha_0-\gamma_0(1-\epsilon)+q(t)) \\
&\leq q(t)(\alpha_0-\gamma_0(1-\epsilon)+q_0+\mu) \\
&\leq 0
\end{aligned} \tag{3.37}$$

(3.38)

(3.39)

(3.40)

because of (3.26). Furthermore,

$$\begin{aligned}
N_2[\underline{s},\bar{r}](x,t) &= -\xi'(t)\overline{R}' + p'(t) + \overline{R}(p(t)-\beta_0 q(t)) - p(t)(1-\overline{R}-\beta_0\underline{S}-p(t)+\beta_0 q(t)) \\
&\geq p'(t) + (1-\epsilon)(p_0-\beta_0 q_0) - \epsilon p(t) \\
&\geq p'(t) + (1-\epsilon)\frac{p(t)}{2} - \epsilon p(t) \text{ because of (3.25)} \\
&\geq \frac{p(t)}{2}(1-3\epsilon-2\mu) \\
&\geq 0
\end{aligned}$$

because of (3.29).

In the intermediary zone Let (x,t) be such that $\epsilon<\underline{S}(x-\underline{c}_{SR}t-\xi(t))<\underline{\alpha}-\epsilon$ or $\epsilon<\overline{R}(x-\underline{c}_{SR}t-\xi(t))<1-\epsilon$. Then because $\underline{S}$ is strictly decreasing, and $\overline{R}$ is strictly increasing, there exists $\eta>0$ such that $\underline{S}'(x-\underline{c}_{SR}t-\xi(t))<-\eta$ and $\overline{R}'(x-\underline{c}_{SR}t-\xi(t))>\eta$. Then:

$$\begin{aligned}
N_1[\underline{s},\bar{r}](x,t) &= -\xi'(t)\underline{S}' - q'(t) + \underline{S}(\underline{\alpha}-\alpha_0+\gamma_0 p(t)-q(t)) + q(t)(\alpha_0-\underline{S}-\gamma_0\overline{R}+q(t)-\gamma_0 p(t)) \\
&\leq \xi'(t)\eta - q(t)(\alpha_0-\gamma_0(1-\epsilon)+q(t)) + q(t)(\alpha_0+q(t)) \\
&\quad \text{because of (3.40)} \\
&\leq (-\xi_0\mu\eta + q_0\gamma_0(1-\epsilon))e^{-\mu t} \\
&\leq 0
\end{aligned}$$

because of (3.31). Furthermore,

$$\begin{aligned}
N_2[\underline{s},\bar{r}](x,t) &= -\xi'(t)\overline{R}' + p'(t) + \overline{R}(p(t)-\beta_0 q(t)) - p(t)(1-\overline{R}-\beta_0\underline{S}-p(t)+\beta_0 q(t)) \\
&\geq -\xi'(t)\eta - p(t)(\beta_0(\underline{\alpha}-\epsilon)-1-\beta_0 q(t)) - p(t)(1+\beta_0 q(t)) \\
&\quad \text{because of (3.36)} \\
&\geq (\xi_0\mu\eta - p_0\beta_0(\underline{\alpha}-\epsilon))e^{-\mu t} \\
&\geq 0
\end{aligned}$$

because of (3.32).

In flat zones We now want to check that $N_1[\underline{s},\bar{r}](x,t)\leq 0$ and $N_2[\underline{s},\bar{r}](x,t)\geq 0$ even if $\underline{s}(x,t)=0$ or $\bar{r}(x,t)=1$.

Let $(x,t)\in\mathbb{R}\times\mathbb{R}^+$ be such that $\underline{s}(x,t)=0$, *i.e.* $\underline{S}(x-\underline{c}_{SR}t-\xi(t))<q(t)$, and $\bar{r}(x,t)<1$. Then $N_1[\underline{s},\bar{r}](x,t)=0$ and up to further reducing q_0, we can suppose $\overline{R}(x-\underline{c}_{SR}t-\xi(t))>3/4$,

thus:

$$\begin{aligned}
N_2[\underline{s},\bar{r}](x,t) &= \partial_t \bar{r} - \partial^2_{xx}\bar{r} - \bar{r}(1-\bar{r}) \\
&= -\xi'(t)\overline{R}' + p'(t) + \overline{R}(1-\beta_0\underline{S}-\overline{R}) - (\overline{R}+p(t))(1-\overline{R}-p(t)) \\
&\geq p'(t) + \overline{R}(p(t)-\beta_0 q(t)) - p(t)(1-\overline{R}) \\
&\geq p'(t) + \frac{1}{2}p(t) - \frac{3}{4}\beta_0 q(t) \\
&\geq (-\mu p_0 + \frac{1}{2}p_0 - \frac{3}{4}\beta_0 q_0)e^{-\mu t} \\
&\geq 0
\end{aligned}$$

because of (3.29) and (3.25).

Now, let $(x,t) \in \mathbb{R}\times\mathbb{R}^+$ be such that $\underline{s}(x,t) > 0$ and $\bar{r}(x,t) = 1$, *i.e.* $\overline{R}(x - \underline{c}_{SR}t - \xi(t)) > 1 - p(t)$. Then $N_2[\underline{s},\bar{r}](x,t) = \beta_0\underline{s} \geq 0$ and

$$\begin{aligned}
N_1[\underline{s},\bar{r}](x,t) &= \partial_t \underline{s}(x,t) - \delta_0\partial^2_{xx}\underline{s}(x,t) - \underline{s}(x,t)(\alpha_0 - \underline{s}(x,t) - \gamma_0) \\
&= -\xi'(t)\underline{S}' - q'(t) + \underline{S}(\underline{\alpha} - \underline{S} - \gamma_0\overline{R}) - (\underline{S} - q(t))(\alpha_0 - \underline{S} - \gamma_0 + q(t)) \\
&\leq -q'(t) + \underline{S}(\underline{\alpha} - \alpha_0 - \gamma_0\overline{R} + \gamma_0 - q(t)) + q(t)(\alpha_0 - \gamma_0 - (\underline{S} - q(t))) \\
&\leq -q'(t) + \underline{S}(\underline{\alpha} - \alpha_0 + \gamma_0 p(t) - q(t)) + q(t)(\alpha_0 - \gamma_0) \\
&\leq q(t)(\mu + \alpha_0 - \gamma_0) \\
&\leq 0
\end{aligned}$$

because of (3.30).

Finally, if (x,t) is such that $\underline{s}(x,t) = 0$ and $\bar{r}(x,t) = 1$, then $N_1[\underline{s},\bar{r}](x,t) = N_2[\underline{s},\bar{r}](x,t) = 0$. □

We have constructed a "sub-super solution" $(\underline{s},\bar{r})$ of (3.1). We now want to compare it to the solution (s,r) with initial condition (3.6). To demonstrate the following lemma, we will finally characterize the constant ξ_1:

Lemma 9. *There exists $T > 0$ and $c_* < c$ such that for every $t \geq T$:*

$$s(c_*t,t) \geq \underline{s}(c_*t,t) \text{ and } r(c_*t,t) \leq \bar{r}(c_*t,t),$$

and for every $x \geq c_*T$:

$$s(x,T) \geq \underline{s}(x,T) \text{ and } r(x,T) \leq \bar{r}(x,T).$$

Proof. Let $c_* < c$ be such that $c_* < -c_R$. Because of Lemma 7, we know that

$$\lim_{t\to+\infty} |s(c_*t,t) - \alpha_0| + |r(c_*t,t)| = 0.$$

Thus, there exists $T_1 > 0$ such that for every $t \geq T_1$, $s(c_*t,t) > \underline{\alpha}$ and $r(c_*t,t) < p_0$. Then, we already have that $s(c_*t,t) \geq \underline{s}(c_*t,t)$ for every $t \geq T_1$.

Furthermore, we know that there exists $X \in \mathbb{R}$ such that $r(x,t) \leq \tilde{U}_R(x - c_Rt - X)$ for all $(x,t) \in \mathbb{R}\times\mathbb{R}^+$, where $\tilde{U}_R$ is the Fisher-KPP front satisfying:

$$\begin{cases} \tilde{U}_R'' + c_R\tilde{U}_R' + \tilde{U}_R(1-\tilde{U}_R) = 0, \\ \tilde{U}_R(-\infty) = 0 \text{ and } \tilde{U}_R(+\infty) = 1. \end{cases}$$

We also know from [KPP37] that $\tilde{U}_R$ satisfies for a certain constant $C > 0$ and any $\zeta \in \mathbb{R}$:

$$\tilde{U}_R(\zeta) \leq C\zeta e^{\frac{c_R}{2}\zeta}.$$

Thus for all $t > 0$, we have

$$r(c_*t, t) \leq \tilde{U}_R((c_* - c_R)t - X) \leq C((c_* - c_R)t - X)e^{\frac{c_R}{2}((c_*-c_R)t-X)}.$$

If we further reduce μ such that $\mu < \frac{c_R}{2}(c_R - c_*)$, there exists $T_2 > 0$ such that for all $t > T_2$,

$$C((c_* - c_R)t - X)e^{\frac{c_R}{2}((c_*-c_R)t-X)} \leq p_0 e^{-\mu t}.$$

Then, by taking $T = \max(T_1, T_2)$, we get that for all $t > T$,

$$s(c_*t, t) \geq \underline{s}(c_*t, t) \text{ and } r(c_*t, t) \leq \bar{r}(c_*t, t).$$

Now consider $(\underline{s}, \bar{r})$ at time T and for $x \geq c_*T$, and recall that $\underline{S}$ is decreasing and $\overline{R}$ increasing:

$$\begin{aligned}
\underline{s}(x, T) &= \max(0, \underline{S}(x - \underline{c}_{SR}T - \xi(T)) - q(T)) \\
&\leq \max(0, \underline{S}(c_*T - \underline{c}_{SR}T - x_1 - x_0 e^{-\mu T}) - q(T)) \\
&= 0
\end{aligned}$$

if we take $\xi_1 < 0$ small enough. In the same way:

$$\begin{aligned}
\bar{r}(x, T) &= \min(1, \overline{R}(x - \underline{c}_{SR}T - \xi(T)) + p(T)) \\
&\geq \min(1, \overline{R}(c_*T - \underline{c}_{SR}T - x_1 - x_0 e^{-\mu T}) + p(T)) \\
&= 1
\end{aligned}$$

by possibly taking ξ_1 smaller. We then get the second part of the lemma.

□

Lemmas 8 and 9 allow us to conclude that, because of the comparison lemma 4,

$$\forall t \geq T, \quad \forall x \geq ct, (\underline{s}, \bar{r})(x, t) \preceq (s, r)(x, t).$$

We thus have the following spreading result:

$$\lim_{t\to+\infty} \inf_{x\geq ct} s(x, t) \geq \underline{\alpha} \text{ and } \lim_{t\to+\infty} \inf_{x\geq ct} r(x, t) \leq 0. \tag{3.41}$$

This is true for any $\underline{\alpha} < \alpha_0$ close enough to α_0, and for any $(x, t) \in \mathbb{R} \times \mathbb{R}^+$ we have $s(x, t) < \alpha_0$, so in conclusion:

$$\lim_{t\to+\infty} \sup_{x\geq ct} |s(x, t) - \alpha_0| + |r(x, t)| = 0,$$

wich concludes the proof of (3.9).

3.4.2 Right side of the interaction zone

This section is devoted to the demonstration of (3.10). We already proved in Subsection 3.3.3 that if $c_S < c_R$, for any c_1, c_2 satisfying $c_S < c_1 < c_2 < c_R$, we have:

$$\lim_{t\to+\infty} \sup_{c_1 t<x<c_2 t} |s(x, t)| + |r(x, t) - 1| = 0.$$

We will now prove that it is in fact true for $c_{SR} < c_1 < c_2 < c_R$.

Let c_1 and c_2 be such that $c_{SR} < c_1 < c_2 < c_R$. In a proof similar to what we did in 3.4.1, we define a pair $(\bar{s}, \underline{r}) : \mathbb{R} \times \mathbb{R}^+ \to \mathbb{R}$ that will satisfy $(s, r) \preceq (\bar{s}, \underline{r})$ on an appropriate domain, with $(\bar{s}, \underline{r})$ almost travelling at a speed faster than c_{SR} and slower than c_1.

Let $1 > \theta > 0$ and $\bar{\alpha} > 0$ to be characterized later, and consider the following system for $c \in \mathbb{R}$ and $(\overline{S}, \underline{R})$:

$$\begin{cases} \delta_0 \overline{S}''(\xi) + c\overline{S}'(\xi) + \overline{S}(\xi)(\bar{\alpha} - \overline{S}(\xi) - \gamma_0 \underline{R}(\xi)) = 0, \\ \underline{R}''(\xi) + c\underline{R}'(\xi) + \underline{R}(\xi)(\theta - \beta_0 \overline{S}(\xi) - \underline{R}(\xi)) = 0, \\ \overline{S}(-\infty) = \bar{\alpha} \text{ and } \overline{S}(+\infty) = 0, \\ \underline{R}(-\infty) = 0 \text{ and } \underline{R}(+\infty) = \theta. \end{cases} \tag{3.42}$$

After the change of variable $\tilde{\xi} = \sqrt{\theta}\xi$ and of states $\overline{S} = \theta\tilde{S}$, $\overline{R} = \theta\tilde{R}$, we find that it is equivalent to the following system:

$$\begin{cases} \delta_0 \tilde{S}''(\tilde{\xi}) + \sqrt{\theta} c \tilde{S}'(\tilde{\xi}) + \tilde{S}(\tilde{\xi})(\frac{\bar{\alpha}}{\theta} - \tilde{S}(\tilde{\xi}) - \gamma_0 \tilde{R}(\tilde{\xi})) = 0, \\ \tilde{R}''(\tilde{\xi}) + \sqrt{\theta} c \tilde{R}'(\tilde{\xi}) + \tilde{R}(\tilde{\xi})(1 - \beta_0 \tilde{S}(\tilde{\xi}) - \tilde{R}(\tilde{\xi})) = 0, \\ \tilde{S}(-\infty) = \frac{\bar{\alpha}}{\theta} \text{ and } \tilde{S}(+\infty) = 0, \\ \tilde{R}(-\infty) = 0 \text{ and } \tilde{R}(+\infty) = 1. \end{cases} \tag{3.43}$$

This corresponds to the Kan-On system of equations: we know because of [KO95] that it admits a solution $(\tilde{S}, \tilde{R})$ when $\tilde{c} = \frac{c}{\sqrt{\theta}}$ is the Kan-On speed of propagation associated to parameters $(\frac{\bar{\alpha}}{\theta}, \beta_0, \gamma_0, \delta_0)$. We deduce that (3.42) has a unique solution $(\overline{S}, \underline{R})$ up to translation if $c = \sqrt{\theta}\tilde{c}$. Note that for this result to hold, we need that $\gamma_0 > \frac{\bar{\alpha}}{\theta} > \frac{1}{\beta_0}$.

If $\bar{\alpha} = \alpha_0$, we have that $c = \sqrt{\theta}\tilde{c} > \sqrt{\theta} c_{SR}$. Numerical tests suggest that in fact, if $\bar{\alpha} = \alpha_0$, we have $c > c_{SR}$: this seems reasonable, since in (3.42), we reduce the growth rate of the right-side placed species. But we do not need this inequality to prove our spreading result. As a matter of fact, for any $\bar{\alpha} > \alpha_0$ close enough to α_0, there exists $\theta < 1$ such that, if $\tilde{c}$ is the Kan-On speed associated to parameters $(\frac{\bar{\alpha}}{\theta}, \beta_0, \gamma_0, \delta_0)$, then $\tilde{c} > \frac{c_{SR}}{\sqrt{\theta}}$.

We choose such $\bar{\alpha}$, θ, and the corresponding speed c, that we will now note $\bar{c}_{SR}$ and that satisfies $\bar{c}_{SR} > c_{SR}$. By possibly taking a bigger θ and a smaller $\bar{\alpha}$, we can suppose $c_{SR} < \bar{c}_{SR} < c_1$ by continuity of the Kan-On speed with respect to the parameters. We can now state the following lemma:

Lemma 10. *Let $(\overline{S}, \underline{R})$ be a solution of (3.42) with $c = \bar{c}_{SR}$. We define $(\bar{s}, \underline{r}) : \mathbb{R} \times \mathbb{R}^+ \to \mathbb{R}^2$ by*

$$\begin{cases} \bar{s}(x,t) = \min(\alpha_0, \overline{S}(x - \bar{c}_{SR}t - \xi(t)) + q(t)), \\ \underline{r}(x,t) = \max(0, \underline{R}(x - \bar{c}_{SR}t - \xi(t)) - p(t)). \end{cases}$$

Then for p, q and ξ well-chosen functions of t, $(\bar{s}, \underline{r})$ satisfies for any $(x,t) \in \mathbb{R} \times \mathbb{R}^+$, $N_1[\bar{s}, \underline{r}](x,t) \geq 0$ and $N_2[\bar{s}, \underline{r}](x,t) \leq 0$.

Proof. The proof of lemma 10 is very similar to the proof of lemma 8. We impose $p(t) = p_0 e^{-\mu t}$, $q(t) = q_0 e^{-\mu t}$ and $\xi(t) = \xi_1 + \xi_0 e^{-\mu t}$. Recall $\bar{\alpha}$ satisfies $\gamma_0 > \frac{\bar{\alpha}}{\theta} > \frac{1}{\beta}$. Let $\epsilon > 0$ be such that $\gamma_0(\theta - \epsilon) - \alpha_0 > 0$, $\theta > \epsilon$, $\bar{\alpha} - \alpha_0 > \epsilon$ and $\beta_0(\bar{\alpha} - \epsilon) > 1$. There exists η such that, if $\epsilon < \overline{S}(\zeta) < \alpha_0 - \epsilon$ or $\epsilon < \underline{R}(\zeta) < \theta - \epsilon$, then $\overline{S}'(\zeta) < -\eta$ and $\underline{R}'(\zeta) > \eta$. Then, the choice of parameters $p_0 > 0$,

$q_0 > 0$, $\mu > 0$ and $\xi_0 < 0$ satisfying:

$$\gamma_0 p_0 < \bar{\alpha} - \alpha_0, \tag{3.44}$$
$$\gamma_0 p_0 + \mu < \gamma_0(\theta - \epsilon) - \alpha_0, \tag{3.45}$$
$$p_0(\mu + 2) < \frac{1-\theta}{2}(\theta - \epsilon), \tag{3.46}$$
$$\beta_0 q_0 < \frac{1-\theta}{2}, \tag{3.47}$$
$$\gamma_0 p_0 < \frac{\bar{\alpha} - \alpha_0 - \epsilon}{2}, \tag{3.48}$$
$$\mu < \frac{\bar{\alpha} - \alpha_0 - \epsilon}{2}, \tag{3.49}$$
$$p_0 + \mu < \beta_0(\bar{\alpha} - \epsilon) - 1, \tag{3.50}$$
$$\xi_0 < -\frac{q_0\gamma_0(\theta - \epsilon)}{\eta\mu}, \tag{3.51}$$
$$\xi_0 < -\frac{p_0\beta_0(\bar{\alpha} - \epsilon)}{\eta\mu}, \tag{3.52}$$

is enough to ensure that, for every $(x,t) \in \mathbb{R}\times\mathbb{R}^+$, we have $N_1[\bar{s},\underline{r}](x,t) \geq 0$ and $N_2[\bar{s},\underline{r}](x,t) \leq 0$. □

As in 3.4.1, we now want to choose ξ_1 and maybe further reduce μ such that $(\bar{s},\underline{r})$ and (s,r) are well-ordered at some time T and on a well-chosen border.

Recall that $c_2 < c_R$. We state the following lemma:

Lemma 11. *There exists $T > 0$ and $c^* > c_2$ such that for every $t \geq T$:*

and for every $x \leq c^*T$:

$$s(x,T) \leq \bar{s}(x,T) \text{ and } r(x,T) \geq \underline{r}(x,T).$$

Proof. We take $c^* > c_2$ such that $c_S < c^* < c_R$. Just as in the proof of lemma 9, we know that

$$\lim_{t\to+\infty} |s(c^*t,t)| + |r(c^*t,t) - 1| = 0.$$

Thus, there exists $T_1 > 0$ such that for any $t > T_1$, $s(c^*t,t) \leq q_0$ and $r(c^*t,t) \geq \theta$.

We also know that there exists $X \in \mathbb{R}$ such that for any $(x,t) \in \mathbb{R}\times\mathbb{R}^+$, $s(x,t) \leq U_S(x - c_St - X)$ where U_S is a Fisher-KPP front defined in (3.3). We also know from [KPP37] that U_S satisfies for a certain constant $C > 0$ and any $\zeta \in \mathbb{R}$:

$$U_S(\zeta) \leq C\zeta e^{-\frac{c_S}{2}\zeta}.$$

Thus for all $t > 0$, we have

$$s(c^*t,t) \leq U_S((c^* - c_S)t - X) \leq C((c^* - c_S)t - X)e^{-\frac{c_S}{2}((c^*-c_S)t-X)}.$$

If we further reduce μ such that $\mu < \frac{c_S}{2}(c^* - c_S)$, there exists $T_2 > 0$ such that for all $t > T_2$,

$$C((c^* - c_S)t - X)e^{-\frac{c_S}{2}((c^*-c_S)t-X)} \leq q_0 e^{-\mu t}.$$

Then, by taking $T = \max(T_1, T_2)$, we get that for all $t > T$,

$$s(c^*t, t) \leq \bar{s}(c^*t, t) \text{ and } r(c^*t, t) \geq \underline{r}(c^*t, t).$$

The parameter ξ_1 remains to be chosen. We can take it large enough that for any $x \leq c^*T$,

$$\bar{s}(x, T) = \bar{\alpha} \text{ and } \underline{r}(x, T) = 0,$$

which concludes the second part of the lemma.

□

We can then apply the comparison lemma 4 with lemmas 10 and 11 to conclude that:

$$\forall t \geq T, \quad \forall x \in [c_1 t, c_2 t], (s, r)(x, t) \preceq (\bar{s}, \underline{r})(x, t).$$

We thus have the following spreading result:

$$\lim_{t \to +\infty} \inf_{c_1 t \leq x \leq c_2 t} s(x, t) \leq 0 \text{ and } \lim_{t \to +\infty} \inf_{c_1 t \leq x \leq c_2 t} r(x, t) \geq \theta. \tag{3.53}$$

This is true for any $\theta < 1$ close enough to 1, and for any $(x, t) \in \mathbb{R} \times \mathbb{R}^+$ we have $r(x, t) < 1$, so in conclusion:

$$\lim_{t \to +\infty} \sup_{c_1 t \leq x \leq c_2 t} |s(x, t)| + |r(x, t) - 1| = 0,$$

wich concludes the proof of Theorem 9.

As stated in 3.1, the proof of these results relies heavily on the Fisher-KPP hypothesis and theorems from [KO95].

Acknowledgements

This work has been carried out in the framework of the NONLOCAL project (ANR-14-CE25-0013) funded by the French National Research Agency (ANR).

Chapter 4

Numerical control of a heterogeneous population of cells

In this chapter, we consider the following medical problem: we want to design protocols for heterogeneous tumours such that, after an initial treatment as short as possible, the tumour size is maintained under a certain threshold. This problem can be expressed, in a Hamilton-Jacobi-Bellman framework, as a viability and a reachability problem. We present the equations involved in solving this problem, and numerical implementations of them. This framework also allows us to take into account uncertainties ; biological events being subject to several stochastic phenomenons, we present the corresponding mathematical methods.

4.1 Introduction

The treatment of cancers with cytotoxic chemotherapies often encounters two major pitfalls: the side toxicity of the drugs on healthy cells and organs, and the emergence of resistance to the treatment. This resistance can occur because of an initial genomic heterogeneity of the tumour: in its early stages, it contains several distinct populations of cells, that differ from one another because of successive mutations [DLL$^+$12]. If one of these lineages is resistant to the first line of treatment, then using strong doses of drug, as it is done in many classical protocols, kills all competing cells, and lets this resistant lineage grow without control. It is thus important to take into account cancer heterogeneity before starting a treatment. Mathematical modelling can, in this framework, give guidelines on how to treat such tumours.

For example, [BG84, BRG$^+$87] study the growth and treatment of heterogeneous tumours, and determine optimal dosages of drugs for fixed time injections. The treatment protocol is there considered as instantaneous injections of drugs. We will work here in a framework of continous treatment. In [LS06], an ODE model of heterogeneous tumour growth is studied under continuous treatment. The optimal control theory is used to give necessary conditions on optimal protocols, in order to reduce the tumour volume while preserving its heterogeneity. We will study a more complex model, with interactions between the two cell lineages.

Optimal control is also used in [1], where an optimal treatment is characterized to treat heterogeneous tumours. We will use the model presented there for tumour growth. It considers two cancerous cells populations, s which is sensitive to the treatment, and r which is resistant to it. They develop in a Petri dish, so that no other cells intervene in their evolution. The model

is the following:

$$\begin{cases} \frac{ds}{dt}(t) = \rho s(t)(1 - \frac{s(t)+mr(t)}{K}) - \alpha s(t)C(t) \\ \frac{dr}{dt}(t) = \rho r(t)(1 - \frac{s(t)+mr(t)}{K}) - \beta s(t)r(t). \end{cases} \tag{4.1}$$

The two lineages follow a logistic growth, with the same growth rate ρ. Because they compete for nutrients and space, the growth is limited by the total available ressources $K-(s(t)+mr(t))$, where K is the maximal size of the tumour, and m represents the difference of metabolism between sensitive and resistant cells. We suppose that, furthermore, resistance to the drug infers a competitive disadvantage for the cells, thus resistant cells see a supplementary competition term $-\beta s(t)r(t)$. Finally, the treatment dosage $C(t) \in [0, C_{\max}]$ only acts on sensitive cells.

The problem of tumour size reduction is then defined by: *for a finite time of experiment T, find a control $C : [0, T] \to [0, C_{max}]$ such that it minimizes the cost:*

$$\psi(s, r) := s(T)^2 + r(T)^2 + \int_0^T (As(t)^2 + Br(t)^2)dt$$

where A and B are tuning parameters. This cost takes into account the size of the tumour during the whole experiment, and penalizes the high values of populations by taking them to the square. To increase the cost of high tumours, one could define a different integral cost for $n \in \mathbb{N}$ by:

$$\psi_n(s, r) := s(T) + r(T) + \left(\int_0^T (As(t)^n + Br(t)^n)dt \right)^{1/n}$$

as it is performed in [Bar90], and let n tend to ∞ or take a large n, to approach a maximum cost. We decide in this chapter to define a different problem, that is more relevant to biological applications. The new objective is to maintain the tumour size under a certain threshold, defined by medical considerations. When this objective is not reachable, for example if the initial tumour is already bigger than the designed threshold, we define an other objective: after an initial protocol, which should be as short as possible, we want to ensure that the tumour size will not exceed the defined threshold. These problems can be expressed, in the framework of Hamilton-Jacobi-Bellman equations, as a problem of viability and a problem of reachability.

A vast litterature of the use of HJB theory for these problems exists. For example, in [BFZ10], the reachability problem is considered with state constraints. This analysis will be useful for the resolution of our problem. In general, we will refer to [ABZ13] for a complete theoretical framework of constraints in HJB equations. The numerical implementation of such methods must be adequate to retrieve optimal solutions ; numerical methods are presented in [ABZ13] for a classic resolution, and in [BMZ09] for a different method. We will present some of the methods that we used for numerical examples. The convergence of the numerical solutions to optimal solutions is demonstrated also in [ABDZ17]. Finally, a framework to take into account uncertainties is presented in [DZC12], with an application to collision avoidance for unmanned vehicles: the uncertainty is here the trajectory of another vehicle.

This chapter is organized as follows. The first part defines the different models, objectives and constraints we will consider. The second part defines the value functions that correspond to each problem, and the Hamilton-Jacobi-Bellman equations that they solve. The third part is devoted to the numerical implementation of these value functions: algorithms and convergence results are presented. The fourth part presents how uncertainties can be take into account in the model, and how some results would be modified. Finally, the fifth part presents some numerical simulations of the different models and problems.

4.2 Problem presentation

We present here some notations that will be usefull for this chapter.

Throughout this paper, $|\cdot|$ is the Euclidean norm and $\langle\cdot,\cdot\rangle$ is the Euclidean inner product on $\mathbb{R}^N$ (for any $N \geq 1$). The notation $\mathbb{B}$ stands for the unit open ball $\{x \in \mathbb{R}^N : \ |x| < 1\}$ and $\mathbb{B}(x,r) := x + r\mathbb{B}$ for any $x \in \mathbb{R}^N$ and $r > 0$.

For a set $S \subseteq \mathbb{R}^N$, $\overset{\circ}{S}$, $\overline{S}$ and ∂S denote its interior, closure and boundary, respectively. The distance function to S is $d_S(x) = \inf\{|x-y| : \ y \in S\}$.

For a given function $\varphi : \mathbb{R}^N \to \mathbb{R} \cup \{+\infty\}$, the epigraph of this function is the set

$$\operatorname{epi} \varphi = \{(x,r) \in \mathbb{R}^N \times \mathbb{R} \mid r \geq \varphi(x)\}.$$

For an embedded manifold of $\mathbb{R}^N$, the tangent space to $\mathcal{M}$ at x is $\mathcal{T}_{\mathcal{M}}(x)$.

For any $M > 0$, the set $L^1(0,+\infty;\ e^{-Mt}dt)$ is the set of functions $f : [0,+\infty) \to \mathbb{R}$ such that $\int_0^{+\infty} |f(t)|e^{-Mt}dt$ is finite: $|f|$ is integrable for the measure $e^{-Mt}dt$.

We consider the following controlled differential system :

$$\dot{y}(t) = f_0(y(t)) + f_1(y(t))C(t) = f(y(t), C(t)) \tag{4.2}$$

where C is the control, and y the vector of state variables ($y(t) \in \mathbb{R}^n$, with $n = 2$ or 3 depending on the problem we consider). We consider only measurable controls taking value between 0 and C_{max} ; in other words,

$$C \in \mathcal{A} := \{c : \mathbb{R}^+ \to [0, C_{max}], c \text{ measurable}\}$$

In the sequel, we will consider models where the vector fields $f_0 : \mathbb{R}^n \to \mathbb{R}^n$ and $f_1 : \mathbb{R}^n \to \mathbb{R}^n$ are Lipschitz functions with a linear growth: there exists a constant $M_0 > 0$ such that:

$$\|f_0(x)\| \leq M_0(1 + \|x\|) \quad \text{and} \quad \|f_0(x)\| \leq M_0(1 + \|x\|) \qquad \forall x \in \mathbb{R}^n.$$

Let $x \in \mathbb{R}^n$ and $C \in \mathcal{A}$ be an admissible control. By a solution to (4.2) we mean an absolutely continuous function $y(\cdot)$ that satisfies

$$y(t) = x + \int_0^t [f_0(y(s)) + f_1(y(s))C(s))]ds \quad \text{for all } t \geq 0.$$

By the Lipschitz continuity of $f_0,\ f_1$ and by their linear growth, the solution of (4.2) is uniquely determined by the control input $C \in \mathcal{A}$ and the initial condition $y(0) = x \in \mathbb{R}^n$and will be denoted by y_x^C. Furthermore, the maximal solution is defined for all times. Note, that by the Gronwall Lemma, we have:

$$\begin{aligned}
&1 + |y_x^C(t)| \leq (1 + |x|)e^{M_0 t} \qquad t \geq 0,\\
&|y_x^C(t) - x| \leq (1 + |x|)(e^{M_0 t} - 1) \qquad t \geq 0,\\
&|\dot{y}_x^C(t)| \leq M_0(1 + |x|)e^{M_0 t} \qquad \text{a.e. } t > 0.
\end{aligned}$$

Moreover, for any $R > 0$, there exists $M_R > 0$ such that:

$$|y_x^C(t) - y_{x'}^C(t)| \leq M_R|x - x'|e^{M_0 t} \qquad \forall x, x' \in \mathbb{B}(0,R).$$

Definition 1. A solution $y : \mathbb{R}^+ \to \mathbb{R}^n$ of (4.2) considered with control $C \in \mathcal{A}$ and initial condition $y(0) = x_0 \in \mathbb{R}^n$ is denoted $y_{x_0}^C$. For any $x \in \mathbb{R}^n$, we denote $S(x)$ the set of solutions of (4.2) with initial condition x:

$$S(x) = \{y_x^C, C \in \mathcal{A}\}$$

In this work, we will be interested in three different systems described in 4.2.1. Before presenting them, we will introduce some notations.

4.2.1 Three models for heterogeneous tumour growth

The first system comes from [1]. It models the growth of two populations of cells in a Petri dish in competition for nutrients: s is the population sensitive to the treatment C, and r the population resistant to it.

$$\begin{cases} \frac{ds}{dt}(t) = \rho s(t)(1 - \frac{s(t)+mr(t)}{K}) - \alpha s(t)C(t) \\ \frac{dr}{dt}(t) = \rho r(t)(1 - \frac{s(t)+mr(t)}{K}) - \beta s(t)r(t) \end{cases} \quad (*)$$

The set $\mathcal{K} := \{(s,r) \in \mathbb{R}^2 / s \geq 0, r \geq 0 \text{ and } s + mr \leq K\}$ is invariant under action of system (*). Since K is the total space available in the Petri dish, $\mathcal{K}$ represents the set of biologically possible situations. Thus, we can modify f_0 and f_1 outside of $\mathcal{K}$ such that for a certain $R > \max(K, K/m)$, $|y| > R$ implies $f_0(y) = f_1(y) = 0$ and f_0 and f_1 are Lipschitzian on $\mathbb{R}^2$.

In the following, we will assume $C_{max} > \frac{\rho}{\alpha}$, meaning that we have access to relatively large doses of treatment.

The second model is very linked to (*): the drug action is slightly different, as it has less effect if sensitive cells are too numerous.

$$\begin{cases} \frac{ds}{dt}(t) = \rho s(t)(1 - \frac{s(t)+mr(t)}{K}) - \alpha \frac{s(t)}{s(t)+s_0} C(t) \\ \frac{dr}{dt}(t) = \rho r(t)(1 - \frac{s(t)+mr(t)}{K}) - \beta s(t)r(t) \end{cases} \quad (**)$$

Coefficient s_0 represents the quantity of sensitive cells s such that the treatment is half as efficient as when very few cells are present. Just as for (*), $\mathcal{K}$ is invariant under action of (**). We thus apply the same modification outside of $\mathcal{K}$ such that f_0 and f_1 are Lipschitzian on $\mathbb{R}^2$.

The third model introduces a new state variable, describing the immune system w. It is produced at a constant rate ρ_w, evacuated from the system at rate μw, and is affected by drug dosages higher than C_{immu}:

$$\begin{cases} \frac{ds}{dt}(t) = \rho s(t)(1 - \frac{s(t)+mr(t)}{K}) - \alpha s(t)C(t) \\ \frac{dr}{dt}(t) = \rho r(t)(1 - \frac{s(t)+mr(t)}{K}) - \beta s(t)r(t) \\ \frac{dw}{dt}(t) = \rho_w - \mu w(t) - \nu w(t) \max(0, C(t) - C_{immu}) \end{cases} \quad (***)$$

This model is inspired by [BFCI03]. The set $\mathcal{K}' := \{(s,r,w) \in \mathbb{R}^3 / s \geq 0, r \geq 0, w \geq 0, s + mr \leq K \text{ and } w \leq \rho_w/\mu\}$ is stable under action of system (***). As previously, we modify f_0 and f_1 outside of $\mathcal{K}'$ such that both are Lipschitzian on $\mathbb{R}^3$.

4.2.2 Objectives and constraints

We consider two types of objectives. They will both consider the tumour size, which we define here:

$$\phi : (s,r) \mapsto s + mr.$$

For the prupose of notation, when we consider System (***), we will denote $\phi(s,r,w) = s + mr$.

The first one is a problem of viability:

Problem 4 (Viability)**.** *Let $Q > 0$ be such that $Q < K$. Given $x_0 \in \mathbb{R}^n$, does there exist a control $C \in \mathcal{A}$ such that its associated trajectory $y^C_{x_0}$ satisfies:*

$$\forall t \geq 0,\ \phi(y^C_{x_0}(t)) \leq Q$$

In other words, given a threshold in tumour size Q, can we find a control such that the effective population never exceed this threshold?

The second problem is an reachability problem:

Problem 5 (Reachability)**.** *Let $Q > 0$ be such that $Q \leq K$, and let $T_0 > 0$. For $x_0 \in \mathbb{R}^n$, does there exists a control $C \in \mathcal{A}$ and a minimal time $t_{in} \in [0, T_0]$ such that the associated trajectory $y^C_{x_0}$ satisfies:*

$$\forall t \geq t_{in},\ \phi(y^C_{x_0}(t)) \leq Q$$

In other words, given a certain time of treatment initialization T_0, minimize the time t_{in} before which the tumour size is stabilized under the threshold Q, without this time exceeding T_0.

These problems will be considered for Systems (*),(**),(***). For system (***), we will furthermore consider the following constraint:

Constraint (Immune system)**.** *Let $w_{min} > 0$ be a constant such that $\frac{\rho_w}{\mu} > w_{min}$. Then Problems 4 and 5 must be solved for System (***) respecting the following constraint:*

$$\forall t \geq 0, w(t) \geq w_{min} \tag{4.3}$$

In other words, we do not allow treatment protocols that let the immune system fall under a certain threshold w_{min}. This constraint can be taken into account immediately in Problem 4 by modifying the tumour size function ϕ:

$$\tilde{\phi} : (s, r, w) \mapsto \max(s + mr, K + \frac{w_{min} - w}{w_{min}})$$

Then for any (s, r, w), we have that $\tilde{\phi}(s, r, w) \leq K$ is equivalent to $\phi(s, r, w) \leq K$ and $w \geq w_{min}$ simultaneously.

However, for Problem 5, it must be considered as a supplementary constraint, since we do not allow any trajectory violating this constraint.

4.3 Stability and reachability

We now describe the objects we will use to address Problems 4 and 5.

4.3.1 Definition of the stability kernels

Let $\mathbb{T} \subset \mathbb{R}^n$. We define the stability kernel of $\mathbb{T}$:

Definition 2. The stability kernel of $\mathbb{T}$ is the set $\mathcal{N}_\mathbb{T} \subset \mathbb{R}^n$ defined by:

$$\mathcal{N}_\mathbb{T} := \{x \in \mathbb{R}^n \,/\, \exists C \in \mathcal{A},\ \forall t > 0,\ y^C_x(t) \in \mathbb{T}\}.$$

It is the set of starting points such that, there exists a control keeping the solution in $\mathbb{T}$ for any time $t \geq 0$.

In our study, we want to determine numerically the stability kernel of $\mathbb{T}_Q := \{(s, r) \in \mathbb{R}^2 / s \geq 0, r \geq 0 \text{ and } s + mr \leq Q\}$, for $Q \in (0, K)$ a threshold value of the tumour size.

Property 1. For Model (*), if $Q > \frac{K}{1+K\beta/\rho}$ then $\mathcal{N}_{\mathbb{T}_Q}$ has a non empty interior. If $Q \leq \frac{K}{1+K\beta/\rho}$ then $\mathcal{N}_{\mathbb{T}_Q} = [0, Q] \times \{0\}$.

Proof. The two parts of this property come from phase plane analysis of System (*).

— Let $Q > \frac{K}{1+K\beta/\rho}$. Consider the point $E = (\frac{1}{2}(Q + \frac{K}{1+K\beta/\rho}), 0)$: a study of the linearized system around it shows that it is stable and locally attractive under constant treatment $C(t) \equiv \frac{\rho}{\alpha}(1 - \frac{1}{2K}(Q + \frac{K}{1+K\beta/\rho}))$. Thus there exists a neighbourhood V_E of E such that $V_E \cap \mathbb{T}_Q \subset \mathcal{N}_{\mathbb{T}_Q}$.

— Let $Q \leq \frac{K}{1+K\beta/\rho}$. Under constant treatment $C(t) \equiv \frac{\rho}{\alpha}(1 - \frac{Q}{K})$, for any $s \in (0, Q]$, we have $y^C_{(s,0)}(t) \underset{t\to+\infty}{\longrightarrow} (Q, 0)$, and $(0, 0)$ is stable under any treatment, thus $[0, Q] \times \{0\} \subset \mathcal{N}_{\mathbb{T}_Q}$. Moreover, for any $(s, r) \in \mathbb{T}_Q$, we have $\frac{dr}{dt}(t) \geq r\beta(\frac{K}{1+K\beta/\rho} - s)$, and $s > \frac{K}{1+K\beta/\rho}$. Thus any trajectory starting in $\mathbb{T}_Q$ will leave it in a finite time.

□

Property 1 is still true for system (**), but the demonstration is slighlty different. For system (***), the result is still true if $C_{immu} > \frac{\rho}{\alpha}(1 - \frac{1}{1+K\beta/\rho})$.

As we are interested in controlling heterogeneous tumours (*i.e.* with $r > 0$), we will only consider $Q > \frac{1}{1+K\beta/\rho}$.

4.3.2 Value function of the viability problem

To compute the viability kernel, we use a *level-set approach* and define a control problem and its value function whose 0-sub-level set coincides exactly with the viability kernel.

For this, we fix $Q > \frac{1}{1+K\beta/\rho}$ and define a Lipschitz continuous function $g_Q : \mathbb{R}^n \to \mathbb{R}$ such that

$$x \in \mathring{\mathbb{T}}_Q \iff g_Q(x) < 0$$

. A particular choice of g_Q could be:

$$g_Q((s, r)) = \max(-s, -r, s + mr - Q)$$

but we could have chosen the signed distance to $\mathbb{T}_Q$.

Now, consider the following control problem parametrized by the initial position $x \in \mathbb{R}^n$:

$$(\mathcal{P}_x) \qquad \min_{C\in\mathcal{A}} \max_{t\geq 0} e^{-\lambda t} g_Q(y^C_x(t))$$

where $\lambda > 0$ is a constant that will be chosen later. We consider also the *value function* (called also *cost-to-go function*) defined by:

$$V_Q(x) = \min(\mathcal{P}_x), \quad \forall x \in \mathbb{R}^n.$$

Before studying this control problem, let us first give point out some straightforward remarks on the value function

Remark 2.

— Since f_0 and f_1 are Lipschitz continuous functions, by Fillipov theorem, for every $t > 0$, the set of trajectories $S_{[0,t]}(x)$ is a compact set in $W^{1,1}([0, t])$ endowed with the C^0-topology. In the case of infinite horizon $t = +\infty$, the set of trajectories $S_{[0,+\infty[}(x)$ is also a compact set in $W^{1,1}(0, +\infty;\ e^{-(M_0+1)t}dt)$ (which is the space of functions $z \in L^1(0, +\infty;\ e^{-(M_o+1)t}dt)$ such that its weak derivative $\dot{z} \in L^1(0, +\infty;\ e^{-(M_o+1)t}dt)$ endowed with the C^0-topology). A consequence of this compactness is that for every $x \in \mathbb{R}$ the control problem $(\mathcal{P}_x)$ admits an optimal solution.

— Furthermore, it is not difficult to check that the viability kernel $\mathcal{N}_{\mathbb{T}_Q}$ can be characterized as the 0-sub-level set of the function V_Q:

$$\mathcal{N}_{\mathbb{T}_Q} = \{x / V_Q(x) \leq 0\}.$$

— Finally, the fact that g_Q is bounded ensures that V_Q is also bounded.

In the sequel, we shall study the properties of the value function V_Q and show a way to get an efficient approximation on $\mathcal{K}$ by solving an appropriate partial differential equation.

Property 2. The value function V_Q is Lipschitz continuous on $\mathbb{R}^n$ if λ is large enough.

Proof. Because f and g are Lipschitz continuous on $\mathbb{R}^n$ for problems (*), (**) and (***), according to the Gronwall lemma, there exists $L > 0$ such that for any x, $x' \in \mathbb{R}^n$, any $t \geq 0$ and any $C \in \mathcal{A}$,

$$|y_x^C(t) - y_{x'}^C(t)| \leq e^{Lt}|x - x'|.$$

We also note L' the coefficient of Lipschitzianity of g_Q. Now let us consider x, $x' \in \mathbb{R}^n$.

$$\begin{aligned}
|V_Q(x) - V_Q(x')| &= |\inf_{C\in\mathcal{A}} \max_{t\geq 0} e^{-\lambda t} g_Q(y_x^C(t)) - \inf_{C\in\mathcal{A}} \max_{t\geq 0} e^{-\lambda t} g_Q(y_{x'}^C(t))| \\
&\leq \sup_{C\in\mathcal{A}} \max_{t\geq 0} e^{-\lambda t} |g_Q(y_x^C(t)) - g_Q(y_{x'}^C(t))| \\
&\leq \max_{t\geq 0} e^{-\lambda t} L' e^{Lt} |x - x'|.
\end{aligned}$$

If we choose $\lambda > L$, then the function V_Q is Lipschitz continuous. □

The value function V_Q satisfies a dynamic programming principle that we can state as:

$$\forall x \in \mathbb{R}^n,\ \forall h > 0,\ V_Q(x) = \min_{C\in\mathcal{A}} \max \left(\max_{t\in[0,h]} e^{-\lambda t} g_Q(y_x^C(t)), e^{-\lambda h} V_Q(y_x^C(h)) \right). \tag{4.4}$$

In the following, we will deduce from (4.4) a Hamilton-Jacobi-Bellman equation that V_Q satisfies in the viscosity sense. Let us first define such solutions:

Definition 3. Consider the following variationnal inequality:

$$\min\left(u(x) - g(x), \lambda u(x) + H(x, \nabla u(x))\right) = 0 \tag{4.5}$$

where $g : \mathbb{R}^n \to \mathbb{R}$ is a bounded, absolutely continuous function, and $H : \mathbb{R}^n \times \mathbb{R}^n \to \mathbb{R}$.

Let u be a bounded and uniformly continuous function on $\mathbb{R}^n$. We say that u is a viscosity solution of (4.5) provided that for any $v \in C^\infty(\mathbb{R}^n)$,

— if $u - v$ has a local maximum at a point $x_0 \in \mathbb{R}^n$, then $\min\left(v(x) - g_Q(x), \lambda v(x) + H(x, \nabla v(x))\right) \leq 0$,

— if $u - v$ has a local minimum at a point $x_0 \in \mathbb{R}^n$, then $\min\left(v(x) - g_Q(x), \lambda v(x) + H(x, \nabla v(x))\right) \geq 0$.

We can now define the Hamilton-Jacobi-Bellman equation that V_Q satisfies:

Theorem 10. *For any $\lambda > M_0$, the value function V_Q is a continuous viscosity solution of the variational inequality (obstacle problem)*

$$\min(\lambda V_Q + H(x, \nabla V_Q),\ V_Q - g_Q(x)) = 0, \quad x \in \mathbb{R}^d, \tag{4.6}$$

where the Hamiltonian $H : \mathbb{R}^n \times \mathbb{R}^n \to \mathbb{R}$ is defined by:

$$H(x, p) := \max_{c\in[0, C_{\max}]} \langle -f(x, c), p\rangle.$$

Proof. First note that H satisfies the following property:

$$\forall x, y \in \mathbb{R}^n, \forall p \in \mathbb{R}^n, |H(x,p) - H(y,p)| \leq \kappa |x-y|(1+|p|)$$

By the dynamic programming principle (4.7), we get that for any $\tau \geq 0$

$$V_Q(x) \geq \inf_{C \in \mathcal{A}} e^{-\lambda \tau} V_Q(y_x^C(\tau)).$$

Hence, with classical arguments, we can obtain

$$\lambda V_Q + H(x, \nabla V_Q) \geq 0,$$

in the viscosity sense. Moreover, by definition of V_Q, for every $x \in \mathbb{R}^d$, we have

$$V_Q(x) \geq \inf_{C \in \mathcal{A}} \max_{t \in [0,\infty[} e^{-\lambda t} g(y_x^C(t)) \geq g_Q(x).$$

Combining these two inequalities, we get

$$\min(\lambda V_Q + H(x, \nabla V_Q), V_Q(x) - g_Q(x)) \geq 0$$

in the viscosity sense, i.e., V_Q is a supersolution of (4.6).

Let us now prove that V_Q is a subsolution. Let $x \in \mathbb{R}^n$ and assume that $V_Q(x) = g_Q(x)$, then clearly in this case V_Q satisfies:

$$\min(\lambda V_Q + H(x, \nabla V_Q), V_Q(x) - g(x)) \leq 0.$$

Now, assume that $V_Q(x) > g_Q(x)$. By continuity of g and V_Q, there exists some $\tau > 0$ such that $e^{-\lambda \tau} V_Q(y_x^C(t)) > e^{-\lambda t} g_Q(y_x^C(t))$ for all $t \in [0, \tau]$ (since $y_x^C(t)$ will stay in a neighborhood of x which is controlled uniformly with respect to C). Hence, by using the DPP, we get that

$$V_Q(x) = \min_{C \in \mathcal{A}} e^{-\lambda h} V_Q(y_x^C(h)), \quad \text{for any } 0 \leq h \leq \tau.$$

We then deduce by classical arguments [Eva10] that $\lambda V_Q(x) + H(x, \nabla V_Q(x,t)) \leq 0$ in the viscosity sense. Therefore, V_Q is a viscosity subsolution of (4.6). □

The fact that V_Q is the unique solution of the equation (4.6) follows from the comparison principle in Theorem 11.

In a more general framework, to ensure certain properties of the solutions to (4.6), we impose on H the following hypothesis: there exists a constant $\kappa > 0$ such that

$$\forall x, y \in \mathbb{R}^n, \forall p \in \mathbb{R}^n, |H(x,p) - H(y,p)| \leq \kappa |x-y|(1+|p|) \tag{H1}$$

$$\forall x \in \mathbb{R}^n, \forall p, q \in \mathbb{R}^n, |H(x,p) - H(x,q)| \leq \kappa |p-q| \tag{H2}$$

Theorem 11 (Unicity of solution)**.** *Let g and h be two continuous functions of $\mathbb{R}^n$ such that $\sup_{x \in \mathbb{R}^n}(g(x) - h(x)) \geq 0$, and suppose H satisfies* (H1) *and* (H2)*.*

We suppose that u and v are two absolutely continuous bounded functions satisfying:

$$\forall x \in \mathbb{R}^n \begin{cases} \min\left(u(x) - g(x), \lambda u + H(x, \nabla u)\right) \leq 0 \\ \min\left(v(x) - h(x), \lambda v + H(x, \nabla v)\right) \geq 0 \end{cases}$$

In other words, u is a sub-solution of the Hamilton-Jacobi-Bellman equation (4.6) *with boundary g, and v is a super-solution of the Hamilton-Jacobi-Bellman equation* (4.6) *with boundary h. Then the following result holds:*

$$\sup_{x\in\mathbb{R}^n}(u(x)-v(x)) \leq \sup_{x\in\mathbb{R}^n}(g(x)-h(x))$$

Moreover, as solutions of (4.6) *are sub and super-solutions, they are unique.*

Proof. Suppose there exists x_0 such that:

$$u(x_0)-v(x_0) > \sup_{x\in\mathbb{R}^n}(g(x)-h(x)).$$

We define $\sigma = u(x_0)-v(x_0)-\sup_{x\in\mathbb{R}^n}(g(x)-h(x)) > 0$.

Let us now define the following function on $\mathbb{R}^{2n}$ for a certain $\epsilon > 0$:

$$\phi : (x,y) \mapsto u(x)-v(y)-\frac{|x-y|^2}{2\epsilon}$$

As u and v are both bounded, ϕ admits a local maximum at (x_ϵ, y_ϵ). As x_ϵ is a local maximum of $x \mapsto u(x)-v(y_\epsilon)-\frac{|x-y_\epsilon|^2}{2\epsilon}$, we can deduce that

$$\nabla u(x_\epsilon) - \frac{x_\epsilon - y_\epsilon}{\epsilon} = 0.$$

Similarly, y_ϵ is a local maximum of $y \mapsto u(x_\epsilon)-v(y)-\frac{|x_\epsilon-y|^2}{2\epsilon}$, thus

$$\nabla v(y_\epsilon) + \frac{x_\epsilon - y_\epsilon}{\epsilon} = 0.$$

Note that $\phi(x_\epsilon, y_\epsilon) \geq \sup_x \phi(x,x) \geq \sigma + \sup_{x\in\mathbb{R}^n}(g(x)-h(x))$. Furthermore, we deduce from this inequality that:

$$\frac{|x_\epsilon - y_\epsilon|^2}{\epsilon} \leq u(x_\epsilon)-v(y_\epsilon)-\sigma-\sup_{x\in\mathbb{R}^n}(g(x)-h(x))$$

and as u and v are both bounded, we have that

$$|x_\epsilon - y_\epsilon| = O(\epsilon^{1/2})$$

Moreover, as $\phi(x_\epsilon, y_\epsilon) \geq \phi(x_\epsilon, x_\epsilon)$, we have:

$$\begin{aligned} u(x_\epsilon)-v(y_\epsilon)-\frac{|x_\epsilon-y_\epsilon|^2}{\epsilon} &\geq u(x_\epsilon)-v(x_\epsilon) \\ \text{wich implies } \frac{|x_\epsilon-y_\epsilon|^2}{\epsilon} &\leq v(x_\epsilon)-v(y_\epsilon) \leq \kappa|x_\epsilon-y_\epsilon| \end{aligned}$$

as v is Lipschitz continuous. Thus $|x_\epsilon - y_\epsilon| = O(\epsilon)$.

We also have that $v(x) \geq h(x)$ for any $x \in \mathbb{R}^n$, thus:

$$\begin{aligned} u(x_\epsilon)-v(y_\epsilon) &\geq \sigma + \sup(g(x)-h(x)) + \frac{|x_\epsilon-y_\epsilon|^2}{2\epsilon} \\ &\geq \sigma + g(x_\epsilon) - h(x_\epsilon) + \frac{|x_\epsilon-y_\epsilon|^2}{2\epsilon} \\ u(x_\epsilon) &\geq \sigma + g(x_\epsilon) + h(y_\epsilon) - h(x_\epsilon) + \frac{|x_\epsilon-y_\epsilon|^2}{2\epsilon}. \end{aligned}$$

Thanks to the estimate for $|x_\epsilon - y_\epsilon|$ and the continuity of h, we can choose ϵ small enough so that $u(x_\epsilon) \geq \frac{\sigma}{2} + g(x_\epsilon)$. Thus we have that $\lambda u(x_\epsilon) + H(x_\epsilon, \nabla u(x_\epsilon)) \leq 0$.

As a consequence:

$$\begin{aligned}\lambda u(x_\epsilon) - \lambda v(y_\epsilon) &\leq H(y_\epsilon, \nabla v(y_\epsilon)) - H(x_\epsilon, \nabla u(y_\epsilon)) \\ &\leq H(y_\epsilon, \frac{x_\epsilon - y_\epsilon}{\epsilon}) - H(x_\epsilon, \frac{x_\epsilon - y_\epsilon}{\epsilon}) \\ &\leq \kappa |x_\epsilon - y_\epsilon|(1 + \frac{|x_\epsilon - y_\epsilon|}{\epsilon}).\end{aligned}$$

For ϵ small enough, we get that $\lambda u(x_\epsilon) - \lambda v(y_\epsilon) \leq \frac{\sigma}{2}$, which is absurd.

If u and v are both continuous bounded solutions of the same HJB equation, it is immediate to see that $u = v$.

□

We can note that the expression of the hamiltonian H can be simplified for the different models we work on:

For model (*)**,** the hamiltonian is:

$$H((s,r),p) = -f_0(s,r) \cdot p + \max(0, \alpha s C_{max} p_1)$$

For model (**)**,** the hamiltonian is:

$$H((s,r),p) = -f_0(s,r) \cdot p + \max(0, \alpha \frac{s}{s+s_0} C_{max} p_1)$$

For model (***)**,** the hamiltonian is:

$$H((s,r,w),p) = -f_0(s,r,w) \cdot p + \max(0, \alpha s C_{immu} p_1, \alpha s C_{max} p_1 + \mu w (C_{max} - C_{immu}) p_3)$$

These expressions will be useful for the numerical implementation of H.

4.3.3 Time minimum function

We now focus on Problem 5.

As trajectories admissible for this problem should stay in $\mathbb{T}_Q$ for any $t > T_0$, in fact they should be in $\mathcal{N}_{\mathbb{T}_Q}$ at $t = T_0$. More precisely, the problem reduces to:

Problem 6 (Simplified Reachability)**.** *For $x \in \mathbb{R}^n$, minimize over $C \in \mathcal{A}$ the time $t_{in}(x)$ such that:*

$$y_x^C(t_{in}) \in \mathcal{N}_{\mathbb{T}_Q}$$

Admissible points are x such that the minimum time $t_{in}(x)$ satisfies $t_{in}(x) < T_0$.

Note that with this definition, for certain $x \in \mathbb{R}^n$, the minimum time $t_{in}(x)$ can be $+\infty$. For example, if $x = (0, K/m)$, then for any $t \geq 0$ and any $C \in \mathcal{A}$, we have $y_x^C(t) = (0, K/m)$. Thus, if $Q < K$, whatever control is chosen, the trajectory will never enter $\mathcal{N}_{\mathbb{T}_Q}$.

To numerically solve this problem, we consider a linked problem:

Problem 7 (Intermediary problem for reachability)**.** *Let $d_Q : \mathbb{R}^n \to \mathbb{R}$ be the signed distance to $\mathcal{N}_{\mathbb{T}_Q}$:*

$$d_Q(x) = \begin{cases} dist(x, \mathcal{N}_{\mathbb{T}_Q}) \text{ if } x \notin \mathcal{N}_{\mathbb{T}_Q} \\ -dist(x, \partial\mathcal{N}_{\mathbb{T}_Q}) \text{ if } x \in \mathcal{N}_{\mathbb{T}_Q} \end{cases}.$$

Let $t \in [0, T_0]$: minimize over $C \in \mathcal{A}$ the quantity $d_Q(y_x^C(t))$.

We then define W, a value function associated to problem 7:

$$\forall x \in \mathbb{R}^n, \forall t \in [0, T_0],\ W(x,t) := \min_{C \in \mathcal{A}} d_Q(y_x^C(t)).$$

The minimum time $t_{in}(x)$ is then expressed by:

$$t_{in}(x) = \min\{t / W(t,x) \leq 0\}.$$

In order to determine t_{in} on $\mathbb{R}^n$, we thus need to calculate $W(x,t)$ for any $x \in \mathbb{R}^n$ and $t \in [0, T_0]$. The value function W satisfies the following dynamical programming principle:

$$\forall h \geq 0, W(x, t+h) = \min_{C \in \mathcal{A}} W(y_x^C(h), t) \tag{4.7}$$

From this, we can derive the Hamilton-Jacobi-Bellman equation satisfied by W:

$$0 = \partial_t W(x,t) + H(x, \nabla W(x,t)) \tag{4.8}$$

where $H(x,p) = \max_{C \in [0, C_{max}]}(f(x,C) \cdot p)$, as in (4.6). Its expression for the different models is thus unchanged. Furthermore, W satisfies the following initial condition:

$$W(x,0) = d_Q(x)$$

With these properties, we are able to numerically implement the value of W for any $x \in \mathbb{R}^n$ and any $t \in [0, T_0]$.

Theorem 12 (Unicity of the solution)**.** *We define viscosity solutions u of* (4.8) *to be uniformly continuous, bounded functions such that:*

— $\forall x \in \mathbb{R}^n$, $u(x,0) = d_Q(x)$

— *Let $v \in \mathcal{C}^\infty(\mathbb{R}^n \times (0,T))$. If $(u - v)$ has a local maximum at (x_0, t_0) then*

$$\partial_t v(x_0,t_0) + H(x_0, \nabla v(x_0,t_0)) \leq 0.$$

Conversely, if $(u - v)$ has a local minimum at (x_0, t_0) then

$$\partial_t v(x_0,t_0) + H(x_0, \nabla v(x_0,t_0)) \geq 0.$$

Then, under hypothesis (H1) *and* (H2)*, there exists at most one solution to* (4.8) *with initial condition $u(x,0) = d_Q(x)$.*

The proof of this theorem can be found in [Eva10]. It relies on the same kind of construction as for our proof of 11: if u and v are two solutions of (4.8) with the same initial condition, we define a function ϕ "doubling the variables":

$$\phi(x, \xi, t, \tau) = u(x,t) - v(\xi, \tau) - \mu(t+\tau) - \frac{1}{\epsilon^2}(|x-\xi|^2 + (t-\tau)^2) - \epsilon(|x|^2 + |\xi|^2)$$

where $\mu < 1$ and $\epsilon > 0$ are to be carefully chosen. If $\sup_{x,t}(u(x,t) - v(x,t)) > 0$, after successive estimates on the 4-uple $(x_\epsilon, \xi_\epsilon, t_\epsilon, \tau_\epsilon)$ that realises the maximum of ϕ, it is possible to draw a contradiction. For a more detailed proof we refer to [Eva10].

An illustration of $\mathcal{N}_{\mathbb{T}_Q}$ and some trajectories reaching it are presented in 4.1.

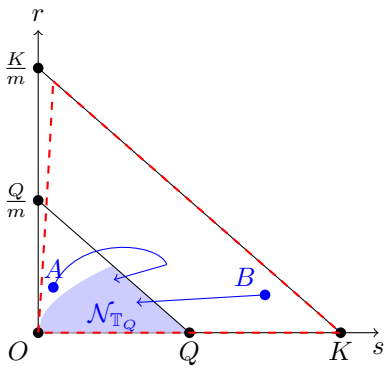

Figure 4.1 – The set $\mathcal{N}_{\mathbb{T}_Q}$ is determined by the calculation of V_Q. Then, the set of points from which $\mathcal{N}_{\mathbb{T}_Q}$ is reachable (inside red dashed line) is determined with W. Point A satisfies $\phi(A) \leq Q$, but all trajectories starting from it exit the triangle $\{x/\,\phi(x) \leq Q\}$. Thus A is not in $\mathcal{N}_{\mathbb{T}_Q}$. A trajectory starting from A and entering $\mathcal{N}_{\mathbb{T}_Q}$ is represented. Point B is not in the triangle $\{x/\,\phi(x) \leq Q\}$, but a trajectory starting from it can reach $\mathcal{N}_{\mathbb{T}_Q}$ faster than T_0.

4.4 Numerical implementation

We will present in this section different algorithms to numerical determine the value functions V and W on $\mathbb{R}^n$ and $\mathbb{R}^n \times [0, T_0]$ respectively. We will not present an exhaustive list of detailed methods, but rather highlight some of them that we implemented, and explain some of their properties with links to litterature. Then, we will consider how to reconstruct optimal trajectories and controls from these value functions.

4.4.1 Viability problem

We are first interested in the numerical resolution of the following Hamilton-Jacobi equation:

$$\forall x \in \mathbb{R}^n,\ \min\left(V(x) - d_Q, \lambda V(x) + H(x, \nabla V(x))\right)$$

where $H(x,p) = \max_{C\in[0,C_{max}]}(-f(x,C)\cdot p)$ is expressed in 4.3.2.

We will present here two main methods to numerically solve this equation: a fixed point algorithm, or value iteration algorithm, and a Howard's algorithm, or policy iteration algorithm.

A fixed point algorithm

The first method we consider is a fixed point algorithm. We will describe it for problems (*) and (**), so that the problem dimension is $n = 2$, but this method is still appliable for (***), up to modify slightly the objects we consider.

The value function will be determined on $[-h, K+h] \times [-h/m, K/m + h/m]$, with $h > 0$. To simplify some notations, we will suppose $m > 1$, so that $\frac{h}{m} < h$. We note $(x)_{1\leq i,j\leq N}$ a discretization of the state variable, with $N = \lfloor \frac{K+2h}{h} \rfloor$, $x_{1,1} = (-h, -h/m)$ and $|x_{i+1,j} - x_{i,j}| = |x_{i,j+1} - x_{i,j}| = h$. We want to approximate the value function V on the points $(x)_{i,j}$: such an approximation is noted V^h and is a $N \times N$ matrix. We define the following function on matrices of size $N \times N$:

$$F^h : M \mapsto \min\left(M - g_Q^h, \lambda M + H^h(M)\right)$$

where $(g_Q^h)_{i,j} = g_Q(x_{i,j})$, and H^h is defined for $i, j < N$ by:

$$H^h(M)_{i,j} = \max_{C \in [0, C_{\max}]} \langle -f(x_{i,j}, C) \cdot \frac{1}{h} \begin{pmatrix} M_{i+1,j} - M_{i,j} \\ M_{i,j+1} - M_{i,j} \end{pmatrix} \rangle$$

and for any (i, j) such that $i = N$ or $j = N$, $H^h(M)_{i,j} = -g_Q^h(x_{i,j})/\lambda$. This way, for such (i, j), we have $F^h(M)_{i,j} = M_{i,j} - g_Q(x_{i,j})$.

For a certain $\omega \in \mathbb{R}$ that will be characterized later, we define the following function:

$$G^h : M \mapsto M - \omega F^h(M)$$

Finding V solving (4.6) is thus approximated by finding V^h solving $V^h = G^h(V^h)$. To perform a classical fixed point algorithm, we have to ensure G^h in a contraction. It suffice to choose ω such that:

$$\forall M \in \mathcal{M}_{N,N}, ||F^h(M)|| \leq \frac{1}{\omega}$$

But F^h as it is defined is not bounded. Thus we need to reduce our domain of choices of M.

Recall that in general, the definition of $\mathcal{N}_{\mathbb{T}_Q}$ does not depend on the exact definition of g_Q, as long as $g_Q(x) < 0$ for any $x \in \mathring{\mathbb{T}}_Q$ and $g_Q(x) > 0$ for any $x \notin \mathbb{T}_Q$. We can thus modify g_Q so that it is bounded:

$$g_Q^h(x) = \min(h, \max(-s, -r, s + mr - Q))$$

Since $V(x) = \min_{C \in \mathcal{A}} \max_{t \geq 0} e^{-\lambda t} g_Q(y_x^C(t))$, we have that with this new definition of g_Q, $V(x) \leq h$ for any $x \in \mathbb{R}^2$. Moreover, $V(x) \geq \min_y g_Q(y)$. Thus we can limit our numerical study to matrices M such that for any i, j, we have:

$$\min_x g_Q(x) \leq M_{i,j} \leq h$$

Property 3. We define $\mathcal{M}^{h, \min g_Q}$ the set of matrices M of size $N \times N$ such that for any i, j, $\min_x g_Q(x) \leq M_{i,j} \leq h$.

Then for well chosen ω and λ, the set $\mathcal{M}^{h, \min g_Q}$ is invariant under the action of G^h.

Proof. Let $M \in \mathcal{M}^{h, \min g_Q}$. Let $(i, j) \in \{1...N\}^2$.

Suppose $F^h(M)_{i,j} = M_{i,j} - (g_Q^h)_{i,j}$. Then:

$$\begin{aligned} G^h(M)_{i,j} &= M_{i,j} - \omega(M_{i,j} - (g_Q^h)_{i,j}) \\ &= M_{i,j}(1 - \omega) + \omega(g_Q^h)_{i,j} \\ &\in [\min_x g_Q(x), h] \end{aligned}$$

Now suppose $F^h(M)_{i,j} = \lambda M_{i,j} + H^h(M)_{i,j}$. Then:

$$\begin{aligned} G^h(M)_{i,j} &= M_{i,j} - \omega(\lambda M_{i,j} + H^h(M)_{i,j}) \\ &\geq M_{i,j} - \omega(M_{i,j} - (g_Q^h)_{i,j}) \text{ since } \lambda M_{i,j} + H^h(M)_{i,j} \leq M_{i,j} - (g_Q^h)_{i,j} \\ &\geq \min_x g_Q(x) \end{aligned}$$

Moreover,

$$\begin{aligned} G^h(M)_{i,j} &= M_{i,j} - \omega(\lambda M_{i,j} + H^h(M)_{i,j}) \\ &\leq M_{i,j}(1-\lambda\omega) + \omega||f||\frac{h-\min g_Q}{h} \\ &\leq h(1-\lambda\omega) + \omega||f||\frac{h-\min g_Q}{h} \text{ if } \lambda\omega < 1 \\ &\leq h + \omega(||f||\frac{h-\min g_Q}{h} - \lambda) \\ &\leq h \text{ if } \lambda \text{ is large enough} \end{aligned}$$

Since we can increase λ and then diminish ω without violating other constraints, we conclude that $\mathcal{M}^{h,\min g_Q}$ is stable under the action of G^h.

□

Since the set $\mathcal{M}^{h,\min g_Q}$ is stable under the action of G^h, and that up to reducing $\omega > 0$, G^h is a contraction on this set, we can apply a fixed point algorithm which will converge towards a $V^h \in \mathcal{M}_{N,N}$ such that:

$$\min(V^h - g_Q^h, \lambda V^h + H^h(V^h)) = 0$$

Once parameters λ and ω are carefully chosen according to the value og g_Q and h, the implementation of this algorithm is quite straightforward. Each iteration requires few computations. However, the convergence of this algorithm is linear, and the convergence rate is of the order of $1-\omega$, where ω is small. Thus many iterations are needed to present a satisfyingly small error.

Howard's algorithm

A second approach of this problem is Howard's algorithm, or policy iteration algorithm. Its idea is the following: one wants to solve the non-linear problem

$$\text{find } x \in \mathbb{R}^N, \ \min_{\alpha \in A^N}(B(\alpha)x - c(\alpha)) = 0 \tag{4.9}$$

where A is a non-empty compact set, for every $\alpha \in A^N$, $B(\alpha)$ is a linear operator on $\mathbb{R}^N$ matrix and $c(\alpha)$ a N-vector, and $\min(x,y)$ where x and y are two N-vectors is the vector of components $\min(x_i, y_i)$.

The Howard's algorithm is then defined by:

- Chose an initial guess $\alpha^0 \in A^N$
- Repeat for $k \geq 0$:
  - Define x^{k+1} by solving the linear system: $B(\alpha^k)x - c(\alpha^k) = 0$. If $x^{k+1} = x^k$ then stop, otherwise:
  - Define $\alpha^{k+1} := \text{argmin}_{\alpha \in A^N}(B(\alpha)x^{k+1} - c(\alpha))$ and iterate.

An extensive study of such algorithms is performed in [BMZ09]. In particular, it is shown that if $B(\alpha)$ is monotone for any $\alpha \in A$, then this algorithm does converge to a solution of (4.9). Moreover, if A is finite, it converges in a finite number of steps.

We describe now the two-step Howard algorithm, which is also described in [BMZ09]: it aims at solving problems of the form

$$\text{find } x \in \mathbb{R}^N, \ \max_{\eta \in E^N} \min_{\alpha \in A^N}(B(\alpha,\eta)x - c(\alpha,\eta)) = 0 \tag{4.10}$$

The two-step Howard algorithm then proceds as follows:

— Chose an initial guess $\eta^0 \in E^N$
— Repeat for $k \geq 0$:
  — Define x^{k+1} by solving $\min_\alpha(B(\alpha, \eta^k)x - c(\alpha, \eta^k) = 0$. This step can be peformed through a normal Howard's algorithm.
  — If $x^{k+1} = x^k$ then stop. Otherwise, define $\eta^{k+1} := \text{argmax}_{\eta \in E^N} \min_\alpha(B(\alpha, \eta)x^{k+1} - c(\alpha, \eta^k)$ and repeat.

If the operator B is monotone for any (α, η), and B and c are continuous functions of the two variables, then according to [BMZ09] this algorithm converges to a solution of (4.10).

In our case, the presence of the hamiltonian H will modify the algorithm. We present here an idea of how to solve the viability problem for systems (*) and (**), but appart from the presence of a third state variable, system (***) can be solved with similar methods.

Now we want to explicit B and c with terms from our Hamilton-Jacobi-Bellman equation (4.6). We transform it into:

$$\text{find } V, \max_{C \in [0, C_{max}]} \min(V(x) - g_Q(x), \lambda V(x) - f(x, C) \cdot \nabla V(x)) = 0$$

As in 4.4.1, we consider a discretization of space into $N \times N$ points. Thus the approximation of V we are looking for is a $N \times N$ matrix, as is $c(\alpha, \eta)$, but also $\alpha \in A^{N \times N}$ and $\eta \in E^{N \times N}$, and $B(\alpha, \eta)$ is a linear function of matrices.

The term ∇V has to be carefully estimated over a discretized value function, so that the monotonicity of the algorithm is preserved. We define a numerical hamiltonian:

$$\mathcal{H}(x, p^-, p^+) = \max_{C \in [0, C_{max}]} \left(\max(0, f_s(x, C))p_1^- + \min(0, f_s(x, C))p_1^+ + \max(0, f_r(x, C))p_2^- + \min(0, f_r(x, C))p_2^+\right)$$

where $f(x, C) = \begin{pmatrix} f_s(x, C) \\ f_r(x, C) \end{pmatrix}$. This expression comes from [BFZ10]: for a different equation of Hamilton-Jacobi-Bellman, they define a numerical approximation of the Hamiltonian H. Other choices of numerical hamiltonians are also presented, which preserve the property of monotonicity.

The theoretical hamiltonian $H(x, \nabla V)$ will then be approximated by $\mathcal{H}(x, D^-V, D^+V)$ where:

$$(D^-V)_{i,j} = \frac{1}{h}\begin{pmatrix} V_{i,j} - V_{i-1,j} \\ V_{i,j} - V_{i,j-1} \end{pmatrix}, \; (D^+V)_{i,j} = \frac{1}{h}\begin{pmatrix} V_{i+1,j} - V_{i,j} \\ V_{i,j+1} - V_{i,j} \end{pmatrix}$$

Thus, by defining $A = [0, C_{max}]$ and $E = \{0, 1\}$, we can express the operator B by:

$$\begin{aligned} B(C, 0)V &= V \\ B(C, 1)V &= \lambda V + \max(0, f_s(x, C))(D^-V)_1 + \min(0, f_s(x, C))(D^+V)_1 \\ &\quad + \max(0, f_r(x, C))(D^-V)_2 + \min(0, f_r(x, C))(D^+V)_2 \end{aligned}$$

and vector c:

$$c(C, 0) = g_Q^h, \; c(C, 1) = 0$$

Property 4. If λ is big enough, for any $\alpha \in A^{N \times N}$ and any $\eta \in E^{N \times N}$, the operator $B(\alpha, \eta)$ is monotone, meaning:

$$\forall V, W \in \mathcal{M}_{N,N}, \; B(\alpha, \eta)V \leq B(\alpha, \eta)W \implies V \leq W$$

where $\leq$ is to be understood element-wise.

Proof. Let $\alpha \in A^{N\times N}$ and $\eta \in E^{N\times N}$, and let V, $W \in \mathcal{M}_{N,N}$ be such that

$$B(\alpha,\eta)V \leq B(\alpha,\eta)W$$

Suppose $V \not\leq W$: we define (i_0, j_0) the pair of indexes such that

$$V_{i_0,j_0} - W_{i_0,j_0} = \max_{i,j}(V_{i,j} - W_{i,j} > 0$$

If $\eta_{i_0,j_0} = 0$ then $V_{i_0,j_0} - W_{i_0,j_0} \leq 0$: this is absurd. Thus $\eta_{i_0,j_0} = 1$. Suppose x_{i_0,j_0} and $C = \alpha_{i_0,j_0}$ are such that $f_s(x_{i_0,j_0}, C) > 0$ and $f_r(x_{i_0,j_0}, C) > 0$. Then:

$$\begin{aligned}
&\lambda V_{i_0,j_0} + \frac{f_s(x_{i_0,j_0},C)}{h}(V_{i_0,j_0} - V_{i_0-1,j_0}) + \frac{f_r(x_{i_0,j_0},C)}{h}(V_{i_0,j_0} - V_{i_0,j_0-1}) \\
&\quad \leq \lambda W_{i_0,j_0} + \frac{f_s(x_{i_0,j_0},C)}{h}(W_{i_0,j_0} - W_{i_0-1,j_0}) + \frac{f_r(x_{i_0,j_0},C)}{h}(W_{i_0,j_0} - W_{i_0,j_0-1}) \\
&\text{thus } (V_{i_0,j_0} - W_{i_0,j_0})(\lambda + \frac{f_s(x_{i_0,j_0},C)}{h} + \frac{f_r(x_{i_0,j_0},C)}{h}) \\
&\quad \leq (V_{i_0-1,j_0} - W_{i_0-1,j_0})\frac{f_s(x_{i_0,j_0},C)}{h} + (V_{i_0,j_0-1} - W_{i_0,j_0-1})\frac{f_r(x_{i_0,j_0},C)}{h}
\end{aligned}$$

Thus if λ is big enough, either $V_{i_0-1,j_0} - W_{i_0-1,j_0} > V_{i_0,j_0} - W_{i_0,j_0}$ or $V_{i_0,j_0-1} - W_{i_0,j_0-1} > V_{i_0,j_0} - W_{i_0,j_0}$. This is a contradiction to the maximality of $V_{i_0,j_0} - W_{i_0,j_0}$. The other cases are treated similarly, always concluding in a contradiction. □

As we can in fact limit the set A of policies in α to $\{0, C_{\max}\}$, the algorithm finishes in a finite number of steps. Furthermore, in [BMZ09] the authors show that the algorithm is equivalent to a Newton-like method, with super-linear convergence.

4.4.2 Reachability and time minimum

In this section, we will present two different algorithms used to solve numerically the following Hamilton-Jacobi-Bellman equation:

$$\begin{cases} \forall x \in \mathbb{R}^n,\ \forall t \in [0,T],\ \partial_t W(x,t) + H(x, \nabla W(x,t)) = 0 \\ \forall x \in \mathbb{R}^n,\ W(x,0) = d_Q(x) \end{cases}$$

where $H(x,p) = \max_C(-f(x,C)\cdot p)$. We recall that d_Q is defined as the signed distance to $\mathcal{N}_{\mathbb{T}_Q}$, which has been numerically determined in 4.4.1.

The first algorithm is a step-by-step construction of W by reconstruction of an optimal path from any point of $\mathcal{N}_{\mathbb{T}_Q}$. The second method actually solves numerically equation (4.8).

Once an approximation of W has been calculated, we can define an approximation to the time minimum function ; its continuous definition being

$$\forall x \in \mathbb{R}^n, t_{in}(x) = \min\{t \,/\, W(x,t) \leq 0\},$$

for a discretization of time t_k, we define the numerical minimum time function as:

$$\forall i,j, t_{in}^{num}(x_{i,j}) = interp(t_k, W_{i,j,k}, t_{k-1}, W_{i,j,k-1})$$

where $t_k = \min_{k'}\{t_{k'} \,/\, W_{i,j,k'} \leq 0\}$ and $interp(t_k, W_{i,j,k}, t_{k-1}, W_{i,j,k-1})$ is an interpolation between t_k and t_{k-1} with weights $W_{i,j,k}$, $W_{i,j,k-1}$ respectively.

Semi-Lagrangian method

The first method, referred to as the semi-Lagrangian algorithm, relies mostly on the dynamical programming principle (4.7). We will first treat the reachability problem for systems (*) and (**), thus without the state constraint (4.3).

We fix a discretization $(x)_{i,j}$ of the state variables as in 4.4.1 with, and a discretization of time $(t)_{0\leq k\leq M}$ with $t_{i+1}-t_i=\Delta t$ for any i, $t_0=0$ and $t_M=T$. We want thus to determine a three dimensional matrix $(W)_{i,j,k}$ which will be an approximation of W in the sense:

$$\forall i,j,k,\ W_{i,j,k}\approx W(x_{i,j},t_k).$$

We also set a discretization of possible values of the control C: $(C)_{0\leq l\leq L}=(0,...,l\Delta C,...,C_{max})$.

We know that $W(x,0)=d_Q(x)$ for any $x\in\mathbb{R}^n$. We thus fix:

$$\forall i,j,\ W_{i,j,0}=d_Q(x_{i,j}).$$

Suppose now that $W_{i,j,k}$ is constructed for any i,j and for a certain k. Let us construct $W_{i,j,k+1}$. The dynamical programming principle applied to $(x_{i,j},t_{k+1})$ becomes:

$$W(x_{i,j},t_{k+1})=\min_{C\in\mathcal{A}}W(y^C_{x_{i,j}}(\Delta t),t_k).$$

For a fixed value of the control C_l, we determine an approximation of $y^{C_l}_{x_{i,j}}(\Delta t)$:

$$y^{C_l}_{x_{i,j}}(\Delta t)\approx x_{i,j}+\Delta t f(x_{i,j},C_l)=y_{i,j,l}.$$

If $y_{i,j,l}$ is one point of the discretized state variables, then $W(y_{i,j,l},t_k)$ has already been approximated. In general it is not the case, we have to estimate it. This can be done by interpolation using the grid points closest to $y_{i,j,l}$, or in a close range of it: we note this interpolation $\tilde{W}(y_{i,j,l},t_k)$. If $y_{i,j,l}$ falls outside of the calculations region, we can assign $\tilde{W}(y_{i,j,l},t_k)=+\infty$ (or a very large value).

Having calculated $\tilde{W}(y_{i,j,l},t_k)$ for $l=0...L$, we assign:

$$W_{i,j,k+1}=\min_l\tilde{W}(y_{i,j,l},t_k).$$

We continue this algorithm until $t_k=T$.

Note that each step requires an estimation of $f(x,C_l)$ for each point of the state variable grid and every C_l. These can be memorized to save computation time. But each time step is still very costly, especially if L is big. We remark that each time step resolution of the ODE is performed *via* a Euler method ; it is possible for more precision to use Runge-Kutta schemes, or other methods of ODE resolution.

For problem (***) with state constraints (4.3), the Hamilton-Jacobi-Bellman equation is different, as an obstacle appears:

$$\min(W(x,t)-g_w(x),\partial_t W(x,t)+H(x,\nabla W(x,t)))=0$$

This case is fully studied in [BMZ09] ; we refer to this article for any technical question on this class of problems.

The spatial interpolation induces an error of order h^2, while solving the ODE with Euler method induces an error of order Δt. Thus for the scheme to be consistent, a CFL condition is $h^2=\tau\Delta t$ where $\tau>0$ is fixed.

Solving the HJB equation

A second method is to numerically solve the Hamilton-Jacobi-Bellman equation. We will once again only cover systems (*) and (**), as (***) is fully covered in [BMZ09].

In view of [BFZ10], we define the following numerical scheme: suppose that $W_{i,j,k}$, an approximation of $W(x_{i,j}, t_k)$ is known for any i, j. Then the next time step approximation $W_{i,j,k+1}$ is defined by:

$$\frac{W_{i,j,k+1} - W_{i,j,k}}{\Delta t} + \mathcal{H}\left(x_{i,j}, \frac{1}{h}\begin{pmatrix} W_{i,j,k} - W_{i-1,j,k} \\ W_{i,j,k} - W_{i,j-1,k} \end{pmatrix}, \frac{1}{h}\begin{pmatrix} W_{i+1,j,k} - W_{i,j,k} \\ W_{i,j+1,k} - W_{i,j,k} \end{pmatrix}\right) = 0$$

where

$$\mathcal{H}(x, p^-, p^+) := \max_{C \in [0, C_{max}]} \left(\max(0, f_s(x,C))p_1^- + \min(0, f_s(x,C))p_1^+ + \max(0, f_r(x,C))p_2^- + \min(0, f_r(x,C))p_2^+\right).$$

We initialize this scheme with $W_{i,j,0} = d_Q(x_{i,j})$.

The general idea for CFL conditions in this case is that, if information crosses less than one cell during Δt, then this scheme is monotone. Thus a CFL condition is that $||f||_\infty \Delta t \leq h$.

It is shown in [CL84] that under CFL conditions on h and Δt, this scheme converges to a solution of (4.8), and the error is of order $(h + \Delta t)^{1/2}$.

4.4.3 Trajectories reconstruction

Once the value functions are constructed up to some error on a grid of calculations, we want to deduce optimal controls for a starting position x_0.

A trajectory staying in $\mathcal{N}_{\mathbb{T}_Q}$

Knowing an approximation of V, we want to construct optimal trajectories staying in $\mathcal{N}_{\mathbb{T}_Q}$ for any time $T \geq 0$.

Let x_0 be a starting point. We define a discretization of the control: $(C)_{0 \leq l \leq L} = (0, .., l\Delta C, ..C_{max})$. We define the following algorithm:

Suppose the optimal control C^* is known until t_k, and note $y_x^{C^*}(t_k) = y_k$.
- For any $l \in \{0, ..L\}$, calculate an approximation for $y_k^l = y_{y_k}^{C_l}(h)$. This step can be done by an Euler method, or a Runge-Kutta method of higher order if needed.
- Approximate, by interpolation for example, the value of V at point y_k^l, noted V_k^l.
- Determine which index l_0 minimizes V_k^l ; choose the corresponding control C_{l_0} as the value for $C^*(t_{k+1})$.
- If $t_{k+1} = T$ then stop, otherwise set $k = k + 1$ and repeat.

A convergence result is presented and proven in [ABDZ17]:

Theorem 13. *Note V_h the approximation of V_Q over a mesh of size h. Suppose that the error $E_h = ||V_h - V_Q(x_{i,j})||$ satisfies $E_h/h \to 0$ as $h \to 0$. Let $x_0 \in \mathbb{R}^n$ and let y^h be the "trajectory" found by the algorithm, starting from x_0, for a mesh of size h. Then:*

— *the approximate trajectories y^h are minimizing sequences in the sense:*

$$V_Q(x_0) = \max\left(\lim_{h \to 0}(\max_k e^{-\lambda t_k^h} g_Q(y_k^h)\right)$$

— *Moreover, the family y^h admits cluster points for the L^∞ as $h \to 0$. For any such cluster point $\bar{y}_{x_0} : [0,T] \mapsto \mathbb{R}^n$, we have $\bar{y}_{x_0} \in S(x_0)$, and $\bar{y}_{x_0}$ is an optimal trajectory for Problem 4.*

Thus, we are able to reconstruct approximations of optimal trajectories from the approximation of the value function.

As there might be several controls such that the trajctory stays in $\mathcal{N}_{\mathbb{T}_Q}$, the control found by this algorithm might present lots of variations.

We recall that the models we are studying come from biology, and that C represents a dose of treatment to give to a patient (or in a Petri dish as a first biological model). Thus it is not interesting for medical pruposes to propose a control with such aliasing, as doses can only be changed each day in the best case. We thus propose the following algorithm to normalize the optimal treatment:

Suppose the optimal control C^* is known until t_k, and note $y_x^{C^*}(t_k) = y_k$.
- For any $l \in \{0, ..L\}$, calculate an approximation for $y_k^l = y_{y_k}^{C_l}(h)$. This step can be done by an Euler method, or a Runge-Kutta method of higher order if needed.
- Approximate, by interpolation for example, the value of V at point y_k^l, noted V_k^l.
- Determine which index l_0 minimizes $V_k^l + \mu U(C_l, C^*)$; choose the corresponding control C_{l_0} as the value for $C^*(t_{k+1})$.
- If $t_{k+1} = T$ then stop, otherwise set $k = k + 1$ and repeat.

In this algorithm, the only difference is in the penalization $\mu U(C_l, C^*)$. The coefficient μ should be chosen "small enough", so that the treatment chosen by the algorithm still chooses a minimal value of V. The penalization function itself can have different values, for different purposes. We give here two examples, but the list is not exhaustive.

- $U(C, C^*) = |C - C_k^*|$ aims at reducing the total variation of the control. This penalization often smoothens the control, which presents large plateaus each time it is changed.
- $U(C, C^*) = |C|$ aims at reducing the total amount of drug given. This penalization often creates peaks of control.

Before presenting results with this penalization, one should always check the actual trajectory without penalization. Indeed, if coefficient μ is too large, the algorithm will favor diminution of the penalization in detriment to minimization of the value function V. Then some trajectories starting in $\mathcal{N}_{\mathbb{T}_Q}$ will exit it in finite time. Moreover, if μ is too small, the penalization might not have any effect on the trajectory. As for the moment we are writing this, we can only indicate guidelines for case-by-case estimation of μ, but more general methods can be found in the litterature.

A convergence theorem for the trajectories found by the penalized algorithm can also be found in [ABDZ17].

Minimizing the time of entry

We now study how to construct optimal trajectories, knowing W, entering $\mathcal{N}_{\mathbb{T}_Q}$ in a minimal time.

The first algorithm we present is a direct application of the value function W. Choose a starting point x_0 such that $W(x_0, T) < 0$, *i.e* there exists a treatment $C \in \mathcal{A}$ such that $y_{x_0}^C(T) \in \mathcal{N}_{\mathbb{T}_Q}$: it is an initial tumour admissible for this kind of chemotherapy. The optimal trajectory can be determined by:

Suppose the optimal control C^* is known until t_k, and note $y_{x_0}^{C^*}(t_k) = y_k$.
- For any $l \in \{0, ..L\}$, calculate an approximation for $y_k^l = y_{y_k}^{C_l}(h)$. This step can be done by an Euler method, or a Runge-Kutta method of higher order if needed.
- Approximate, by interpolation for example, the value of W at point y_k^l and time t_{k+1}, noted W_k^l.
- Determine which index l_0 minimizes W_k^l ; choose the corresponding control C_{l_0} as the value for $C^*(t_{k+1})$.
- If either $t_{k+1} = T$ or $W_k^{l_0} < 0$ then stop, otherwise set $k = k + 1$ and repeat.

Note that it might occur that despite the fact that $W(x_0, T) < 0$, the algorithm stops without the trajectory having reached the viability set $\mathcal{N}_{\mathbb{T}_Q}$. This is caused either by a lack of precision in the resolution of the ODE in the first step, by a loose discretization of control $(C)_{0 \leq l \leq L}$, or even by a bad approximation of the value function W. To tackle this problem, one should then either choose a higher order method for resolution of ODE, choose more points for discretization of C or re-evaluate the mapping $W_{i,j,k}$ with smaller time step Δt and smaller space steps h for example.

By using this algorithm, note that we have to keep in memory the whole mapping $W_{i,j,k}$. Instead, we can use the time minimum function mapping t_{in}, which is of one dimension less than W, to reconstruct optimal trajectories. The algorithm now becomes, for a starting point $x_0 \in \mathbb{R}^n$:

Suppose the optimal control C^* is known until t_k, and note $y_{x_0}^{C^*}(t_k) = y_k$.
- For any $l \in \{0, ..L\}$, calculate an approximation for $y_k^l = y_{y_k}^{C_l}(h)$. This step can be done by an Euler method, or a Runge-Kutta method of higher order if needed.
- Approximate, by interpolation for example, the value of t_{in} at point y_k^l, noted $t_{in}^{k,l}$.
- Determine which index l_0 minimizes $t_{in}^{k,l}$; choose the corresponding control C_{l_0} as the value for $C^*(t_{k+1})$.
- If either $t_{k+1} = T$ or $y_k^l \in \mathcal{N}_{\mathbb{T}_Q}$ then stop, otherwise set $k = k + 1$ and repeat.

As precendently, the algorithm might stop while we have not reached $\mathcal{N}_{\mathbb{T}_Q}$; the reasons and solutions we propose are still the same.

Remark that, theoretically, one should have over the optimal trajectory C^* the following equality:

$$t_{in}(y_x^{C^*}(t)) = \Delta t + t_{in}(y_x^{C^*}(t + \Delta t)).$$

Thus instead of choosing the index minimizing t_{in} in the third step of the algorithm, we should try to satisfy this equality. However, this might not be possible due to numerical errors and the discretization of control ; it is thus easier numerically to consider a minimization.

Once again, the optimal control chosen by the algorithm might be very noisy. Methods to regularize it will be similar to what we proposed in 4.4.3.

In conclusion of this section, thanks to convergence results from [ABZ13, ABDZ17], we are able with these numerical implementations to recover a practical answer to the theoretical Problems 45.

4.5 Uncertainties

We will investigate in this section some theoretical means of taking into account uncertinties on the parameters.

In particular, in our models, the efficiency of the drug, modelled by parameter α, can vary a lot during experiments. It is due to the fact that cytotoxic drugs kill cells that are dividing ; the proportion of cancer cells in that configuration is subject to a lot of stochastic variations.

We will present the general ideas behind the theory with (*) as an example ; models (**) and (***) would present similar results.

Consider α no longer as a parameter, but as a supplementary control:

$$\begin{cases} \frac{ds}{dt}(t) = \rho s(t)(1 - \frac{s(t)+mr(t)}{K}) - \alpha(t)s(t)C(t) \\ \frac{dr}{dt}(t) = \rho r(t)(1 - \frac{s(t)+mr(t)}{K}) - \beta s(t)r(t). \end{cases} \tag{*'}$$

This system is summed up in the following notation: $\dot{(y)}(t) = f^{unc}(y, \alpha(t), C(t))$.

We now have an ODE system controlled by both $\alpha(t) \in [\alpha_{min}, \alpha_{max}]$ and $C(t) \in [0, C_{max}]$. We suppose α_{min} and α_{max} are known or at least estimated, otherwise the control of this system might prove itself impossible. During actual experiments, C is the quantity the experimenter can control directly, while α is considered as an adverse player, on which we have no control, that maybe we cannot measure for each time t, and that in any case we cannot predict. We define the set of possible functions α as:

$$\mathcal{B} := \{\alpha : t \mapsto [\alpha_{min}, \alpha_{max}], \alpha\text{measurable}\}.$$

Our control C will thus have to adapt to the actual value of α ; we will no longer talk about an optimal control, but about an optimal strategy. Let us first define, from game theory, the set of non-anticipative strategies $\mathcal{AS}$:

$$\begin{aligned} \mathcal{AS} := \{C : \mathcal{B} \to \mathcal{A} \,/\, \forall(\alpha, \alpha') \in \mathcal{B} \text{ and } \forall t \leq 0, \\ (\alpha(\tau) = \alpha'(\tau) \forall \tau \in [0, t]) \implies (C[\alpha](\tau) = C[\alpha'](\tau) \forall \tau \in [0, t])\}. \end{aligned}$$

We will denote $y_x^{\alpha, C}$ the solution of (*') with initial value $y(0) = x$.

The problem of viability with uncertainties is now the following:

Problem 8 (Optimal strategy)**.** *Given a threshold $Q > 0$, find the set of points $\mathcal{NS}_{\mathbb{T}_Q}$ such that for any point $x \in \mathcal{NS}_{\mathbb{T}_Q}$, there exists a strategy $C[\cdot] \in \mathcal{AS}$ such that:*

$$\forall \alpha \in \mathcal{B}, \forall t \geq 0, y_x^{\alpha, C[\alpha]}(t) \in \mathbb{T}_Q.$$

In other words, we want to determine the set of starting for which, even in the worst case, there exists a control C so that the trajectory stays in $\mathbb{T}_Q$.

We define the following value function for the uncertainties problem:

$$V_Q^{unc}(x) = \min_{C \in \mathcal{AS}} \max_{\alpha \in \mathcal{B}} \max_{t \geq 0} \left(e^{-\lambda t} g_Q(y_x^{\alpha, C[\alpha]}(t)) \right).$$

Then the set $\mathcal{NS}_{\mathbb{T}_Q}$ is characterized by $\mathcal{NS}_{\mathbb{T}_Q} = \{x \in \mathbb{R}^2 \,/\, V_Q^{unc}(x) \leq 0\}$.

By using the same reasonning as in 4, we find that this value function satisfies the following differential equation:

$$\min(V(x) - g_Q(x), \lambda V(x) + H(x, \nabla V(x)) = 0 \tag{4.11}$$

where

$$H^{unc}(x, p) = \max_{C \in [0, C_{max}]} \min_{\alpha \in [\alpha_{min}, \alpha_{max}]} (-f^{unc}(x, C, \alpha) \cdot p).$$

Parameter	Symbol	Value for numerical simulations
Growth rate	ρ	1
Capacity	K	3
Metabolism difference	m	2
Drug efficiency	α	0.1
Competition force	β	2/3
Maximal drug dosage	$C_{\max}$	10
Size threshold	Q	1.3
Maximal time of treatment	T_0	10 or 20
Immune system creation	ρ_w	1
Immune system evacuation	μ	1
Drug effect of the immune system	ν	1
Drug threshold for the immune system	C_{immu} 6	

Table 4.1 – List of parameters and their values for numerical simulations

We are then able, with methods from 4.4.1, to numerically determine this value function on a certain calculation space. A study of these methods and some properties can be found in [DZC12].

The reconstruction of actual optimal trajectories can then be performed through an algorithm described here. We suppose that at each time step t_k we have access to the actual value of $\alpha(t_k)$. For a starting point x_0 in $\mathcal{NS}_{\mathbb{T}_Q}$, and a final time of experiment T:

Suppose the optimal control C^* is known until t_k, and note $y_x^{C^*}(t_k) = y_k$.
- For any $l \in \{0, ..L\}$, calculate an approximation for $y_k^l = y_{y_k}^{\alpha(t_{k+1}),C_l}(h)$. This step can be done by an Euler method, or a Runge-Kutta method of higher order if needed.
- Approximate, by interpolation for example, the value of V at point y_k^l, noted V_k^l.
- Determine which index l_0 minimizes V_k^l ; choose the corresponding control C_{l_0} as the value for $C^*(t_{k+1})$.
- If $t_{k+1} = T$ then stop, otherwise set $k = k + 1$ and repeat.

This algorithm is non anticipative, and does produce an approximation of an optimal trajectory.

4.6 Numerical Simulations

Several simulations have been performed to analyse the stability properties of the numerical procedure. Results from the model (**) are not shown, since they did not differ from results of the model (*) for the range of parameters we used. The simulations were performed on ROC-HJ by Hasnaa ZIdani. The values of the different parameters are listed in table 4.1. These parameters were chosen arbitrarily to show some general numerical results.

4.6.1 Models without immune system

Figure 4.2 shows the viability kernel for the model (*). Some trajectories and the corresponding control functions are also represented

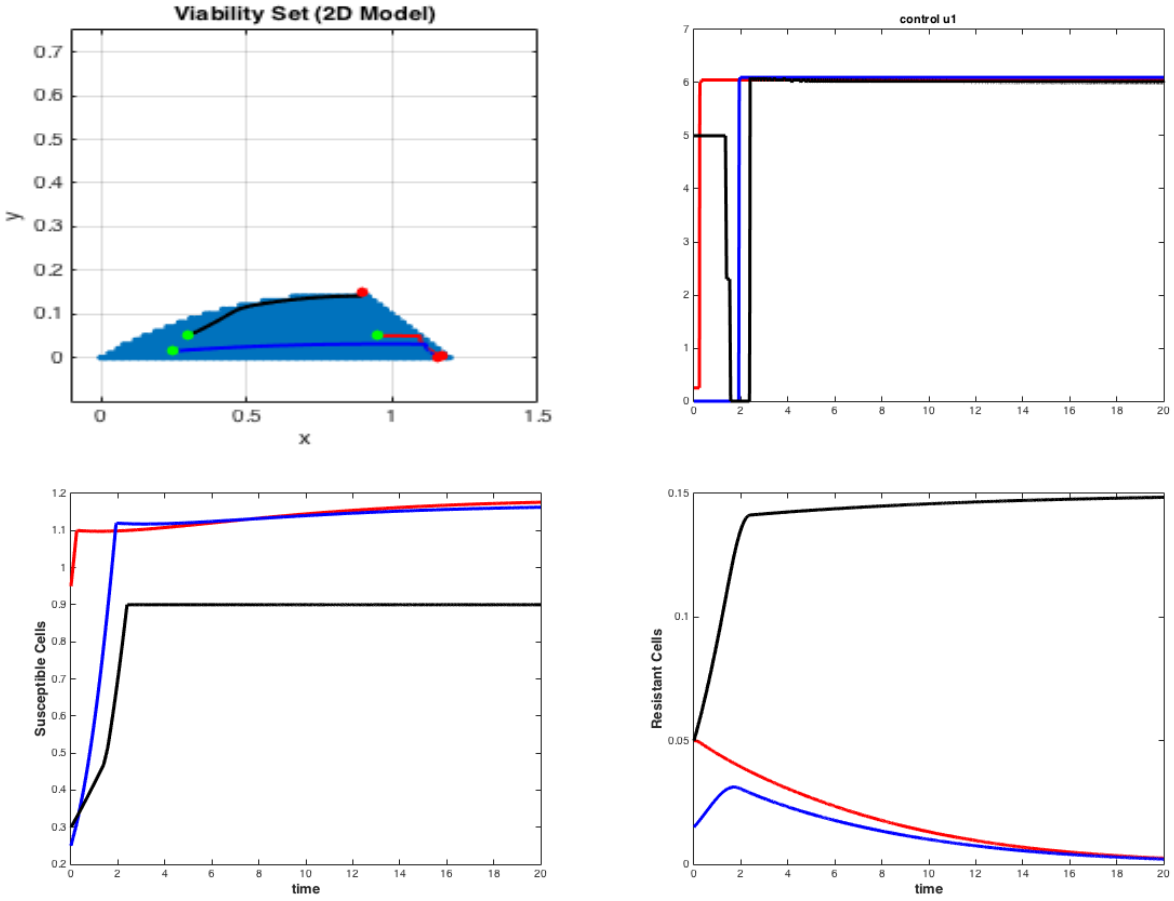

Figure 4.2 – Viability set and some optimal trajectories - Model (*)

The next figure (figure 4.3) shows the capture basin corresponding to the positions from where there exist trajectories that can reach the kernel of viability in a time less than $t = 10$. In the same figure, the trajectories represented correspond to the optimal paths starting from outside the viability kernel and that reach the kernel in minimum times.

We can note that for the viability problem, the algorithm favors intermediary values of the treatment. These simulations thus hint at the efficiency of low-dose treatments to maintain small, heterogeneous tumours. This joins the results of [1], where an adaptive treatment is designed to reduce the tumour volume.

However, the simulations of the reachability problem suggest that high dosage treatments are crucial to achieve the objectives of the problem. High values of the drug dosage given for too long periods of time can be very harmful for the patient. Thus, Model (***) introduces a modelling of the immune system to limit such damages.

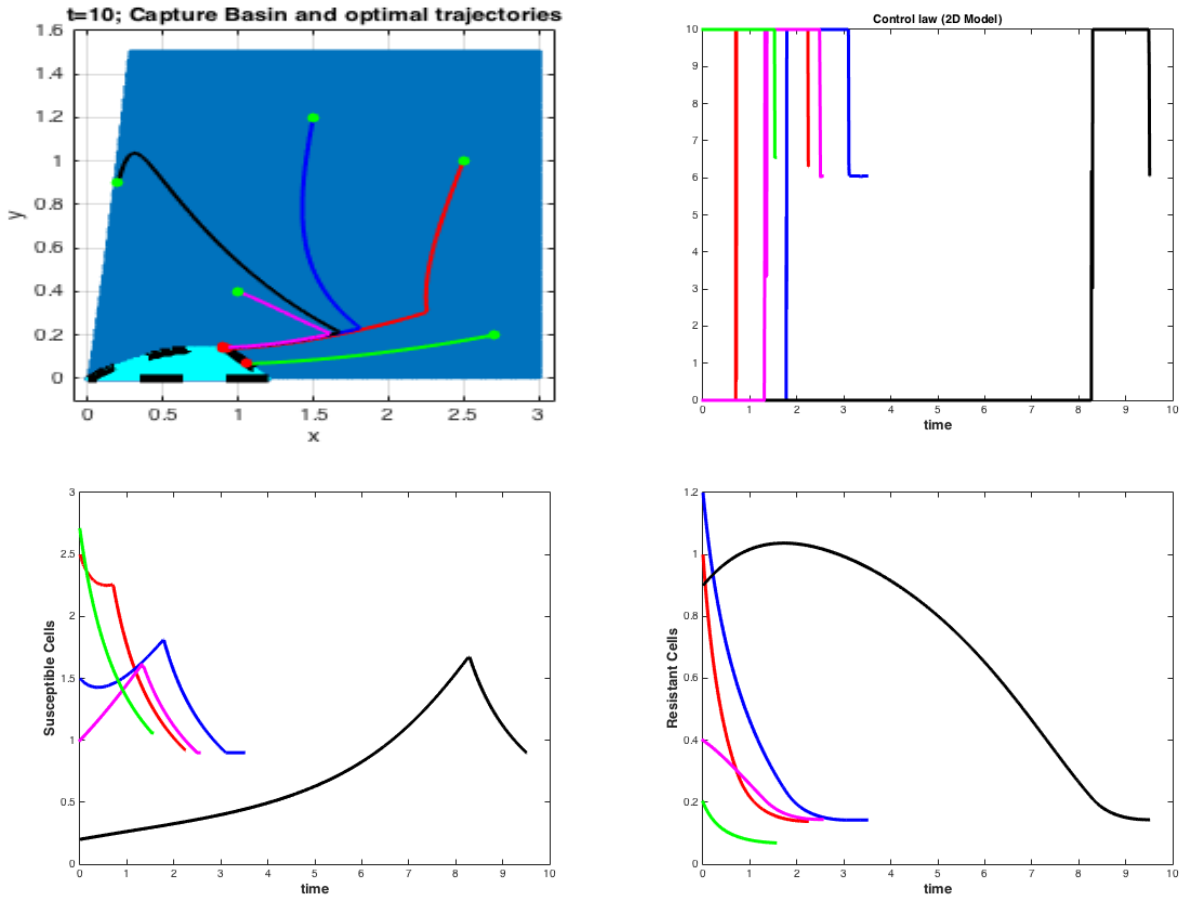

Figure 4.3 – Viability set and some optimal trajectories - Model (*)

4.6.2 Model with immune system

Here, we consider the model (***). As for the model (*), we first compute the viability kernel and then we compute the set of positions from where it is possible to find admissible trajectories that can reach the viability kernel in a time less than $t = 20$.

The next figure (figure 4.5) shows the capture basin corresponding to the positions from where there exist trajectories that can reach the kernel of viability in a time less than $t = 10$. In the same figure, the trajectories represented correspond to the optimal paths starting from outside the viability kernel and that reach the kernel in minimum times.

We note that the algorithms still favor the use of maximal treatment dose for the reachability problem, but for shorter periods of time, as the immune system is immediately damaged by it. Then, intermediary doses of treatment are preferred.

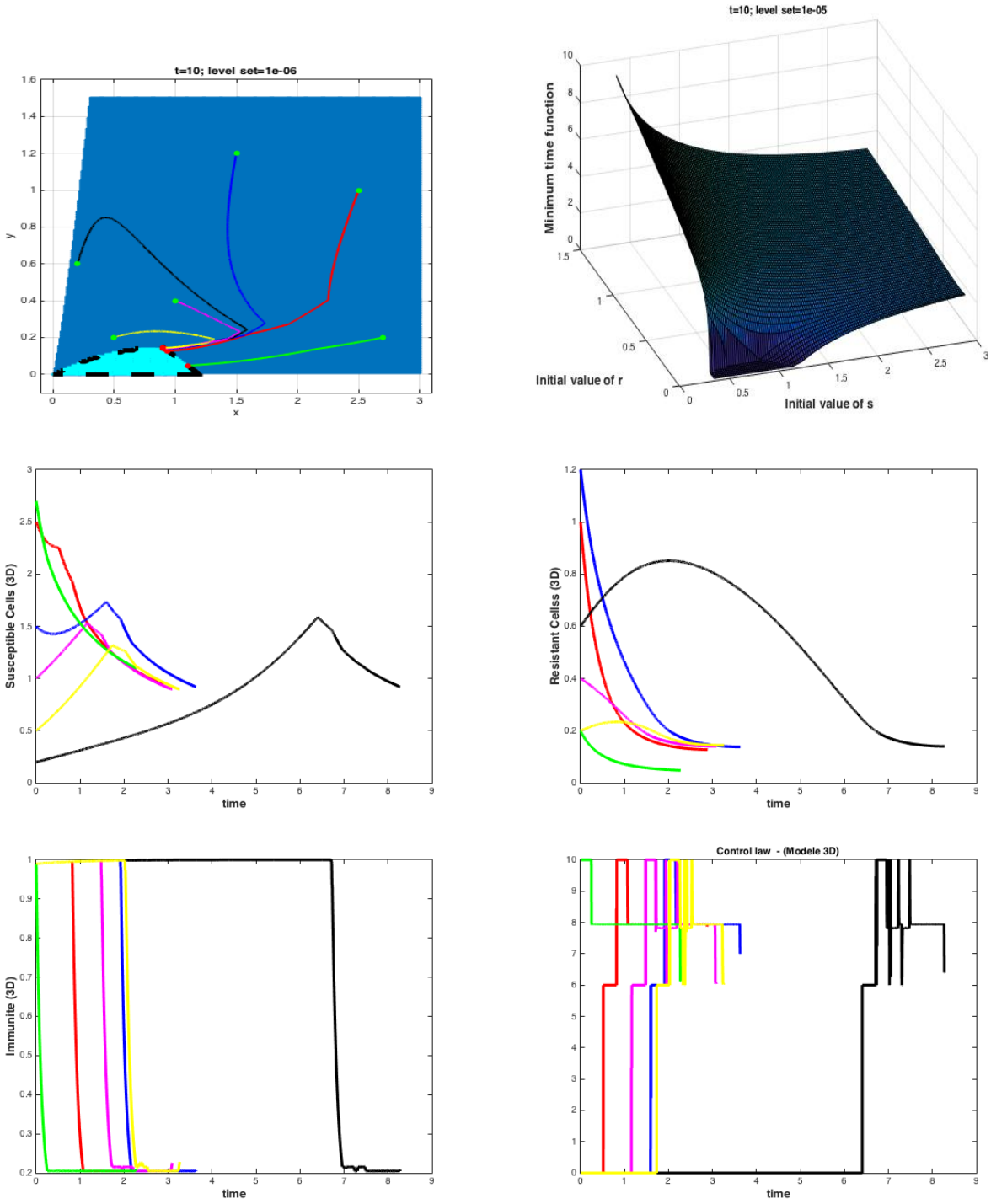

Figure 4.4 – Capture basin and some optimal trajectories - Model (***)

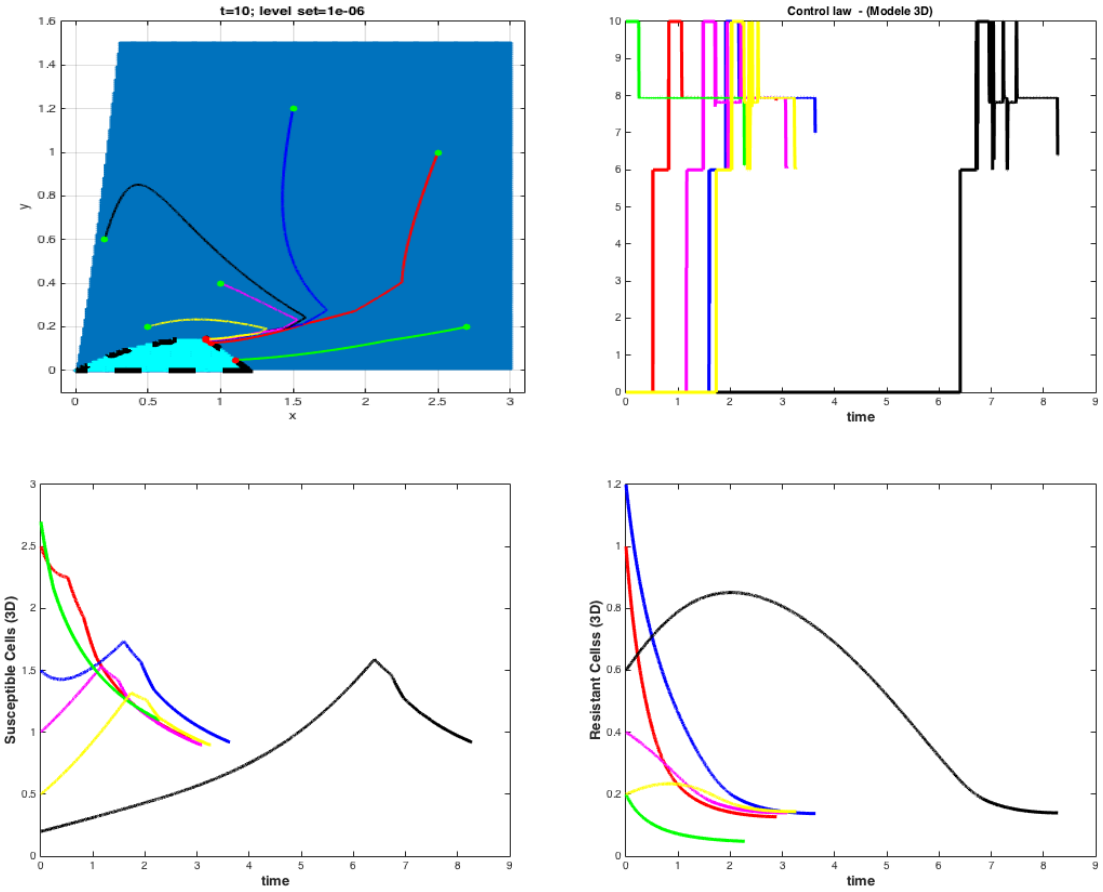

Figure 4.5 – Viability set and some optimal trajectories - Model (***)

Bibliography

References

[ABB+13] N. André, D. Barbolosi, F. Billy, G. Chapuisat, F. Hubert, E. Grenier, and A. Rovini. Mathematical model of cancer growth controled by metronomic chemotherapies. In *CANUM 2012, 41e Congrès National d'Analyse Numérique*, volume 41 of *ESAIM Proc.*, pages 77–94. EDP Sci., Les Ulis, 2013.

[ABDZ17] Mohamed Assellaou, Olivier Bokanowski, Anna Désilles, and Hasnaa Zidani. Value function and optimal trajectories for a maximum running cost control problem with state constraints. application to an abort landing problem. 2017.

[ABZ13] Albert Altarovici, Olivier Bokanowski, and Hasnaa Zidani. A general hamilton-jacobi framework for non-linear state-constrained control problems. *ESAIM: Control, Optimisation and Calculus of Variations*, 19(2):337–357, 2013.

[AW78] Donald G Aronson and Hans F Weinberger. Multidimensional nonlinear diffusion arising in population genetics. *Advances in Mathematics*, 30(1):33–76, 1978.

[BAB+12] S. Benzekry, N. André, A. Benabdallah, J. Ciccolini, C. Faivre, F. Hubert, and D. Barbolosi. Modeling the impact of anticancer agents on metastatic spreading. *Math. Model. Nat. Phenom.*, 7(1):306–336, 2012.

[Bar90] EN Barron. The pontryagin maximum principle for minimax problems of optimal control. *Nonlinear Analysis: Theory, Methods & Applications*, 15(12):1155–1165, 1990.

[BBHV09] Dominique Barbolosi, Assia Benabdallah, Florence Hubert, and Federico Verga. Mathematical and numerical analysis for a model of growing metastatic tumors. *Mathematical biosciences*, 218(1):1–14, 2009.

[BC03] Bernard Bonnard and Monique Chyba. *Singular trajectories and their role in control theory*, volume 40 of *Mathématiques & Applications (Berlin) [Mathematics & Applications]*. Springer-Verlag, Berlin, 2003.

[BD09] Helen Byrne and Dirk Drasdo. Individual-based and continuum models of growing cell populations: a comparison. *J. Math. Biol.*, 58(4-5):657–687, 2009.

[BDD+10] Estelle Borne, Eve Desmedt, Alain Duhamel, Xavier Mirabel, Véronique Dziwniel, Cyril Maire, Valérie Florin, Véronique Martinot, Nicolas Penel, Sophie Vercambre-Darras, et al. Oral metronomic cyclophosphamide in elderly with metastatic melanoma. *Investigational new drugs*, 28(5):684–689, 2010.

[BFCI03] Dominique Barbolosi, Gilles Freyer, Joseph Ciccolini, and Athanassios Iliadis. Optimisation de la posologie et des modalités d'administration des agents cytotoxiques à l'aide d'un modèle mathématique. *Bulletin du Cancer*, 90(2):167–75, 2003.

[BFZ10] Olivier Bokanowski, Nicolas Forcadel, and Hasnaa Zidani. Reachability and minimal times for state constrained nonlinear problems without any controllability assumption. *SIAM Journal on Control and Optimization*, 48(7):4292–4316, 2010.

[BG84] BG Birkhead and WM Gregory. A mathematical model of the effects of drug resistance in cancer chemotherapy. *Mathematical biosciences*, 72(1):59–69, 1984.

[BH13] Sebastien Benzekry and Philip Hahnfeldt. Maximum tolerated dose versus metronomic scheduling in the treatment of metastatic cancers. *Journal of theoretical biology*, 335:235–244, 2013.

[BHD08] David Basanta, Haralambos Hatzikirou, and Andreas Deutsch. Studying the emergence of invasiveness in tumours using game theory. *The European Physical Journal B-Condensed Matter and Complex Systems*, 63(3):393–397, 2008.

[BMZ09] Olivier Bokanowski, Stefania Maroso, and Hasnaa Zidani. Some convergence results for howard's algorithm. *SIAM Journal on Numerical Analysis*, 47(4):3001–3026, 2009.

[BP07] Alberto Bressan and Benedetto Piccoli. *Introduction to the mathematical theory of control*, volume 2 of *AIMS Series on Applied Mathematics*. American Institute of Mathematical Sciences (AIMS), Springfield, MO, 2007.

[Bra83] Maury Bramson. *Convergence of solutions of the Kolmogorov equation to travelling waves*, volume 285. American Mathematical Soc., 1983.

[BRG+87] Brian G Birkhead, Elaine M Rankin, Stephen Gallivan, Leanne Dones, and Robert D Rubens. A mathematical model of the development of drug resistant to cancer chemotherapy. *European Journal of Cancer and Clinical Oncology*, 23(9):1421–1427, 1987.

[BRS+09] Frédérique Billy, Benjamin Ribba, Olivier Saut, Hélène Morre-Trouilhet, Thierry Colin, Didier Bresch, Jean-Pierre Boissel, Emmanuel Grenier, and Jean-Pierre Flandrois. A pharmacologically based multiscale mathematical model of angiogenesis and its use in investigating the efficacy of a new cancer treatment strategy. *J. Theoret. Biol.*, 260(4):545–562, 2009.

[BSDB14] François Bertaux, Szymon Stoma, Dirk Drasdo, and Gregory Batt. Modeling dynamics of cell-to-cell variability in trail-induced apoptosis explains fractional killing and predicts reversible resistance. *PLoS computational biology*, 10(10):e1003893, 2014.

[BTM+16] Sebastien Benzekry, Amanda Tracz, Michalis Mastri, Ryan Corbelli, Dominique Barbolosi, and John ML Ebos. Modeling spontaneous metastasis following surgery: an in vivo-in silico approach. *Cancer research*, 76(3):535–547, 2016.

[BW13] Xiongxiong Bao and Zhi-Cheng Wang. Existence and stability of time periodic traveling waves for a periodic bistable lotka–volterra competition system. *Journal of Differential Equations*, 255(8):2402–2435, 2013.

[CBVG15] Jessica J Cunningham, Joel S Brown, Thomas L Vincent, and Robert A Gatenby. Divergent and convergent evolution in metastases suggest treatment strategies based on specific metastatic sites. *Evolution, medicine, and public health*, 2015(1):76–87, 2015.

[CCP+17] Joe Collis, Anthony J Connor, Marcin Paczkowski, Pavitra Kannan, Joe Pitt-Francis, Helen M Byrne, and Matthew E Hubbard. Bayesian calibration, validation and uncertainty quantification for predictive modelling of tumour growth: a tutorial. *Bulletin of mathematical biology*, 79(4):939–974, 2017.

[CD91] Michael Cross and T Michael Dexter. Growth factors in development, transformation, and tumorigenesis. *Cell*, 64(2):271–280, 1991.

[CG86] A. J. Coldman and J. H. Goldie. A stochastic model for the origin and treatment of tumors containing drug-resistant cells. *Bull. Math. Biol.*, 48(3-4):279–292, 1986. Simulation in cancer research (Durham, N.C., 1986).

[CILS12] Thierry Colin, Angelo Iollo, Damiano Lombardi, and Olivier Saut. System identification in tumor growth modeling using semi-empirical eigenfunctions. *Mathematical Models and Methods in Applied Sciences*, 22(06):1250003, 2012.

[CILS14] Thierry Colin, Angelo Iollo, Jean-Baptiste Lagaert, and Olivier Saut. An inverse problem for the recovery of the vascularization of a tumor. *Journal of Inverse and Ill-posed Problems*, 22(6):759–786, 2014.

[CL84] Michael G Crandall and P-L Lions. Two approximations of solutions of hamilton-jacobi equations. *Mathematics of Computation*, 43(167):1–19, 1984.

[CLC16] Rebecca H Chisholm, Tommaso Lorenzi, and Jean Clairambault. Cell population heterogeneity and evolution towards drug resistance in cancer: biological and mathematical assessment, theoretical treatment optimisation. *Biochimica et Biophysica Acta (BBA)-General Subjects*, 1860(11):2627–2645, 2016.

[COS+06] M Colleoni, L Orlando, G Sanna, A Rocca, P Maisonneuve, G Peruzzotti, R Ghisini, MT Sandri, L Zorzino, F Nole, et al. Metronomic low-dose oral cyclophosphamide and methotrexate plus or minus thalidomide in metastatic breast cancer: antitumor activity and biological effects. *Annals of Oncology*, 17(2):232–238, 2006.

[dC16] Institut National du Cancer. Les cancers en france en 2016, l'essentiel des faits et chiffres. Technical report, INCA, 2016.

[DGM] Arnaud Ducrot, Thomas Giletti, and Hiroshi Matano. Spreading speeds for multidimensional reaction-diffusion systems of the prey-predator type. a.

[DGM14] Arnaud Ducrot, Thomas Giletti, and Hiroshi Matano. Existence and convergence to a propagating terrace in one-dimensional reaction-diffusion equations. *Transactions of the American Mathematical Society*, 366(10):5541–5566, 2014.

[DLL+12] Li Ding, Timothy J Ley, David E Larson, Christopher A Miller, Daniel C Koboldt, John S Welch, Julie K Ritchey, Margaret A Young, Tamara Lamprecht, Michael D McLellan, et al. Clonal evolution in relapsed acute myeloid leukaemia revealed by whole-genome sequencing. *Nature*, 481(7382):506–510, 2012.

[dLMS09] Alberto d'Onofrio, Urszula Ledzewicz, Helmut Maurer, and Heinz Schättler. On optimal delivery of combination therapy for tumors. *Math. Biosci.*, 222(1):13–26, 2009.

[Dur15] Richard Durrett. Branching process models of cancer. In *Branching Process Models of Cancer*, pages 1–63. Springer, 2015.

[DZC12] Anna Desilles, Hasnaa Zidani, and Eva Crück. Collision analysis for an uav. In *AIAA Guidance, Navigation, and Control Conference*, page 4526, 2012.

[ECH10] Heiko Enderling, Mark AJ Chaplain, and Philip Hahnfeldt. Quantitative modeling of tumor dynamics and radiotherapy. *Acta biotheoretica*, 58(4):341–353, 2010.

[ENKD+16] Pedro M Enriquez-Navas, Yoonseok Kam, Tuhin Das, Sabrina Hassan, Ariosto Silva, Parastou Foroutan, Epifanio Ruiz, Gary Martinez, Susan Minton, Robert J

Gillies, et al. Exploiting evolutionary principles to prolong tumor control in preclinical models of breast cancer. *Science translational medicine*, 8(327):327ra24–327ra24, 2016.

[Eva10] Lawrence C Evans. Partial differential equations. 2010.

[Fis37] Ronald Aylmer Fisher. The wave of advance of advantageous genes. *Annals of eugenics*, 7(4):355–369, 1937.

[FM77] Paul C Fife and J Bryce McLeod. The approach of solutions of nonlinear diffusion equations to travelling front solutions. *Archive for Rational Mechanics and Analysis*, 65(4):335–361, 1977.

[Fri04] Avner Friedman. A hierarchy of cancer models and their mathematical challenges. *Discrete Contin. Dyn. Syst. Ser. B*, 4(1):147–159, 2004. Mathematical models in cancer (Nashville, TN, 2002).

[Gar82] Robert A Gardner. Existence and stability of travelling wave solutions of competition models: A degree theoretic approach. *Journal of Differential equations*, 44(3):343–364, 1982.

[GBCC+09] Enrique González-Billalabeitia, Julia Calzas, Daniel Castellano, Cesar Mendiola, Susana Bezares, Vicente Valentín, Javier Hornedo, Eva Ciruelo, and Hernan Cortés-Funes. Long-term follow-up of an anthracycline-containing metronomic chemotherapy schedule in advanced breast cancer. *The breast journal*, 15(5):551–553, 2009.

[GG96] Robert A Gatenby and Edward T Gawlinski. A reaction-diffusion model of cancer invasion. *Cancer research*, 56(24):5745–5753, 1996.

[GN15] Léo Girardin and Grégoire Nadin. Travelling waves for diffusive and strongly competitive systems: relative motility and invasion speed. *European Journal of Applied Mathematics*, 26(04):521–534, 2015.

[GR16] Quentin Griette and Gaël Raoul. Existence and qualitative properties of travelling waves for an epidemiological model with mutations. *Journal of Differential Equations*, 260(10):7115–7151, 2016.

[GSGF09] Robert A Gatenby, Ariosto S Silva, Robert J Gillies, and B Roy Frieden. Adaptive therapy. *Cancer research*, 69(11):4894–4903, 2009.

[GV03] Robert A Gatenby and Thomas L Vincent. Application of quantitative models from population biology and evolutionary game theory to tumor therapeutic strategies. *Molecular cancer therapeutics*, 2(9):919–927, 2003.

[GW89] Mats Gyllenberg and Glenn F Webb. Quiescence as an explanation of gompertzian tumor growth. *Growth, development, and aging: GDA*, 53(1-2):25–33, 1989.

[HFH03] Philip Hahnfeldt, Judah Folkman, and Lynn Hlatky. Minimizing long-term tumor burden: The logic for metronomic chemotherapeutic dosing and its antiangiogenic basis. *J. theor. Biol.*, 220:545–554, 2003.

[HMB+16] Emilie Hénin, Christophe Meille, Dominique Barbolosi, Benoit You, Jérôme Guitton, Athanassios Iliadis, and Gilles Freyer. Revisiting dosing regimen using pk/pd modeling: the model1 phase i/ii trial of docetaxel plus epirubicin in metastatic breast cancer patients. *Breast cancer research and treatment*, 156(2):331–341, 2016.

[HPFH99] Philip Hahnfeldt, Dipak Panigrahy, Judah Folkman, and Lynn Hlatky. Tumor development under angiogenic signaling. *Cancer research*, 59(19):4770–4775, 1999.

[HR10] François Hamel and Lionel Roques. Fast propagation for kpp equations with slowly decaying initial conditions. *Journal of Differential Equations*, 249(7):1726–1745, 2010.

[IHRTEN+17] Arig Ibrahim-Hashim, Mark Robertson-Tessi, Pedro M Enriquez-Navas, Mehdi Damaghi, Yoganand Balagurunathan, Jonathan W Wojtkowiak, Shonagh Russell, Kam Yoonseok, Mark C Lloyd, Marilyn M Bui, et al. Defining cancer subpopulations by adaptive strategies rather than molecular properties provides novel insights into intratumoral evolution. *Cancer Research*, 77(9):2242–2254, 2017.

[JB00] Trachette L. Jackson and Helen M. Byrne. A mathematical model to study the effects of drug resistance and vasculature on the response of solid tumors to chemotherapy. *Math. Biosci.*, 164(1):17–38, 2000.

[JCK] Adrianne Jenner, Adelle CF Coster, and Peter Kim. Mathematical modelling of oncolytic virotherapy: The effects of a peg-modified adenovirus conjugated with herceptin. *The Australian Mathematical Society*, page 297.

[JGA15] Gunther Jansen, Robert Gatenby, and C Athena Aktipis. Opinion: Control vs. eradication: Applying infectious disease treatment strategies to cancer. *Proceedings of the National Academy of Sciences USA*, 112:937–938, 2015.

[KK04] Robert S Kerbel and Barton A Kamen. The anti-angiogenic basis of metronomic chemotherapy. *Nature Reviews Cancer*, 4(6):423–436, 2004.

[KO95] Yukio Kan-On. Parameter dependence of propagation speed of travelling waves for competition-diffusion equations. *SIAM journal on mathematical analysis*, 26(2):340–363, 1995.

[KPP37] Andrei N Kolmogorov, IG Petrovsky, and NS Piskunov. Etude de l'équation de la diffusion avec croissance de la quantité de matiere et son application à un probleme biologique. *Moscow Univ. Math. Bull*, 1(1-25):129, 1937.

[Lai64] Anna Kane Laird. Dynamics of tumour growth. *British journal of cancer*, 18(3):490, 1964.

[LCB+16] Mark C Lloyd, Jessica J Cunningham, Marilyn M Bui, Robert J Gillies, Joel S Brown, and Robert A Gatenby. Darwinian dynamics of intratumoral heterogeneity: not solely random mutations but also variable environmental selection forces. *Cancer research*, 76(11):3136–3144, 2016.

[LLC+15] Alexander Lorz, Tommaso Lorenzi, Jean Clairambault, Alexandre Escargueil, and Benoît Perthame. Modeling the effects of space structure and combination therapies on phenotypic heterogeneity and drug resistance in solid tumors. *Bull. Math. Biol.*, 77(1):1–22, 2015.

[LS06] Urszula Ledzewicz and Heinz M Schättler. Drug resistance in cancer chemotherapy as an optimal control problem. *Discrete and Continuous Dynamical Systems Series B*, 6(1):129, 2006.

[LS14] Urszula Ledzewicz and Heinz Schättler. An optimal control approach to cancer chemotherapy with tumor-immune system interactions. In *Mathematical models of tumor-immune system dynamics*, volume 107 of *Springer Proc. Math. Stat.*, pages 157–196. Springer, New York, 2014.

[MBC+16] Christophe Meille, Dominique Barbolosi, Joseph Ciccolini, Gilles Freyer, and Athanassios Iliadis. Revisiting dosing regimen using pharmacokinetic/pharmacodynamic mathematical modeling: densification and intensification of combination cancer therapy. *Clinical pharmacokinetics*, 55(8):1015–1025, 2016.

[MBK+15] P Mazzocco, Célia Barthélémy, G Kaloshi, Marc Lavielle, D Ricard, A Idbaih, D Psimaras, M-A Renard, A Alentorn, J Honnorat, et al. Prediction of response to temozolomide in low-grade glioma patients based on tumor size dynamics and genetic characteristics. *CPT: pharmacometrics & systems pharmacology*, 4(12):728–737, 2015.

[MBOVD04] L Marcu, E Bezak, I Olver, and T Van Doorn. Tumour resistance to cisplatin: a modelling approach. *Physics in medicine and biology*, 50(1):93, 2004.

[MMGL87] S. Michelson, B. E. Miller, A. S. Glicksman, and J. T. Leith. Tumor micro-ecology and competitive interactions. *J. Theoret. Biol.*, 128(2):233–246, 1987.

[NCO+03] Marco Novelli, Antonio Cossu, Dahmane Oukrif, Alberto Quaglia, Sunil Lakhani, Richard Poulsom, Peter Sasieni, Piera Carta, Marcella Contini, Anna Pasca, et al. X-inactivation patch size in human female tissue confounds the assessment of tumor clonality. *Proceedings of the National Academy of Sciences*, 100(6):3311–3314, 2003.

[OAMB09] Markus R. Owen, Tomás Alarcón, Philip K. Maini, and Helen M. Byrne. Angiogenesis and vascular remodelling in normal and cancerous tissues. *J. Math. Biol.*, 58(4-5):689–721, 2009.

[OSM+11] Markus R Owen, I Johanna Stamper, Munitta Muthana, Giles W Richardson, Jon Dobson, Claire E Lewis, and Helen M Byrne. Mathematical modeling predicts synergistic antitumor effects of combining a macrophage-based, hypoxia-targeted gene therapy with chemotherapy. *Cancer research*, 71(8):2826–2837, 2011.

[Pan96] John Carl Panetta. A mathematical model of periodically pulsed chemotherapy: tumor recurrence and metastasis in a competitive environment. *Bulletin of mathematical Biology*, 58(3):425–447, 1996.

[PBZ+13] Angela Oliveira Pisco, Amy Brock, Joseph Zhou, Andreas Moor, Mitra Mojtahedi, Dean Jackson, and Sui Huang. Non-darwinian dynamics in therapy-induced cancer drug resistance. *Nature communications*, 4, 2013.

[PHA+17] Holger Perfahl, Barry D Hughes, Tomás Alarcón, Philip K Maini, Mark C Lloyd, Matthias Reuss, and Helen M Byrne. 3d hybrid modelling of vascular network formation. *Journal of Theoretical Biology*, 414:254–268, 2017.

[PKA10] Eddy Pasquier, Maria Kavallaris, and Nicolas André. Metronomic chemotherapy: new rationale for new directions. *Nature reviews Clinical oncology*, 7(8):455–465, 2010.

[PW12] Murray H Protter and Hans F Weinberger. *Maximum principles in differential equations*. Springer Science & Business Media, 2012.

[RKP+12] Benjamin Ribba, Gentian Kaloshi, Mathieu Peyre, Damien Ricard, Vincent Calvez, Michel Tod, Branka Čajavec-Bernard, Ahmed Idbaih, Dimitri Psimaras, Linda Dainese, et al. A tumor growth inhibition model for low-grade glioma treated with chemotherapy or radiotherapy. *Clinical Cancer Research*, 18(18):5071–5080, 2012.

[RTGGA15] Mark Robertson-Tessi, Robert J Gillies, Robert A Gatenby, and Alexander RA Anderson. Impact of metabolic heterogeneity on tumor growth, invasion, and treatment outcomes. *Cancer research*, 75(8):1567–1579, 2015.

[SG10] Ariosto S Silva and Robert A Gatenby. A theoretical quantitative model for evolution of cancer chemotherapy resistance. *Biology direct*, 5(1):1, 2010.

[SPSW91] Jerry W Shay, Olivia M Pereira-Smith, and Woodring E Wright. A role for both rb and p53 in the regulation of human cellular senescence. *Experimental cell research*, 196(1):33–39, 1991.

[Tré05] Emmanuel Trélat. *Contrôle optimal*. Mathématiques Concrètes. [Concrete Mathematics]. Vuibert, Paris, 2005. Théorie & applications. [Theory and applications].

[UMK+14] Jan Unkelbach, Bjoern H Menze, Ender Konukoglu, Florian Dittmann, Nicholas Ayache, and Helen A Shih. Radiotherapy planning for glioblastoma based on a tumor growth model: implications for spatial dose redistribution. *Physics in medicine and biology*, 59(3):771, 2014.

[VA82] Vinay G Vaidya and Frank J Alexandro. Evaluation of some mathematical models for tumor growth. *International journal of bio-medical computing*, 13(1):19–35, 1982.

[VVV94] Aizik I Volpert, Vitaly A Volpert, and Vladimir A Volpert. *Traveling wave solutions of parabolic systems*, volume 140. American Mathematical Soc., 1994.

[Wei13] Robert Weinberg. *The biology of cancer*. Garland science, 2013.

[Wel97] Peter G Welling. *Pharmacokinetics: Processes, mathematics, and applications*. Amer Chemical Society, 1997.

[Xin00] Jack Xin. Front propagation in heterogeneous media. *SIAM review*, 42(2):161–230, 2000.

[ZPQH14] Joseph Xu Zhou, Angela Oliveira Pisco, Hong Qian, and Sui Huang. Nonequilibrium population dynamics of phenotype conversion of cancer cells. *PloS one*, 9(12):e110714, 2014.

My articles

[1] Cécile Carrère. Optimization of an in vitro chemotherapy to avoid resistant tumours. *Journal of Theoretical Biology*, 413:24–33, 2017.

[2] Cécile Carrère. Spreading speeds for a two-species competition-diffusion system. 2017.